Near-Infrared High-Resolution Polarimetry Observations towards Protoplanetary Disks in Binary/Multiple Systems

YANG YI

Doctor of Philosophy

Department of Astronomical Science
School of Physical Sciences
SOKENDAI (The Graduate University for Advanced Studies)

Near-Infrared High-Resolution Polarimetry Observations towards Protoplanetary Disks in Binary/Multiple Systems

Yi Yang

Department of Astronomical Science
SOKENDAI (The Graduate University for Advanced Studies)

This dissertation is submitted for the degree of
Doctor of Philosophy

2018

I would like to dedicate this thesis to:
Mrs Lan Lin, my astronomy teacher in high school, who brought me into Hanggao Observatory, where I started my exploration of the universe;
Prof. D. N. C. Lin, my supervisor in Peking University, who led me into the world of exoplanet.

Declaration

I hereby declare that except where specific reference is made to the work of others, the contents of this dissertation are original and have not been submitted in whole or in part for consideration for any other degree or qualification in this, or any other university. This dissertation is my own work and contains nothing which is the outcome of work done in collaboration with others, except as specified in the text and Acknowledgements.

Yi Yang
2018

Acknowledgements

First of all, I would like to acknowledge all of my supervisors. I greatly thank Prof. Motohide Tamura for giving me the opportunity to study at National Astronomical Observatory of Japan, teaching me much knowledge about exoplanets, protoplanetary disks and high contrast observation techniques. I will also thank my three other supervisors: Prof. Saeko Hayashi, Prof. Tomonori Usuda and Prof. Satoshi Mayama, for their endless help and research advice during my 5-year PhD study. I am very glad to have them as my supervisors.

Besides my supervisors, I would like to acknowledge my co-investigators. I specially thank Dr. Jun Hashimoto, Dr. Daehyeon Oh, and Dr. Jungmi Kwon, for teaching me how to deal with high contrast PDI data and giving me many suggestions about my research. I thank Prof. Roman Rafikov, and Dr. Ruobing Dong for giving their suggestions from theoretical view. I thank Prof. Eiji Akiyama for teaching me how to analyze ALMA sub-millimeter data using CASA. I want to thank all the SEEDS group members for either giving me research suggestions, or maintaining high-contrast observation instruments HiCIAO I use for my research. I would also like to thank all the astronomers who discussed with me and gave me suggestions in various conferences.

I would also like to thank my PhD referees: Prof. Fumitaka Nakamura, Prof. Katsunori Shibata, Prof. Tomoya Hirota, Prof. Takayuki Muto and Prof. Hideko Nomura. Their suggestions and comments help a lot in improving my thesis.

Then I would like to thank all the students, postdocs, professors and other staff in NAOJ Mitaka campus and NAOJ Hilo campus. I specially thank Dr. Takuya Suenaga and Dr. Daehyon Oh for helping me get used to the life in Japan. Without their support, I cannot finish my study.

Finally, I would like to acknowledge my parents and my friends. Their encouragement supports me to overcome all the difficulties during my study.

Abstract

About 4000 exoplanets have been discovered so far and among them about 200 are in binary or multiple systems. It is also known that stars tend to form in binary or multiple systems, which indicates that many planets would form in environments of binary or multiple systems. Therefore, to understand planet formation, it is quite necessary to investigate planet formation processes in binary systems.

Previous researches have made a big progress on planet formation in single star systems. However, we still do not clearly understand the planet formation process in binary systems. To understand this, we need to know the disk evolution process in binary systems. Some theories of disk evolution process in binary systems have been developed in recent years, but the observational evidence is still lacked due to the previous low spatial resolutions and low contrasts of the instruments, especially for the disk evolution process in close (separation < 100 AU) binaries. To improve current theories, observational evidence is quite important. Fortunately, as the development of high-contrast observation techniques, we can now observe the protoplanetary disk structures in close binaries.

In this thesis, we aim at finding observational evidence of the disk evolution in young binary systems by investigating the disk structures around them. To achieve this goal, we use high-contrast imaging polarimetric observations in near-infrared wavelengths and investigate the detailed disk structures around close binaries. We also used the Atacama Large Millimeter Array (ALMA) high spatial resolution data at submillimeter wavelengths to complement the near-infrared data.

We mainly investigated four young binaries. Firstly, we focused on the GG Tau A binary. By performing non-masked polarimetry imaging with the High Contrast Instrument for the Subaru Next Generation Adaptive Optics (HiCIAO) instrument mounted on the Subaru Telescope, polarized scattered light from the inner region of the disk around the GG Tau A system was successfully detected in the H-band ($\sim$1.6 μm) with a spatial resolution of approximately 0.07$''$, revealing the complicated inner disk structures around this young binary. An arc-like structure to the north of GG Tau Ab and part of a circumstellar structure that is noticeable around GG Tau Aa extending to approximately 28 AU from the primary star is detected in the near-infrared band for the first time. The speckle noise around GG Tau

Ab constrains its disk radius to <13 AU. Based on the size of the circumbinary ring and the circumstellar disk around GG Tau Aa, the semi-major axis of the binary's orbit is likely to be 62 AU. A comparison of the present observations with previous ALMA and near-infrared H_2 emission observations suggests that the north arc could be part of a large streamer flowing from the circumbinary ring to sustain the circumstellar disks. According to the previous studies, the circumstellar disk around GG Tau Aa has enough mass and can sustain itself for a duration sufficient for planet formation; thus, this study indicates that planets can form within close (separation < 100 AU) young binary systems.

Secondly, we observed the triple-star system T Tau. We conducted high-contrast polarimetry observations in the direction of T Tau in the H-band, by using the HiCIAO instrument mounted on the Subaru Telescope, revealing structures as near as $0.1''$ from the stars, T Tau N and T Tau S. The whole T Tau system is discovered to be surrounded by nebula-like envelopes, and there are several outflow-related structures detected in these envelopes. After analyzing the detailed polarization patterns near each component of this triple young star system, we suggest that the face-on circumstellar disk of T Tau N should not be larger than $0.8''$, or 117 AU. As for T Tau S, we suggest that it is surrounded by an inclined circumbinary disk with a radius of about 44 AU which is quite misaligned with the binary orbit, and is likely to trigger the famous E-W outflow, and a precessing southwest outflow. But we did not detect any cavity in the disk around T Tau S, which may be due to that the gap opened in a misaligned disk is smaller than a coplanar one, and it is hard to observe such a gap in such an inclined disk. Our observations give a much more direct view of the disk structures in this system than the previous researches; it could be quite helpful for the following researches.

Thirdly, we investigated the FS Tau A system. By analyzing the H-band image obtained by HiCIAO as well as the archived CO 2-1 data obtained by ALMA, we found out that the surrounding structures around FS Tau A can be classified as blue-shifted component 1 and red-shifted component 2. For component 1, we identify one structure representing a 56-AU nearly edge-on inner circumbinary disk which is quite misaligned with the binary orbit, and a bar-like structure located at the southeast of the central stars. For component 2, we identify a crescent-like structure in CO 2-1 image which is consistent with the structures detected in near-infrared band, which may represent a ring or an arm. We notice that the binary orbit, inner 56-AU circumbinary disk and the previous detected outer circumbinary disk are misaligned with each other. For FS Tau A holds a low-eccentric orbit, it is hard to explain this misalignment from the precession triggered by the binary. We also take a look at H-band image of the binary system Coku Tau 4 obtained by Subaru/HiCIAO, suggesting that it may have a gap with radius about 23 AU in its 70-AU circumbinary disk.

Based on the circumbinary disks we observed, as well as the results from other telescopes, we made a brief analysis about the disk evolution in binary systems, mainly focusing on gap opening and misalignment of circumbinary disks. We found out that current gap opening and disk misalignment theory can explain most of the gaps and disk misalignment in observed circumbinary disks. However, there still exist some circumbinary disks whose gap size and misalignment cannot be explained well by the current theories, and this indicates that improving circumbinary disk evolution is still necessary. Besides, although from our observation results a detailed discussion about planet formation is hard, we can still suggest that planet formation may be possible in the circumstellar disks around the stars in binary systems and circumbinary disks, and the discovery of so many misaligned circumbinary disk implies there should exists planet whose orbital plane is misaligned with the orbital plane of its host binary.

Table of contents

List of figures

List of tables

Chapter 1

Introduction

1.1 Planets and Their Formation in Binary Systems

1.1.1 Planets in Binary Systems

Extrasolar planets, or exoplanets for short, mean that planets located outside our Solar System. Although γ Cep Ab "Tadmor", an exoplanet in a binary system, was suggested in 1988 [18] (confirmed in 2003 [50]), the first confirmed discovery of exoplanet is in 1992: Wolszczan and Frail [133] reported two exoplanets around PSR B1257+12 "Lich", a pulsar locates about 710 pc from us [135]. The first confirmed exoplanet around a main sequence star is 51 Peg b “Dimidium", a "hot-Jupiter" around the star 51 Peg [86]. Till now there have been about 3700 confirmed exoplanet discoveries (http://www.openexoplanetcatalogue.com/, retrieved on 2018/01/07).

Many exoplanets show different characteristics from the planets in our solar system. One example is that some exoplanets are discovered in binary or multiple star systems. Despite γ Cep Ab, the first discovery of them is PSR B1620-26 (AB)b: it is an exoplanet first announced in 1993, and confirmed in 2003, located in a pulsar-white dwarf system in the global cluster M4 [124, 116]. The first confirmed exoplanets in main-sequence binary stars are τ Boötis Ab and 55 Cancri Ab "Galileo", discovered in 1997 [16]. Now there are about 185 planets discovered in 133 binary or multiple star systems (http://www.openexoplanetcatalogue.com/, retrieved on 2017/09/26). Roell et al. [111] suggested that at least 12% planet systems have binary or multiple star hosts, by simply matching some exoplanet candidates discovered by radial velocity and transit with online multiplicity catalog. In an earlier research, Raghavan et al. [104] investigated the proper motions of 131 exoplanet candidates discovered by radial velocity and concluded that about 23% planet-host stars are binary or multiple systems. And Horch et al. [56] estimated that approximately 40-50% planet systems are binary or multiple

systems, by using high-resolution imaging and statistical methods. In any case, there are a lot of planets in binary or multiple systems, so it could be quite important to learn their properties, like their orbits, habitability, and formation.

Now planets in binary systems can be classified into three types. S-type planets mean that planets orbit around only one of the stars in the binary system, P-type planets mean that planet orbits around the binary system. There is also one kind planets called Trojan planets, or T-type planets, which means that planets locate at the Lagrangian points L4 or L5 of the binary. Till now there are no discovery of T-type planets, so the discussion about planets in binaries are mainly focused on S-type and P-type planets.

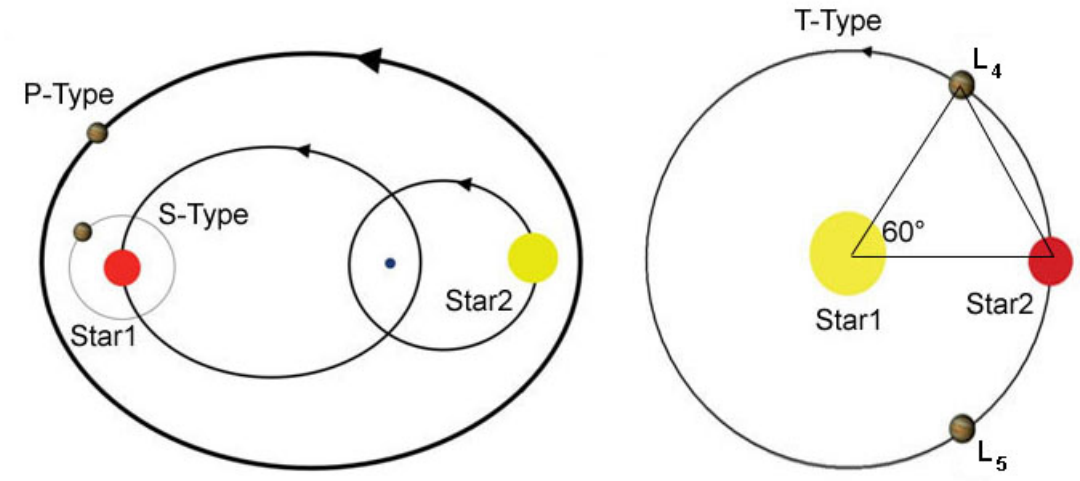

Fig. 1.1 An illustration of S-type, P-type and T-type planets. Figure 1 in Schwarz et al. [115]

An additional star will obviously affect the planets' orbit. One of the famous mechanisms showing the planets affected by the stars is the Lidov-Kozai mechanism [71, 78]:

$$L_z = \sqrt{1-e^2} cos\ i \tag{1.1}$$

here L_z is a constant, indicating the specific z component of the planet's angular momentum, while e and i represent the eccentricity and inclination of the planets, respectively. This mechanism will lead the planets in a binary system to change their orbits from a near-circular, high-inclined one to an eccentric, low-inclined one. This will lead the periaston distances of the orbits to become smaller. With some other mechanisms such as tidal dissipation it will lead the gas giant planets to migrate inward and become hot Jupiters (e.g., Wu and Murray

Table 1.1 An incomplete list of planets discovered in binary or multiple systems

Name	Planet properties			Host star properties			Reference
	$M_p(M_J)$	$a_p(AU)$	e_p	$M_s(M_\odot)$	$a_s(AU)$	e_s	
PSR B1620-26 (AB)b	2.5	23	–	1.35/0.34	0.775	0.025	[124, 6, 116]
γ Cep Ab	1.6	2.14	0.12	1.40/0.41	20.2	0.41	[50, 92]
τ Boötis Ab	5.95	0.048	0.023	1.35[1]	43[2]	–	[16, 17, 15]
55 Cancri Ab	0.824	0.115	0.014	0.905[3]	1050[4]	–	[16, 104, 42, 129]
Kepler-16(AB) b	0.333	0.7048	0.0069	0.69/0.20	0.224	0.159	[30]

M_p: planet mass in Jupiter mass; a_p: semi-major axis of planet orbit; e_p: eccentricity of planet orbit; M_s: host stellar mass in solar mass; a_s semi-major axis of binary orbit; e_s: eccentricity of binary orbit

[1] the mass of the primary star, the secondary star is a M2 target [14] and its mass is unknown;

[2] The calculated projected separations of the binaries, based on Fabricius et al. [40], Butler et al. [17], Adelman-McCarthy and et al. [1];

[3] Only the mass of the primary star (55 Cancri A) is given, 55 Cancri B is a M4 star [104] and its mass is unknown;

[4] The projected separation of the binaries;

[134]). If the planet reaches a critical inclination (Kozai angle, for circular binary orbit it is given by $i = \arccos\sqrt{\frac{3}{5}} \approx 39.2^\circ$), the orbit will oscillate around 90° or 270°.

Binarity is also believed to affect the habitability of the planets, because a companion star will not only influence the orbits of planets, but also alter the habitable zone, whose temperature is believed to be suitable for liquid water to exist. However, research like Eggl et al. [38] has revealed that it is not so rare that a planet in binary system has a stable orbit and is habitable. So it is still promising to find a habitable planet in binary systems.

Finally, binaries will significantly affect the planet formation and disk evolution processes. A detailed discussion will be made in the next section.

1.1.2 Planet Formation in Binary Systems

Since we have discovered about 200 planets in binary or multiple systems by now, it is necessary for astronomers to explain their formation. In addition, previous researches found out that the binary fraction in young stars, e.g., T-Tauri stars, is significant higher than that of the field stars [33]. This implies that planets in single stars may also be affected by a companion star during their formation. Therefore, to understand planet formation processes, it is quite important to investigate how the binaries affect planet formation and disk evolution processes.

Some previous researches have shown that, for wide (separations $>\sim$100 AU) binaries, planet formation is not so difficult and could be just the same as the planet formation around single stars, but for close (separation $<\sim$100 AU) binary systems, planet formation could be

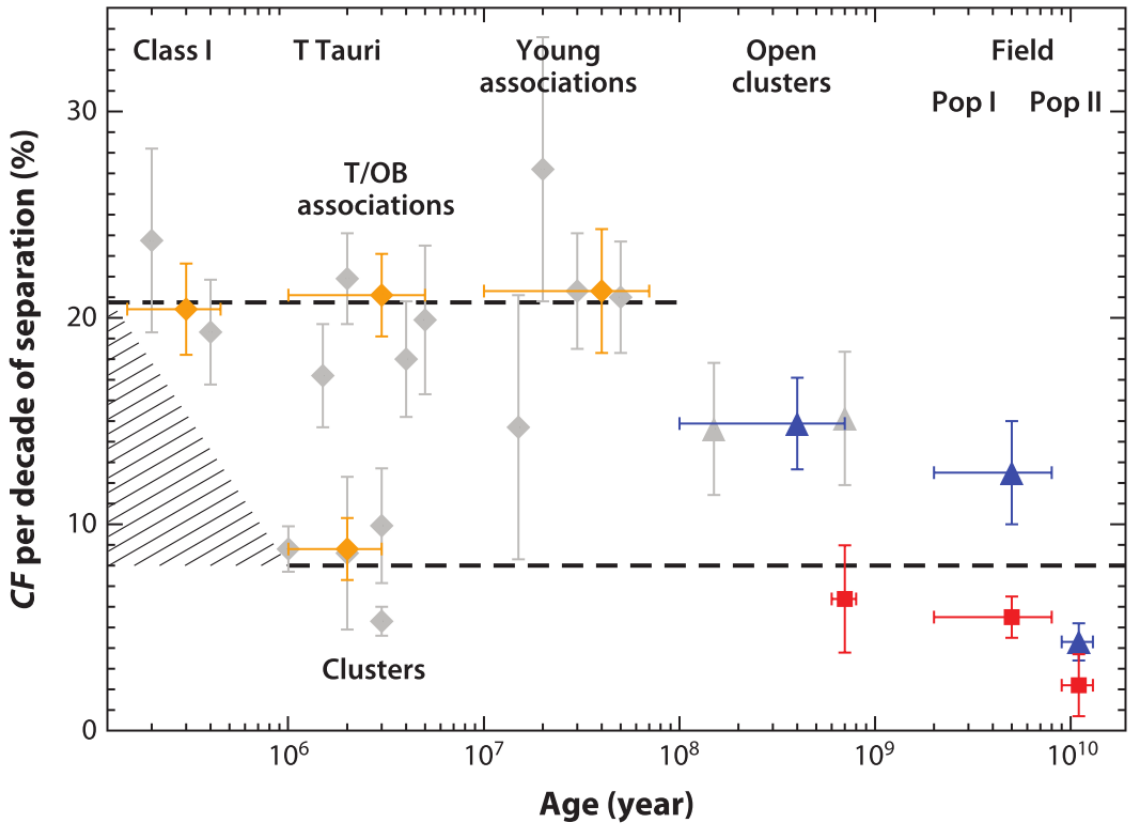

Fig. 1.2 Binary fractions in different ages of stars. It can be seen that in young stars, like Class I, T Tauri stars, binary fractions is significantly higher than field stars. Here blue triangles stand for solar-type stars ($\sim 0.7-1.5M_{\odot}$), red squares stand for low mass stars ($\sim 0.1-0.5M_{\odot}$) and orange diamonds stand for overall ranges of young stars ($\sim 0.1-2M_{\odot}$). Gray symbols indicate results of individual surveys used in Duchêne and Kraus [33]. Black dashed lines indicate the binary fractions of predicted behaviors of low-density associations (top line) and dense clusters (bottom line). The hashed region indicates the predicted ranges of binary fractions for stellar clusters in the embedded phases. Figure 5 in Duchêne and Kraus [33]

quite difficult, because the motion of the binary will make the disk dissipate quickly (e.g., Duchêne [31]). However, many planets in close binaries have been discovered, like γ Cep Ab and Kepler-16(AB) b [30]. These discoveries force astronomers to seek some theory to explain their formation. Some theories include that the gravity due to the disk mass will help reduce the orbital eccentricity excitation and velocities of the planetesimals so that they can grow to planet size [102], and there exists non-turbulent midplane layer (dead zone) in the disk where planets can form safely [46].

Obviously, to improve current planet formation theory in binary or multiple systems, we need observation evidence, i.e., we need to observe the planet formation process using telescopes. However, currently it is still very difficult to observe a forming planet, because they are very far and faint. One capable way is to investigate the protoplanetary disks where planets form. From how the binary systems alter the disk evolution process, we may extrapolate the planet formation process in binary or multiple systems.

1.2 Disk Evolution in Binary Systems

Protoplanetary disks are pancake or ring-like structures often found around Young Stellar Objects (YSOs), consisting of mainly gas and dust. They can be regarded as accretion disks of YSOs, and are believed to be the birthplace of planets. Therefore, to learn the planet formation process, it is quite important to learn the evolution process of protoplanetary disks.

Disk evolution is a quite complicated process, till now our understanding of it is still quite limited. However, based on numerical simulations and observations, a typical evolution process can still be summarized. A typical evolution of protoplanetary disk actually includes many processes, like accretion, far ultraviolet (FUV) photoevaporation, and grain growth. At the first stage massive flared disk (Figure 1.3a), the disk is full of gas and grains, and the evaporation due to FUV photons and mass accretion onto the central star will cause the disk to lose its mass. Then at the second stage settled disk (Figure 1.3b), grains begin to settle in the midplane of the disk and grow larger and larger to become planetesimals, and the decreasing of the scale height of the dust due to this process makes the disk flatter. As the accretion rate decreases lower than the photoevaporation rate, the inner disk cannot get enough supply from the outer disk. The FUV photoevaporation will starts to blow the gas and dusts out from the most inner parts of the disk, making a central hole of radius about a few AUs, then the disk generally enters its third stage photoevaporating disk (Figure 1.3c). After that the inner disk edge will be exposed under the FUV and the gas and grains in the disk will keep losing. When almost all the gas and small grains are blown out of the disk,

the disk enters its final stage debris disk (Figure 1.3d), only large grains, planetesimals, and planets, will be left.

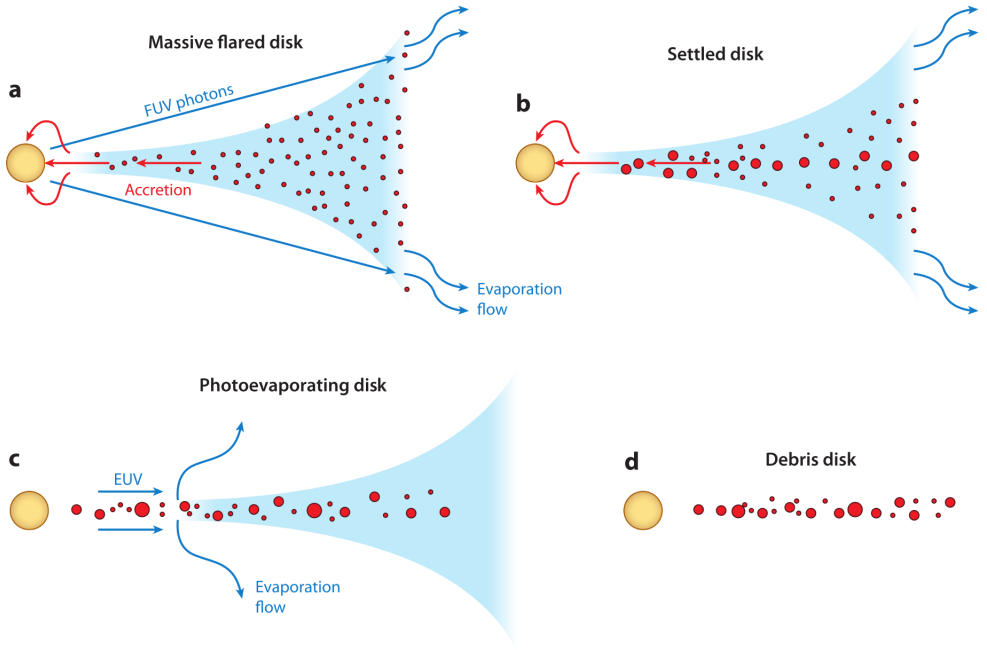

Fig. 1.3 An illustration of typical disk evolution process. The blue indicates the gas distributions in the disk and the red dots indicate the dust size and distributions in the disk. a: massive flared disk, the disk loses mass due to photoevaporation caused by the far ultraviolet (FUV) light and accretion onto the central star; b: settled disk, grains start to growth and settle down to the middle plane of the disk; c: photoevaproating disk, the accretion rate decreases and gas is blown out by the extreme ultraviolet (EUV) light from the disk; d: debris disk, all the gas is dissipated, only large grains, planetesimals and/or planets are left. Figure 6 in Williams and Cieza [131]

However, in binary and multiple systems, one or more additional companions will have significant influence towards the disk. Compared to the typical disk evolution process in single stars, previous theoretical researches have revealed that binary may affect the disk in many ways.

The most obvious effect of the binary is that it will significant alter the appearance of the disks around them. Firstly, they can open gaps in the circumbinary disk which will make the disk structures in binary systems become 3 parts: a large circumbinary ring, with a inner radius usually 2-3 times of the binary's semi-major axis, around both stars, and a circumstellar disk around each star, e.g., Artymowicz and Lubow [5] discussed a coplanar circumbinary disk with different binary mass ratios and eccentricities, found that the binary will open a gap with about 2-3 times of the binary semi-major axis, and the circumstellar disks around each

star have radii about 0.2-0.4 times of the binary semi-major axis; secondly, the interaction between the circumbinary disk and the binary will make the disk misaligned with the binary orbit, e.g., Martin and Lubow [83] simulated a disk with initial inclination 60° and radius 2-5 times of the binary semi-major axis around an equal-mass binary with eccentricity 0.5 and found out that the binary can trigger the disk to precess to polar-alignment, and Zanazzi and Lai [136] used semi-analytic theory to study circumbinary disk with around eccentric binaries implying that eccentric binaries are more possible to have highly misaligned circumbinary disks; also, tidal forces from the binary will constrain the disk size, making the disk become eccentric, e.g., Regály et al. [108] simulated a circumstellar disk with initial radius 40 AU and a companion with semi-major axis 40 AU under different parameters including binary mass ratios and binary eccentricities, found out that the disk will become smaller and more eccentric under the interactions with the companion star. In addition, since binaries will alter the motion of the dusts and gas in the disks, it is foreseeable that the binary will affect the grain growth process, and we can know this by investigating the dust size distributions in the circumbinary disks. Finally, the disturbance to the motion of dusts and gas may also alter the temperatures of the disks.

Previous observations have revealed some disks in binaries, like resolving the streaming structures around the binary SR 24, a binary with separation about 800 AU, in near infrared band [84], and the $\sim 60-68^\circ$ misaligned circumstellar disks around each star in HK Tau system, a binary with separation about 386 AU (e.g., Jensen and Akeson [59]). These researches are mainly focused on relatively wide binaries, i.e., binaries with separations about hundreds of AU. There are also some researches focused on close binaries, like the discovery of the famous circumbinary ring around GG Tau A, a binary with separation about 40 AU (e.g., Krist et al. [76]). However, for disk structures near the close binaries, previous researches are quite limited. Previous researches ever showed that the peak of distribution of physical separations for solar-type pre–main sequence binaries is expected to around 30 AU in field stars (e.g., Duquennoy and Mayor [34], Raghavan et al. [105]). This indicates that close binaries may be the majority of the binaries. Therefore, to learn disk evolution as well as in binary systems, it is necessary to learn the disk structures in close binaries.

Considering the close binaries have separations about tens of AU, the disk structures, like the circumstellar disk and the gap opened in the circumbinary disks, generally have sizes about tens to hundreds of AU according to the simulation results by Artymowicz and Lubow [5]. In this case, we expect spatial resolution near the diffraction limit ($\sim 0.''05$ in H-band, corresponding to 7 AU at 140 pc, which is the typical distance of young stellar objects, e.g., Kenyon et al. [64], and see Loinard et al. [80], Torres et al. [127, 128, 126]) of a 10-m class telescope, and inner working angle $0.''1$ (corresponding to 14 AU at 140 pc) to help reveal the

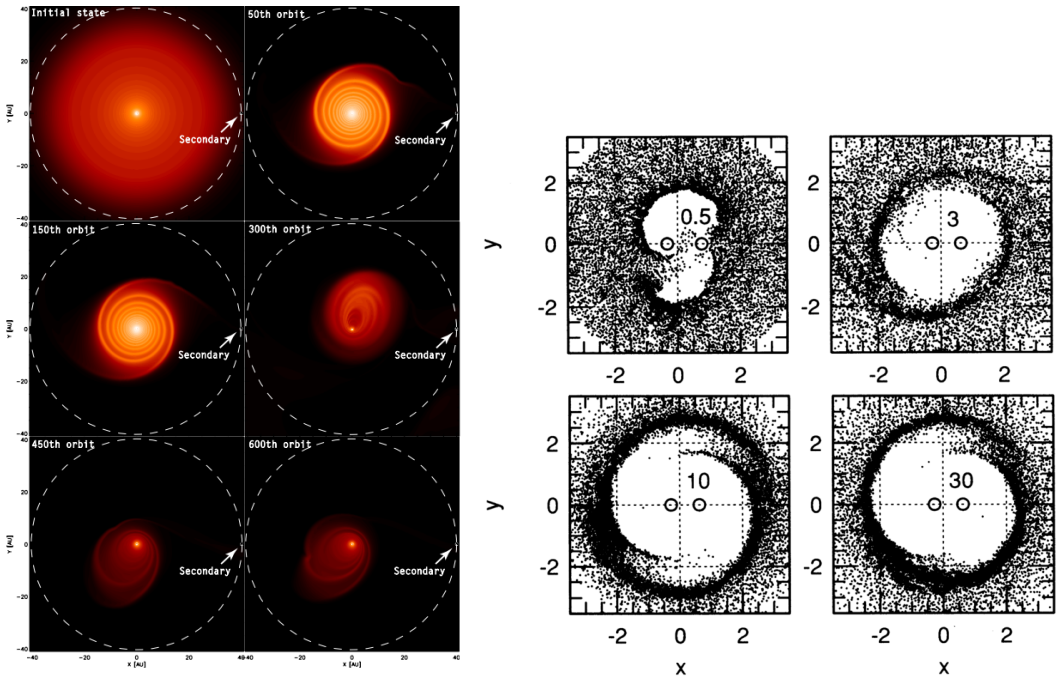

(a) (b)

Fig. 1.4 (a): one simulation showing the evolution of the disk surface density with a companion star at $t = 0, 50P, 150P, 300P, 450P, 600P$, showing how a companion star constrain the disk size and make the disk become eccentric. The dashed white lines show the circular orbit of the companion star, and the mass ratio of the binary in this simulation is 0.3. Figure 1 in Regály et al. [108]; (b): an simulation showing how a binary open gaps in the center of a circumbinary disk, with mass ratio 0.3 and eccentricity 0.1. The four images, from top left to bottom right, show the gaps after $t = 0.5P, 3P, 10P, 30P$ respectively, here P is the period of the binary. Figure 9 in Artymowicz and Lubow [5].

disk structures near the close binaries. Fortunately, with the development of high-spatial and high-contrast resolution instruments, now it is possible to observe such small scale structures. With the new Subaru Telescope instrument HiCIAO and AO 188, we can easily achieve a spatial resolution about $0.''07$ in H-band and inner working angle about $0.''1$, this could be enough for our study.

1.3 Motivation of this thesis

The motivation is to investigate the disk structures in close binary or multiple systems, hoping to reveal how the binary affects the disk, then it will help understand the planet formation process in binary systems in some future research.

Our research starts from GG Tau A. It is a typical young binary system with masses similar to our Sun and has been studied a lot. It has a well-known circumbinary ring, but due to the limitation of spatial resolution, previous researches did not discuss much about the structures inside the circumbinary ring, and learning the structures near the binaries is crucial for us to learn the planet formation process of S-type planet in close binaries, like γ Cep Ab. Therefore, to learn planet formation process in binaries, GG Tau A is an ideal target.

The second target we choose is T Tau. It is the prototype of T Tauri star, and is a triple system. Previous research suggested that the close binary T Tau S could hold a nearly edge-on disk which is quite misaligned with its orbital plane from indirect method like analysis of its extinction, but direct imaging of its disks lacks. So to understand disk misalignment in binary systems, it is worth investigating.

The third target is FS Tau A. It is a low mass binary system with a total mass about $0.78M_{\odot}$, and previous researches like Hioki et al. [53] suggested that the circumstellar disks around the binaries could be misaligned with the outer circumbinary disk. So from it we may be able to find out the clue about disk misalignment in binaries. And there is another target: Coku Tau 4. Previous SED fitting results like D'Alessio et al. [27] suggested that it could have a central gap with a radius about 10 AU, but it lacks direct observation. Thus investigating this target could help with understanding gap opening in binary systems.

Then, from these observation results we can compare with the theoretical predictions of gap size and disk misalignment, to see if they can be explained well by current theories. This can help to understand how disk evolution is affected by different masses of binaries.

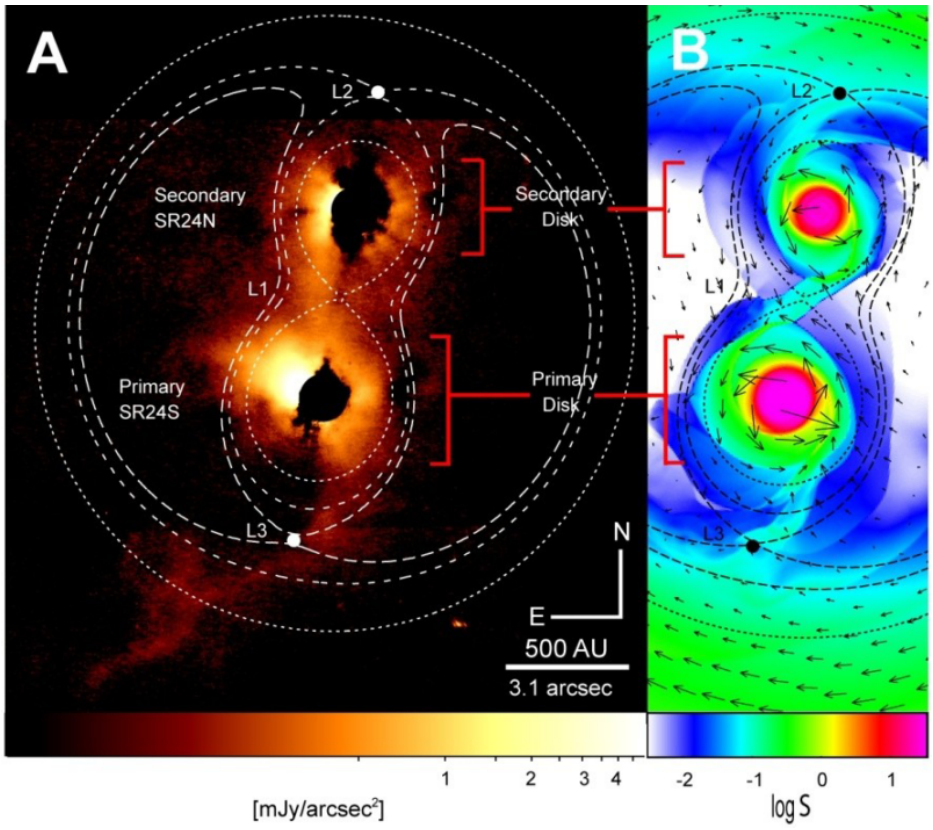

(a)

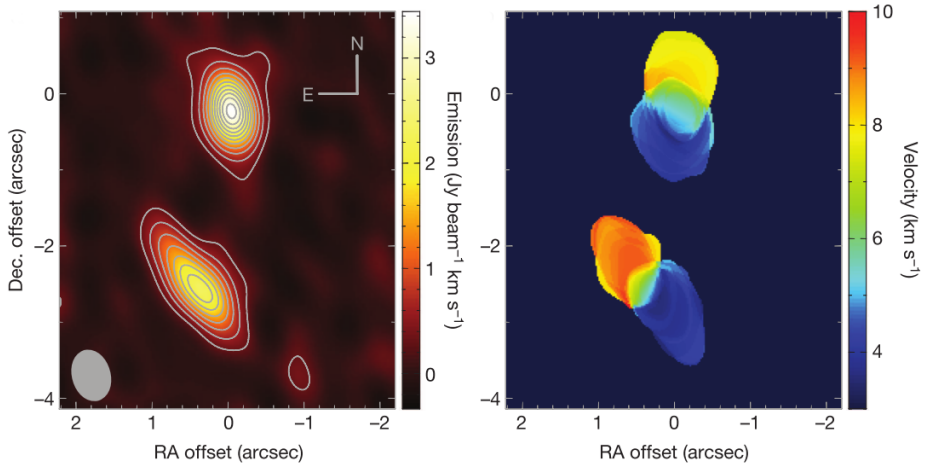

(b)

Fig. 1.5 Previous observations of disk in binary systems. (a): Near infrared Subaru/CIAO H-band observations of the disk structure around the wide binary SR 24 (*left*), and corresponding simulation (*right*), showing a binary with separation about 800 AU and surrounding disk and stream structures. The dotted and dashed lines on the H-band and simulated image represent the inner and outer Roche Lobes, and L1, L2, L3 represents the three Lagrangian points in this binary system. Figure 1 in Mayama et al. [84]; (b): ALMA CO 3-2 emission line observations of HK Tau, a binary with separation about 386 AU. The intensity map (*left*) and velocity map (*right*) shows two misaligned circumstellar disks with misaligned angles 60-68°. Figure 1 in Jensen and Akeson [59].

1.4 Observation Techniques

1.4.1 Adaptive Optics (AO)

Because protoplanetary disk host stars are quite far (about 140 pc) and faint, thus some special techniques are needed to resolve the disk structures. For observation band we choose the near-infrared band, because it is sensitive to young stars, and can give a high spatial resolution. Our observations use the HiCIAO instrument mounted on the 8.2m Subaru Telescope. Since planets and disks are very faint compared to their hosts star, some techniques are needed to observe them.

One basic technique for high-contrast observations is called Adaptive Optics (AO). Since we need to resolve the detailed structures in the disk to understand how the binary system alters the disk, we need a high spatial resolution. However, for large ground-based telescopes like Subaru Telescope, it is difficult to reach its theoretical spatial resolution because of the atmosphere distortion of light. To help ground-based telescopes to reach their theoretical spatial resolutions, the AO technology is developed.

In the AO system, firstly the telescope will observe a guide star. This guide star could be a real star, or an artificial laser guide star. Then the light from this guide star will be received by a wavefront sensor. Based on the signals got by the wavefront sensor, one computer will calculate the atmosphere distortion, then controls a deformable mirror to change its shape and to correct the distorted wavefront. After that, the atmosphere distortion will be largely reduced and the telescope can reach its theoretical spatial resolution.

1.4.2 Polarimetry Differential Imaging (PDI)

Another basic technique used in disk imaging is called Polarimetry Differential Imaging (PDI), which observes polarized light scattered by the dusts in the protoplanetary disk. The light from the stars is not polarized, while the light scattered by the protoplanetary disks is polarized. Therefore, by observing the polarized light we can easily resolve the disk structures around the young stars. In addition, since the polarized light is scattered by the aligned dusts in the disk, if we draw a vector map which shows the polarization position angles, we will see the vectors on disk structures are generally centrosymmetric, this could be helpful for us to distinguish the disk structures near the stars.

Polarization means that waves can oscillate more than one direction. It is the unique property of the transverse waves, like the electromagnetic waves. For pure polarization state, it can be classified as three types: linear polarization, circular polarization, elliptical polarization.

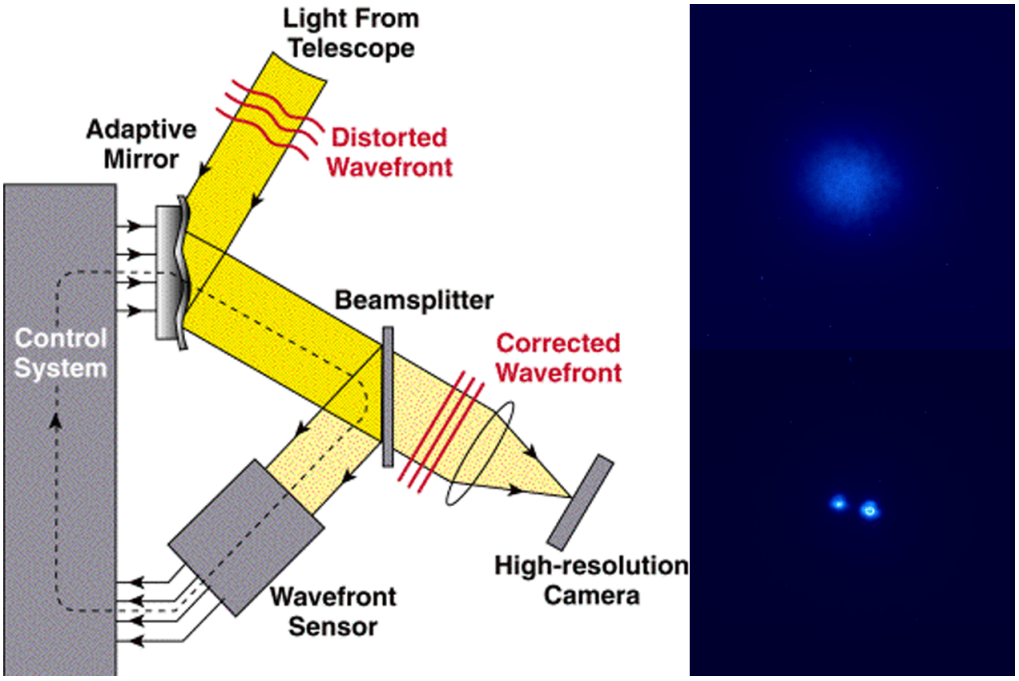

Fig. 1.6 *left*: an example of Adaptive Optics system. The light from telescope is split into two beams by the beamsplitter, and one beam is received by the wavefront sensor. Based on the signals from the wavefront sensor, the control system changes the shape of the deformable adaptive mirror to correct the distorted wavefront. Source: http://lyot.org/img/AOfigure.gif; *right*: the GG Tau A image before (*top*) and after (*bottom*) correction.

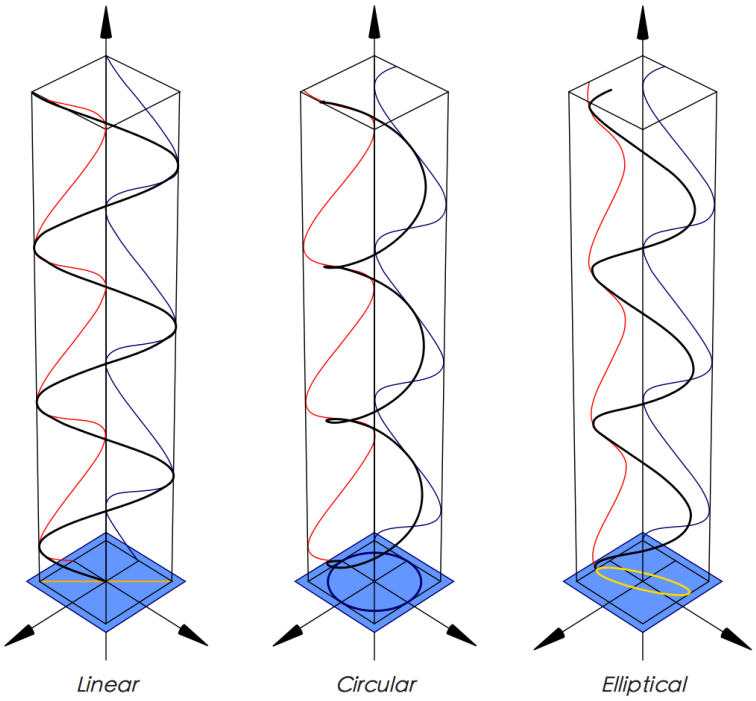

Fig. 1.7 An illustration of different pure polarization types: *left*: linear polarization; *middle*: circular polarization; *right*: elliptical polarization. Source: *Wikimedia Commons*

Light from the protoplanetary disks are considered as partially polarized, which means that the light contains polarized part and non-polarized part. To describe partially polarized light, we need to use Stokes parameters. Consider a transverse wave transferring along the z-axis, the oscillations along the x-axis and y-axis, E_x and E_y, should be like:

$$\begin{aligned} E_x(t) &= E_{x0} cos(\omega t + \varphi_1) \\ E_y(t) &= E_{y0} cos(\omega t + \varphi_2) \end{aligned} \tag{1.2}$$

Here E_{x0}, E_{y0} means the amplitudes of the oscillations along the x-axis and y-axis, ω means the angular frequency, and φ_1 and φ_2 means the phases of the oscillations along the x-axis and y-axis, respectively. The Stokes parameters (I, Q, U, V) are defined as:

$$\begin{aligned} I &= < E_{x0}^2 > + < E_{y0}^2 > \\ Q &= < E_{x0}^2 > - < E_{y0}^2 > \\ U &= < 2E_{x0}E_{y0} cos(\Delta\varphi) > \\ V &= < 2E_{x0}E_{y0} sin(\Delta\varphi) > \end{aligned} \tag{1.3}$$

Here:

$$\Delta\varphi = \varphi_2 - \varphi_1 \tag{1.4}$$

I is the intensity, Q stands for the difference of intensity between the x-axis and y-axis linearly polarized light, U stands for the difference of intensity between the $+45°$ and $-45°$ linear polarization, and V stands for the difference of intensity between left and right circular polarization, "<>" here indicates that the value is time-averaged. $\sqrt{Q^2+U^2+V^2} \leq I$, where the equality indicates the case of totally polarized light.

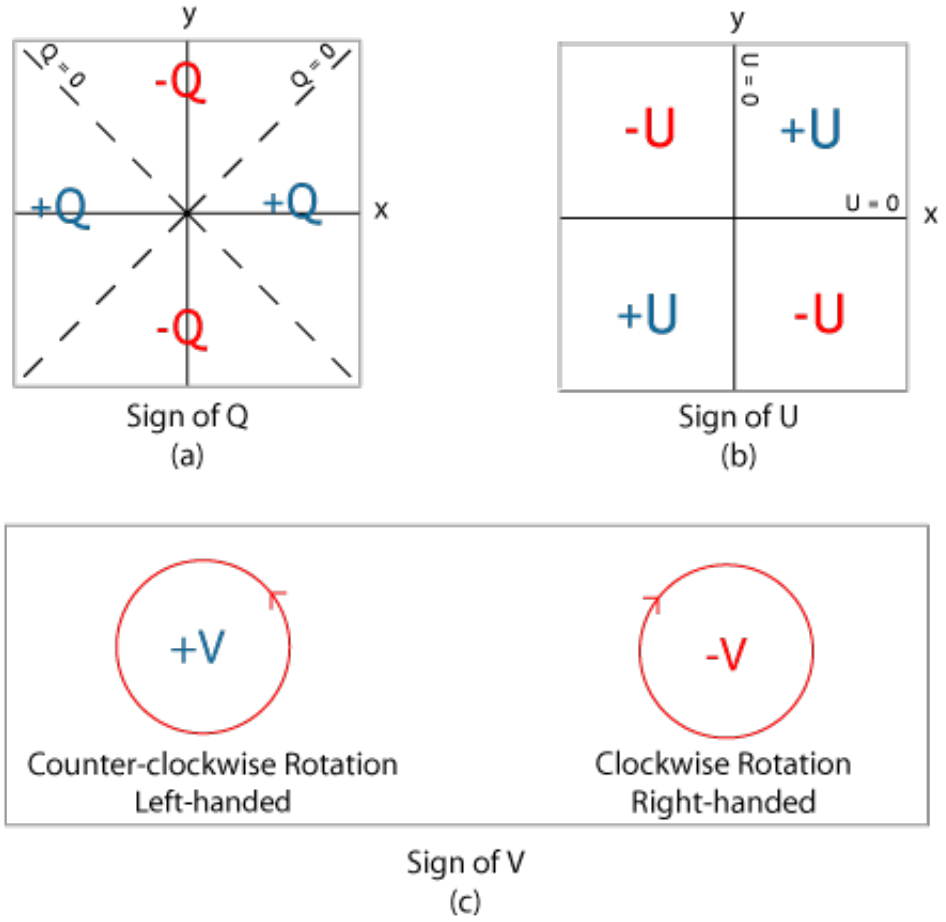

Fig. 1.8 An illustration of Stokes parameters. (a) Stokes Q parameter, showing the difference of intensity between the x-axis and y-axis linear polarization; (b) Stokes U parameter, showing the difference of intensity between $+45°$ and $-45°$ linear polarization (c) Stokes V parameter, showing the difference of intensity between left and right circular polarization Source: *Wikimedia Commons*

Stokes parameters can describe all polarization patterns, including unpolarized, partially polarized, totally polarized light, and can be calibrated by instruments. To calibrate the

Stokes parameters, we need to use a polarimeter. A typical polarimeter consists of a retarder and a polarizer.

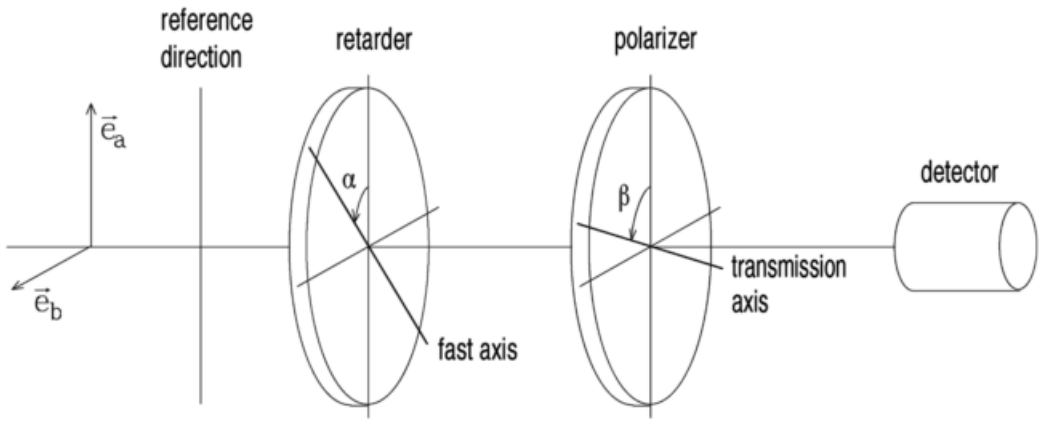

Fig. 1.9 An illustration of Polarimeter. The light needs to pass a retarder and a polarizer to reach a detector. Figure 1.9 in Degl'innocenti and Landolfi [28]

The signals passed a polarimeter will obey the following formula [28]:

$$\begin{aligned} D(\alpha,\beta,\delta) = \frac{1}{2}[I &+ (Qcos2\alpha + Usin2\alpha)cos2(\beta-\alpha) \\ &- (Qsin2\alpha - Ucos2\alpha)sin2(\beta-\alpha)cos\delta \\ &+ Vsin2(\beta-\alpha)sin\delta] \end{aligned} \tag{1.5}$$

here α means the angle between the fast axis of the retarder and the reference direction, β means the angle between the transmission axis of the polarizer and the reference direction, and δ is the phase retardance of the retarder.

Since the light scattered by the disk contains little circular polarization, we only need to calibrate linear polarization, i.e., Stokes Q and U parameters. In this case, we just need to use a half-wave plate ($\delta = \pi$) for the retarder. As for the polarizer, we use a Wollaston prism. Wollaston prism consists of two orthogonal calcite prisms whose optical axes are perpendicular with each other. In this case the incident light will be split into two beams, the horizontal polarized "o" light and the vertical polarized "e" light, and we will see two channels on the detector. This is the standard polarimetry differential imaging mode, or sPDI mode. There is another PDI mode called quad-PDI mode, or qPDI mode. This mode uses a double-Wollaston prism to split the light into four beams to help reduce the saturation radius.

When in PDI observations, the half wave plate will rotate to four different angles, i.e., α =0°, 45°, 22.5°, 67.5°. And considering the properties of Wollaston prism, the light are splitted into two beams of light whose oscillation directions are perpendicular, we can regard

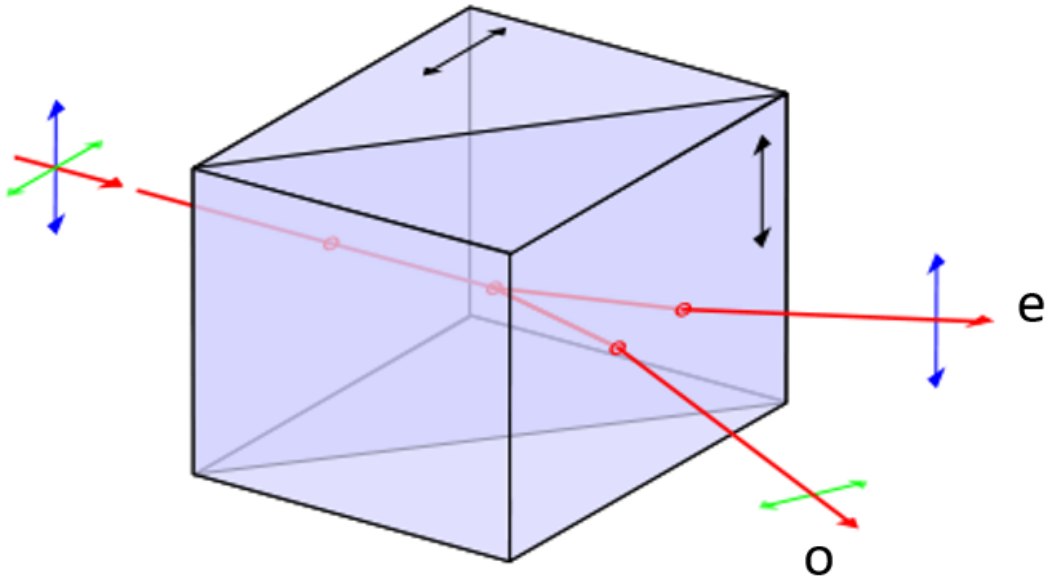

Fig. 1.10 An illustration of Wollaston prism. It will split the light into o-light and e-light with perpendicular polarization directions. Source: *Wikimedia Commons*

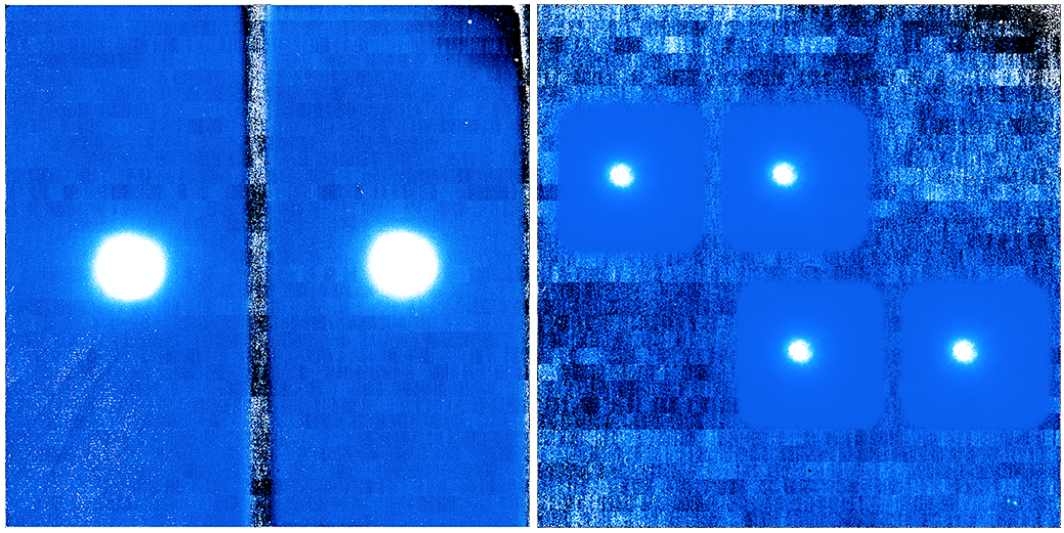

(a) sPDI (b) qPDI

Fig. 1.11 The field of view of PDI mode. (a): sPDI mode, consists of two 2048×1024-pixel channels (about $20''\times10''$); (b): qPDI mode, consists of four 512×512-pixel channels (about $4.''9\times4.''9$).

Table 1.2 Stokes parameters in each channels during observations

$\alpha(^\circ)$	o	e	o-e
0	$\frac{1}{2}(I+Q)$	$\frac{1}{2}(I-Q)$	$+Q$
45	$\frac{1}{2}(I-Q)$	$\frac{1}{2}(I+Q)$	$-Q$
22.5	$\frac{1}{2}(I+U)$	$\frac{1}{2}(I-U)$	$+U$
67.5	$\frac{1}{2}(I-U)$	$\frac{1}{2}(I+U)$	$-U$

o-light as $\beta = 0^\circ$, and e-light as $\beta = 90^\circ$. Using the formula (1.5), we can calculate the Stokes parameters for each channels when the half wave plate rotates to different angles during the observation, as Table 1.2 shows.

From Table 1.2, we can see that by subtracting the e-light channel from o-light channel, we can derive $+Q$, $+U$, $-Q$, and $-U$ parameters. Then by using the formula $Q = ((+Q) - (-Q))/2$, $U = ((+U) - (-U))/2$, we can derive Stokes Q and Stokes U image, and the difference between the two channels can also be eliminated. After that, we can derive the polarized intensity (PI) image by $PI = \sqrt{Q^2 + U^2}$.

The signal-noise ratio (SNR) of the PI image can be calculated from Stokes Q and U images. Since $PI = \sqrt{Q^2 + U^2}$, then the uncertainties N_{PI} in PI image is:

$$N_{PI} = \sqrt{(\frac{\partial PI}{\partial Q} N_Q)^2 + (\frac{\partial PI}{\partial U} N_U)^2} = \frac{\sqrt{Q^2 N_Q^2 + U^2 N_U^2}}{PI} \tag{1.6}$$

here N_Q and U_Q are the error/noise in Stokes Q and U images. Since Stokes Q and Stokes U parameters generally follow a Poisson distribution, then the noise $N = \sqrt{|S|}$, here $|S|$ is the absolute value of signal. Then equation (1.6) can be converted to:

$$N_{PI} = \frac{\sqrt{|Q|^3 + |U|^3}}{PI} \tag{1.7}$$

In polarimetry observations, anything with SNR below 4, i.e., 4σ is suspicious.

Chapter 2

Near-Infrared Imaging Polarimetry of Inner Region of GG Tau A Disk

Part of this chapter has been published as Yang, Y., Hashimoto J., Hayashi S., et al., 2017, The Astronomical Journal, 152, 7.

2.1 Introduction

Many stars in our galaxy form binary or multiple systems. Duchêne and Kraus [33] noted that for solar-type ($0.7M_{\odot}$–$1.3M_{\odot}$) main sequence stars, the multiple frequency can reach 44%. Furthermore, many planets have been found in binary or multiple systems such as τ Boötis Ab [16], Kepler-16 (AB) b [30], and ROXs 42Bb [23].

Roell et al. [111] estimated that at least 12% of planet-hosting stars may be binary or multiple systems, whereas Raghavan et al. [104] estimated this value to be 23%, and Horch et al. [56] very optimistically estimated that approximately 40–50% planet-hosting stars are binary stars. This begs the question of how planets form and evolve in binary or multiple systems. In addition, the proportion of young stars in binary or multiple systems appears to be two times higher that for solar-type field stars [33]. This may imply that stars tend to form from binary or multiple systems. Furthermore, this indicates that even planets discovered around single stars may have been affected by companion stars during their formation and evolution. Therefore, to understand the early stages of the planet formation process, research on planets and disks around binary or multiple systems is necessary.

Previous studies (e.g., Wang et al. [130]) have demonstrated that the efficiency of planet formation in wide-separation ($\gtrsim$100 AU) binaries is not very different from their single star analogs. On the other hand, disks in smaller-separation binaries ($\lesssim$100 AU) may be too

disturbed by the companion's gravity and too short-lived to produce planets [31]. Despite this fact, some planets have been discovered in close binaries. For example, S-type planets, which are planets that orbit around one of the binary stars, have been found in binaries with separations of approximately 20 AU (e.g., γ Cep Ab, Hatzes et al. [50]), and P-type planets, which are planets that orbit around both binary stars, have been found in binaries with separations of approximately 0.22 AU (e.g., Kepler-16 (AB)-b, Doyle et al. [30]). In a census of a star formation region, Kraus et al. [74] determined that although approximately 2/3 of the close binaries with a separation of $\lesssim$ 40 AU lose their disks within approximately 1 Myr, the remainder of approximately 1/3 of the disks appear to experience an evolutionary timescale similar to that of disks around single stars; thus, planets may have opportunities to form in binary systems. These results indicate that some mechanism may help planets form in such close binaries. Some theories suggest that an additional star might have helped the planet formation process, such as changing the orbit of a planet through the Kozai–Lidov mechanism [71, 78], causing the protoplanetary disks to become eccentric by truncating them (e.g., Regály et al. [108]), or opening large gaps in circumbinary disks (e.g., Artymowicz and Lubow [5]). Thus, the planet formation process around binaries could be quite different from and more complicated than that around single stars. To obtain a better understanding of this, it is necessary to investigate disk structures in binaries to determine how the disks in binary systems evolve.

GG Tau is a well-known young multiple star system in the Taurus–Auriga molecular cloud at a distance of approximately 140 pc from the Solar System [64, 80, 127, 128, 126]. This is a double binary system: GG Tau Aa/Ab and GG Tau Ba/Bb. GG Tau A is an eccentric ($e \simeq 0.35$, Beust and Dutrey [10]) T Tauri binary system with an age of approximately 2.3 Myr [96]. It consists of GG Tau Aa ($0.73 M_\odot$) and GG Tau Ab ($0.64 M_\odot$) with a separation of approximately $0.25''$ (35 AU; Kraus and Hillenbrand [72]). In addition, Di Folco et al. [29] reported that GG Tau Ab is a binary with a separation of approximately $0.03''$ (4.2 AU) and a period of approximately 16 yr; thus, this system is actually a triple system, though it may still be regarded as a binary system in observations with $0.07''$ resolution.

The GG Tau A system is noteworthy for its circumbinary ring, which was first discovered by ground-based adaptive optics (AO) imaging [110] and has been observed many times in various wavelengths, e.g., Guilloteau et al. [47] in the millimeter band, Krist et al. [75] in the optical band, and Itoh et al. [58] in the NIR band. Millimeter and submillimeter observations [47, 35] have shown that this ring rotates clockwise and the northern edge is nearest to us. Additionally, a gap has been observed in the northwestern region of the ring; e.g., Silber et al. [117] observed it in 1998 with the Near Infrared Camera and Multi-Object Spectrometer installed on the Hubble Space Telescope (HST/NICMOS), and Krist et al. [76] observed it in

1997 with the Wide Field and Planetary Camera 2 installed on the Hubble Space Telescope (HST/WFPC2). This gap is believed to be a shadow cast by circumstellar materials [75, 58].

Several groups have investigated the disk structure inside the circumbinary ring of GG Tau A. Piétu et al. [99] suggested the possible (2σ) existence of a streamer extending from the northeastern edge of the outer ring to the inner disk based on the observations from the IRAM Plateau de Bure interferometer in a 1.1 mm continuum band. Beck et al. [8] observed the H_2 $v = 1-0$ $S(1)$ emission around the stars using the Gemini North Telescope, arguing that the strong emissions around the disk are likely caused not by X-ray excitation but by shock waves due to an accretion flow in the disk. Dutrey et al. [35] detected a feature in their observations of the gas in CO J=6–5 transition by the Atacama Large Millimeter Array (ALMA) implying the presence of streamers and speculated that the streamer may feed material from the outer region of the disk to a planet, sustaining planet formation. These studies strongly indicate that the region inside the circumbinary disk may not have been cleared yet, but they have not revealed the detailed structure of this region because of their low spatial resolution. Investigating the details inside the circumbinary ring will be quite helpful in improving our understanding of planet formation in this system; thus, it is very important to observe this region around GG Tau A with a higher spatial resolution in the NIR band. In the past studies, high-spatial-resolution NIR observations have helped to reveal the structures around the binary system SR24 [84], and it is thus a promising method for improving our understanding of disk structures.

This chapter discusses the successful observation of the detailed structures inside the circumbinary ring around GG Tau A, which shows a "north arc" structure in the H-band that is believed to be part of a streamer flowing from the circumbinary ring to GG Tau Ab. In Section 2.2, the observation and data reduction processes are introduced. Section 2.3 presents the observation results of GG Tau A. In Section 2.4, we compare the observations made in this study with theory and previous observations. Conclusions are given in Section 2.5.

2.2 Observations and Data reduction

The presently reported observation of GG Tau A was performed on 8 January 2015 Hawaii Standard Time using the Subaru 8.2 m Telescope with the High Contrast Instrument for the Subaru Next Generation Adaptive Optics (HiCIAO [122]) and the adaptive optics (AO) instrument AO188 [51]. This observation was part of the survey program Strategic Explorations of Exoplanets and Disks with Subaru (SEEDS), which began in 2009. This observation employed the quad-polarized differential imaging (qPDI) mode, which uses a double-Wollaston prism to split the light into four 512×512 channels on the detector with

pixel scale of 9.50 mas/pixel. To help reduce the saturated radius, two of these four channels each corresponded to o- and e-polarizations. During this observation, the AO system limited the full width at half maximum of the stellar point spread function to $0.07''$, which is close to the diffraction limit of $0.04''$. In a previous observation of GG Tau A by Itoh et al. [58] in 2011, a mask with a $0.6''$ diameter was used to obscure structures near the stars. To help reveal the inner region of the disk, no mask was used in the present observation. A half-wave plate was used in the observation, and it was rotated among position angles of 0°, 22.5°, 45°, and 67.5° to measure the Stokes parameters. This cycle was repeated 15 times during observation. Ultimately, 60 frames were collected, each with an exposure time of 5 s and 4 coadds. The total integration time was 20 minutes.

The data reduction process was completed using the Image Reduction and Analysis Facility (IRAF) pipeline. Flat field was corrected, and stripes, bad pixels, and distortions were removed. After these steps, the images were first cross-correlated in different channels. The Stokes parameters $+Q$, $+U$, $-Q$, and $-U$ were then obtained by subtracting the e-images from the o-images. Next, these Stokes images were aligned, and the Q and U images were constructed as $Q = ((+Q) - (-Q))/2$, $U = ((+U) - (-U))/2$. The Stokes I image, or intensity image, was derived by averaging the sum of the o- and e- images in all frames. After the instrumental polarization was corrected, a polarized intensity (PI) image was constructed as $PI = \sqrt{U^2 + Q^2}$. Because the PSF reference star was not obtained during the observation, it was difficult to remove the PSF from the Stokes I image, which is actually a mixture of the total intensity image of the disk and the much brighter PSF of the binary. Therefore, the total intensity image as well as the polarization degree image (P image) of the disk could not be derived, and the present discussion will be mainly based on the PI image rather than the P image.

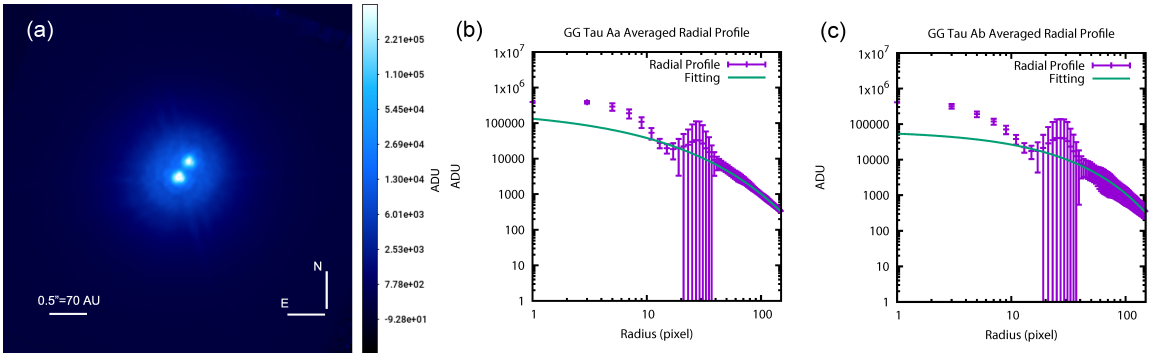

Fig. 2.1 (a) Stokes I image of GG Tau A, taken by Subaru/HiCIAO in H-band. Radial profile (purple) and fitting results (green) for (b) GG Tau Aa and (c) GG Tau Ab. The profiles were fit from 15 to 140 pixels so that only the PSF halo part was fitted. The large uncertainties at approximately 30 pixels were caused by the other star and did not affect the fitting results.

Even with the AO system, residual seeing error still remains after correction. This type of residual called a PSF halo, distorts the final image and its polarization directions, as shown in Figure 2.3 (a). Therefore removal of PSF halo is necessary. The general process of removing the polarized halo which was not fully corrected by the AO system involves rebuilding the polarized halos for Stokes Q and U images then subtracting them from the original images. After that, the corrected image can be used to produce a halo-corrected polarized intensity image.

To create an artificial PSF halo around the binary, the radial brightness profile of the two stars must first be calibrated in the Stokes I image Figure 2.1 (a). The radial profiles of the two stars can be derived using IRAF and Python scripts, and the luminosity L and radius r are then fit by the function

$$L = A\exp(-r^B/C^2), \tag{2.1}$$

where A, B, and C are fitting parameters. The radial profile and fitting results are shown in Figure 2.1 (b) and (c). Considering that only the polarized halos require fitting, the profiles are fit from 15 to 140 pixels to exclude the disturbances from the central Airy disk PSF.

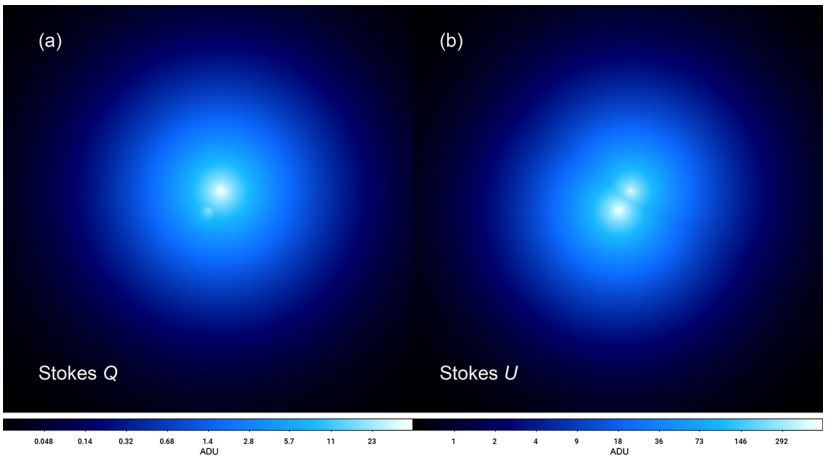

Fig. 2.2 Generated PSF halos for (a) Stokes Q and (b) U images.

After A, B, and C have been determined for each halo, the observed brightness ratio of the halo in the Stokes Q and U images must be compared to that of the Stokes I image to help regenerate the polarized halos in the Stokes Q and U images. For every Stokes image, photometry is conducted by first calibrating the flux with apertures of 15 and 140 pixels for GG Tau Aa and Ab, respectively. Then subtracting the flux within 15 pixels from the flux calibrated within 140 pixels for each star. Thus, the flux of the PSF halo can be obtained for each star in all Stokes images. The ratio of the halo brightness in the Stokes Q and U images

to that of the Stokes I image is then obtained. Based on the fitting and photometry results, the polarized halo for each star can be regenerated in the Stokes Q and U images in the end.

For the case of a single star, the next step is to subtract the generated PSF halo from the original Stokes Q and U images. However, in the case of a binary, an extra step is required to combine the halos of the two companion stars in the Stokes Q and U images. Considering that the halos are generated from the observation results, the PSF halo from the star itself and the effect of the other star are both included in the fitted halos. That is why the two halos cannot be combined by simply adding them together. Here, the maximum values of the two halos were mixed, i.e., for the halo H_a around GG Tau Aa and that H_b around GG Tau Ab, the final combined halo would be $H_c = \max(H_a, H_b)$. The combined halos for the Stokes Q and U images are shown in Figure 2.2. After these combined halos have been obtained, they are subtracted from each of the corresponding original Stokes images to obtain the halo-corrected PI images (Figure 2.3 (b)). In Figure 2.3 (b), it can be seen that the vectors are generally centrosymmetric rather than aligned in one direction, which demonstrates that the vectors were corrected successfully using this method.

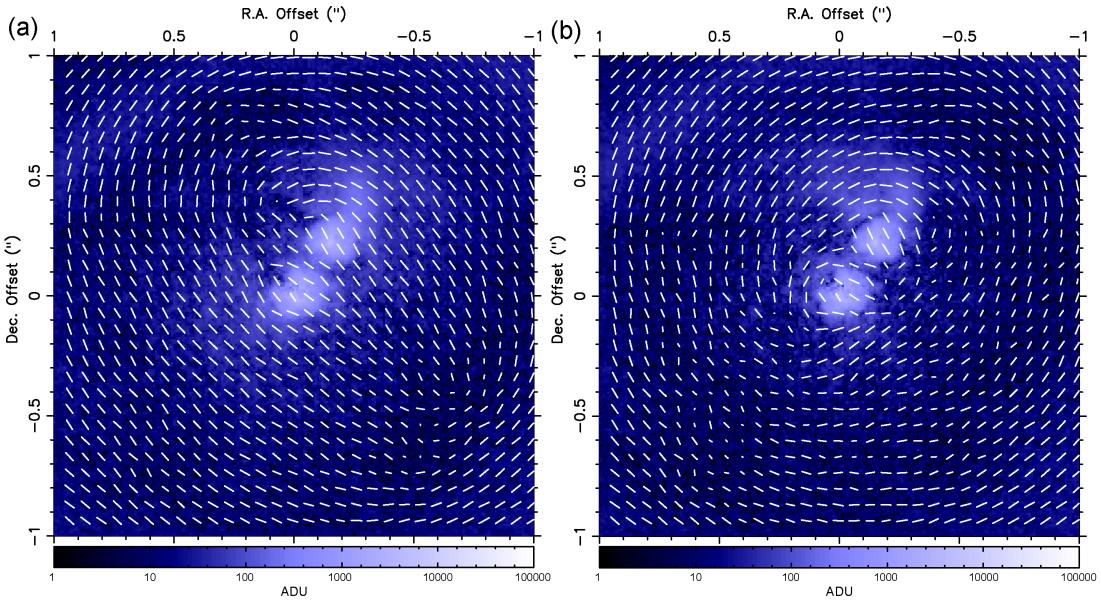

Fig. 2.3 Vector map (a) before and (b) after PSF halo subtraction, showing the $2'' \times 2''$ area of GG Tau A and its disk.

2.3 Results

The *PI* image tracing the light scattered by the dust grains of GG Tau A is shown in Figure 2.4, which provides a wide view of GG Tau A and its disk. The field of view is 512×512 pixels, corresponding to approximately $4.9'' \times 4.9''$. This image shows the circumbinary ring, the two companion stars GG Tau Aa/Ab and some disk structures near them. Polarimetry observation is a powerful method of revealing circumstellar disk structures because it traces the polarized light scattered from the disks. The nonpolarized light from the central stars is subtracted during data reduction. However, it should also be noted that a lack of polarized light does not necessarily mean that there is no scattered light or scattering structures (e.g., Perrin et al. [98]). For the present discussion, the part of the disk inside the circumbinary ring is defined as the "inner region" of the circumbinary disk around GG Tau A.

The separation between the two companion stars was derived as $0.27 \pm 0.01''$, which corresponds to 38 ± 1 AU[1]. The position angle (PA) of GG Tau Aa/Ab binary is $327 \pm 1^\circ$ (measured from north to east). The GG Tau Ab binary reported by Di Folco et al. [29] could not be resolved.

In the *PI* image, the circumbinary ring looks asymmetric. There seem to be offsets among the center of the outer edge ellipse, that of the inner edge ellipse, and the barycenter of the binary. To estimate the basic parameters of the circumbinary ring, we developed a toy model. In this model, we assumed the outer edge of the ring to be circular, the inclination 37°, and the PA 277°, as in the previous observations. In addition, we attributed the barycenter of the binary to be near one of the foci of the inner edge ellipse. The result is shown in Figure 2.4 (b). It was determined that the inner edge can be generally fitted by an ellipse with an eccentricity of approximately 0.2 and there are offsets among the center of the inner edge ellipse, that of the outer edge ellipse, and the barycenter of the GG Tau A binary. The center of the inner edge (yellow cross) is located approximately 15 pixels ($0.14''$ or 20 AU) to the south of the barycenter, which should be near one of the foci of the inner edge (yellow star), and that of the outer ring (red cross) is approximately 25 pixels ($0.24''$ or 33 AU) to the south of the center of the inner edge. This reveals the asymmetric characteristics of the circumbinary ring and that the binary is much closer to the north side of the circumbinary ring.

In addition, some have suggested that the gap in the northwestern edge of the circumbinary ring, which can also be seen in Figure 2.4(a) and (b) as darker areas, is a shadow cast by

[1]The sizes in AU are calculated by assuming that GG Tau A lies at a distance of 140 pc from the Solar System.

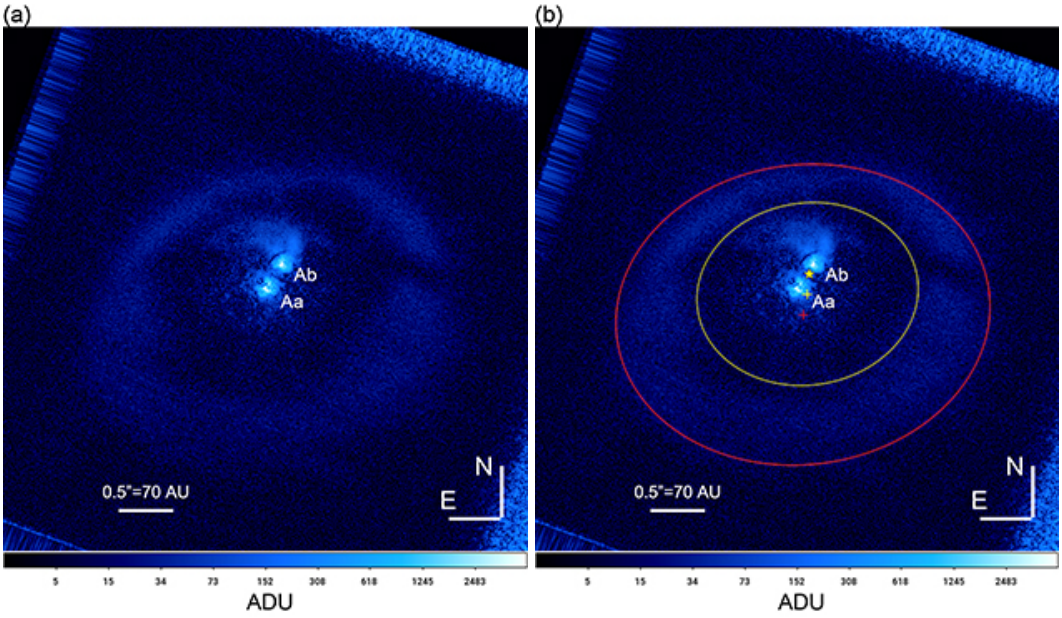

Fig. 2.4 (a): Polarized intensity image (*PI* image) of GG Tau A (512×512 pixels, corresponding to $4.9'' \times 4.9''$), taken by Subaru/HiCIAO in H-band. The rectangle-like structure around the image is an artifact caused by the data reduction process. (b): Comparison between the modeled circumbinary ring and the present observation. The inner and outer edges are shown in yellow and red, respectively. The yellow and red crosses represent the centers of the inner and outer edges, respectively. The yellow star represents one of the foci of the inner edge. Based on the theory, the barycenter of the binary should be near this focus.

some circumstellar materials [75, 58]. However, none of the inner disk structures discovered in this study appear to be responsible for it, and thus the origin of this gap remains unknown.

Both stars in the *PI* image are surrounded by bright nebula-like structures with radii of approximately 0.14″ (20.0 AU) and 0.10″ (13 AU) for GG Tau Aa and GG Tau Ab, respectively. These nebula-like structures look like circumstellar disks around each stars, but they could also be dominated by speckles. To help distinguish between speckles and real disk structures in the inner region, a vector map of the *PI* image was constructed. The fact that some vectors show centrosymmetric characteristics surrounding the central stars implies the presence of real disk structures. It is much more difficult to judge what the noncentrosymmetric vectors imply at this stage; thus, we will leave discussions on such vectors to the future study.

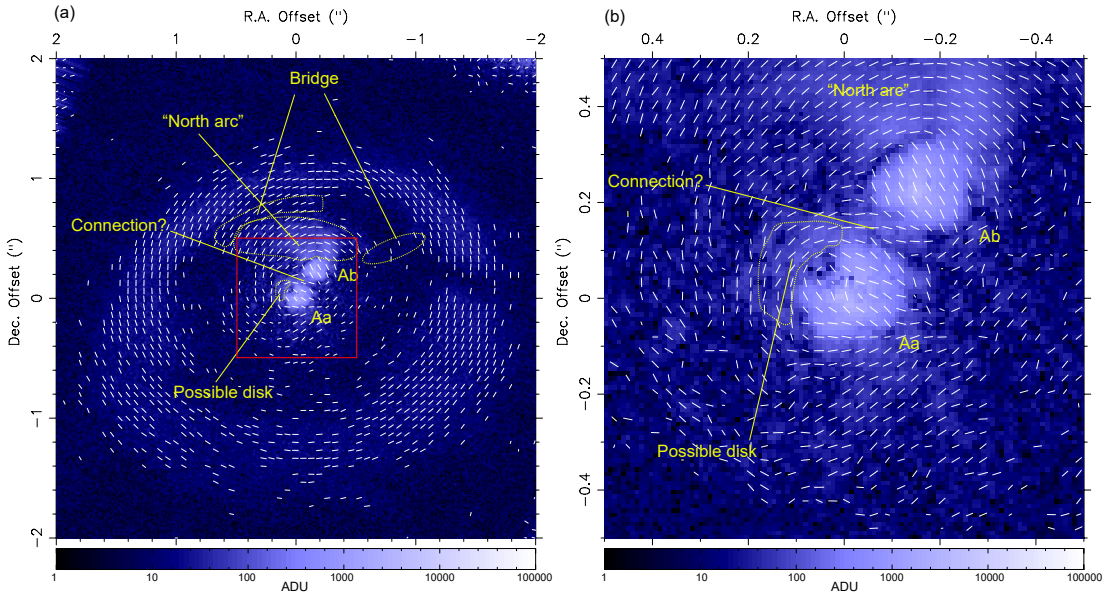

Fig. 2.5 Polarization vector maps of GG Tau A near the central region for the *PI* image with fields of view of (a) $4'' \times 4''$ and (b) $1'' \times 1''$ centered on GG Tau A. (b) is an enlarged view of the area outlined by a red square in (a). The polarization angles $\theta_{\rm p}$ were calculated using the formula $\theta_{\rm p} = 0.5\tan^{-1}(U/Q)$ in bins of (a) 7 and (b) 3 pixels, and only areas brighter than 15 analog-to-digital unit (ADU) counts are drawn. The two bridges described by Itoh et al. [58] are barely observable in this image. In the bright nebular-like structure around GG Tau Aa and Ab, the vectors are clearly not centrosymmetric, implying the presence of speckles. The north arc structure to the north of GG Tau Ab and the structures to the northeast of GG Tau Aa show centrosymmetric characteristics, representing possible real structures.

The vector maps centered on GG Tau Aa with sizes of $4'' \times 4''$ and $1'' \times 1''$ are shown in Figures 2.5 (a) and (b), respectively, where the white bars show the polarization angles (PAs). We calculated PAs θ_p using the formula $\theta_{\rm p} = 0.5\tan^{-1}(U/Q)$ with binned data of 7 and 3

pixels for Figures 2.5(a) and (b), respectively. The errors of the PAs were estimated from the noise of the Stokes Q and U images. The typical error of the PAs was approximately 5° for the circumbinary ring, and that for the inner region of the disk was approximately 3°. The vectors in the bright nebula-like structures around both stars do not show centrosymmetric characteristics, which may indicate that these bright nebular appearances are dominated by speckles.

However, the vectors to the north of GG Tau Ab show a region with obvious centrosymmetry, extending approximately 0.40″ (56 AU) to the north of GG Tau Ab with a signal-to-noise ratio (SNR) of larger than approximately 5σ. The brightest part in this region could have an SNR of approximately 11σ. Here, the SNRs of the *PI* image were calculated from the SNRs of the Stokes Q and U images. Therefore, this area shows a real structure that may correspond to the north arc reported by Krist et al. [76]. We refer it hereafter as "the north arc". Its inner side appears to be close to 0.10″ from GG Tau Ab and to connect the two "bridges" mentioned by Itoh et al. [58], which are barely noticeable in this image. The eastern bridge has an SNR of approximately 4σ, indicating it may be real. On the other hand, the western bridge has an SNR of only approximately 3σ; therefore, the detection of this bridge remains uncertain. In the southern part of the inner disk, such obvious disk structures were not observed. This overall feature suggests that the inner region may be asymmetric.

The vectors outside the bright structures in GG Tau Aa, especially vectors to the northeast of the star, tend to be centrosymmetric, which indicates that part of the disk structures around GG Tau Aa were captured in this image. The outermost boundary appears to extend to approximately 0.20″ (28 AU) in projection. This is slightly larger than but still in fair agreement with the radius of approximately 20 AU previously reported for the circumstellar disk of GG Tau Aa (e.g., 35). No such circumstellar structures are discernible in the present image of GG Tau Ab. Based on the speckle radius of GG Tau Ab, the radius of the disk structure around the GG Tau Ab1/Ab2 binary is constrained to < 13 AU.

The bright structure between the two stars indicated in Figure 2.5 appears to be connected, but the vectors are not centrosymmetric. Considering the possible complexity of the polarization pattern between two stars, it is still unclear whether this structure is real or simply speckles. Observations in other bands could be helpful in improving our understanding of this potential structure.

2.4 Discussions

2.4.1 Binary Orbit

According to Beust and Dutrey [10], the semi-major axis (SMA) of the GG Tau A binary could be either 32 or 62 AU. Strict fitting of the astrometric data yielded an SMA of 32 AU. However, a binary with such a small SMA could not open such a large gap in the circumbinary disk. Another attempt taking into larger error bars of the astrometric data gave SMA = 62 AU that could fit the size of the ring but had a significance of only 3σ. They concluded that the disk and the binary were likely to be coplanar but the astrometric data errors were underestimated. Köhler [66] noted that not only the underestimation of astrometric data errors but also the misalignment of the binary orbit plane and disk could be responsible for the discrepancy between the astrometric data and the ring size.

We compared present binary position with the observation performed by Beck et al. [8] in late 2009, approximately five years prior to the observation considered in this study. The PA was found to have changed by approximately 7° over that time. In the study by Beust and Dutrey [10], both the 32- and 62-AU models have a PA rate of approximately $1.4°/yr$, which is consistent with the present results. However, in this case, the SMA of the binary could not be constrained using only astrometry. Thus, the binary orbit was constrained using the disk structure model. Pelupessy and Zwart [97] developed a formula relating the radius of the density peak in the circumbinary disk to the SMA and eccentricity of the binary orbit:

$$a_{peak} = (3.2 + 2.8 e_{binary}) a_{binary}, \tag{2.2}$$

where e_{binary} and a_{binary} are the eccentricity and SMA of the binary, respectively, and a_{peak} is the radius of the density peak in the disk.

First, we attempted to constrain the SMA from the surface brightness peak and the density peak locations. For both $a_{binary} = 32$ AU and $a_{binary} = 62$ AU (with an eccentricity of $e = 0.35$) the locations of the surface density peak are 130 and 260 AU, respectvitly, using the equation by Pelupessy and Zwart [97]. Both numbers did not coincide with that of the surface brightness peak at 180 AU. The surface brightness and surface density are likely to peak at different radii because the former is sensitive primarily to the disk shape and less sensitive to the density. Therefore we concluded that the surface density peak lies outside the peak of the surface brightness since scattering is likely dominated by the material closest to the inner cavity where the illumination comes directly from the stars. This favors the $a = 62$ AU solution for the binary SMA.

The binary orbit could also affect the circumstellar disk around both stars. In the simulation performed by Regály et al. [108], they determined that for $a_{binary} = 40$ AU and $e = 0.3$, the circumstellar disks around the companion stars should be approximately 13 AU. It is expected that if $a_{binary} = 62$ AU, the disk radius should be larger than 13 AU, whereas if $a_{binary} = 32$ AU, the disk radius is much smaller than 13 AU. In the simulation performed by Nelson and Marzari [91], they demonstrated that a binary with $a_{binary} = 62$ AU and $e = 0.3$ should have a circumstellar disk radius equal to 10 AU, whereas this radius is only 4 AU for $a_{binary} = 32$ AU. In the present observation, a possible disk structure was detected around GG Tau Aa extending to a projected distance of approximately 28 AU, and Dutrey et al. [35] noted that the circumstellar disk should have a radius on the order of approximately 20 AU. Both of these results suggest that GG Tau Aa has a relatively large disk. Although it has not been definitively determined whether the circumbinary ring and the binary are misaligned, the results of the present study indicate that $a_{binary} = 62$ AU is more likely than $a_{binary} = 32$ AU.

In addition, based on the calculation results of Miranda and Lai [88], they suggested that the gap size in a near coplanar circumbinary disk around an equal mass binary is about 2.1-3 times of the binary SMA, considering the gap size of GG Tau A's disk is about 140 AU, the SMA of GG Tau A is about 46-67 AU. Also in the results of Miranda and Lai [88], they suggested that the coplanar circumstellar disks an equal-mass binary are generally 0.2-0.4 times of the binary SMA, considering the disk around GG Tau Aa is about 28 AU, corresponding to SMA 70-140 AU. If combining these two results, the SMA of GG Tau A is around 70 AU, and with a small eccentricity (near zero). This result also suggest that 62 AU is a more possible SMA of GG Tau A.

2.4.2 Structure in the Inner Region

The observations made in this study provided the first high-resolution image of the inner region around GG Tau A. Generally, it appears to be asymmetric. An arc structure was detected north of GG Tau Ab; however, no such large disk-related feature was detected in the southern part. One would expect a binary comprising two stars with almost the same mass have a symmetric disk structures. To better understand the structure in the inner region, we compare the present observations with theory and previous observations, especially regarding CO gas and dust continuum emissions.

Farris et al. [41] calculated the accretion of binary black holes in circular orbits. Because the GG Tau A binary has a mass ratio q of approximately 0.88, its accretion would be similar to the $q = 0.82$ case shown in Figure 3 of Farris et al. [41]. This figure shows that the streamers are asymmetric even though the binary orbit was circular in their simulation. They

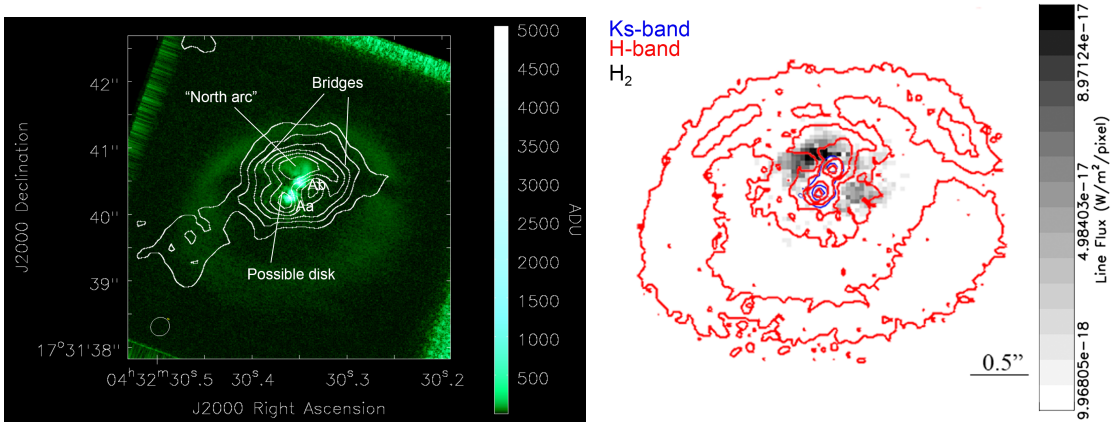

Fig. 2.6 (a): GG Tau A *PI* image (color scale) with ALMA CO 6-5 intensity image (white contour) taken by Dutrey et al. [35] overplotted. Contours are 0.3, 0.4, 0.5, 0.6, 0.7, 0.8 of the peak intensity 3.07 Jy/beam. (b): Gemini North Telescope H_2 emissions taken by Beck et al. [8] with our GG Tau A *PI* image overplotted (red contour). The contours represent 13, 28, 87, 324, 1267, 5020 ADU. Blue contours were the United Kingdom Infrared Telescope K_s band image obtained by Beck et al. [8], representing 0.1, 0.4 and 0.7 times of the peak intensity.

concluded that the asymmetry may be caused by the eccentric shape of the inner edge of a circumbinary disk driven by the binary tides, which lead to the different distances from the circumbinary disk to the binary in different directions. Such asymmetric streamers have also been described by Nelson and Marzari [91], who made simulation of the GG Tau A binary in an orbit with an eccentricity of 0.3. Considering that the north arc appears to connect the northern side of the ring and GG Tau Ab, the north arc may be part of a large streamer extending from the circumbinary ring to the inner disk. As mentioned in Section 3, the circumbinary ring is asymmetric, and the binary is much closer to the north; thus, the streamer from the north is larger than that in the south.

In previous CO J=6–5 observations by Dutrey et al. [35] with ALMA , two asymmetric CO cores were detected in the inner disk; implying possible interfaces of the streamers from the outer ring to the circumstellar disks around both stars. For a detailed comparison, the CO 6–5 image is superimposed on the present *PI* image in Figure 2.6(a). The north arc coincides with the position of the northern CO core observed by Dutrey et al. [35], suggesting that the north arc observed in this study could be part of a streamer observed in the NIR band.

For an advanced investigation, we checked the CO 6–5 velocity map in detail. The analysis of the CO 6–5 velocity field near the northern part of the CO 6–5 core of the inner region performed by Dutrey et al. [35] revealed a large velocity dispersion of approximately

2–2.5 km/s, which is larger than the predicted Keplerian rotation velocity dispersion of 1.2 km/s. This could be further evidence of the existence of the streamer.

We also compared the present observations with the H_2 emission observations by Beck et al. [8], which revealed the temperature distribution in the inner disk. Figure 2.6(b) shows a peak in the H_2 emission represented by the darkest region that partly coincides with the north arc on its southern boundary, indicating a high temperature (approximately 2000 K) in this location. Such high temperatures tend to be the result of shockwaves in the inner disk, which are likely caused by inflows as suggested by Beck et al. [8], whereas the north arc observed in this study is slightly north of the peak of the H_2 emission. The peak of the hydrogen emission is located between the north arc and GG Tau Ab. One simple explanation for this is that the north arc observed in scattered light does not have a very high temperature and the temperature increases only when material begins to drop rapidly to GG Tau Ab.

The CO 6–5 core near the circumstellar disk around GG Tau Aa coincides with the possible disk structure. In the CO J=3–2 map presented by Tang et al. [123], there is one structure extending from GG Tau Aa; thus, part of this possible disk structure could also be part of a streamer feeding the circumstellar disk around GG Tau Aa. This may explain why it is slightly larger than the previously reported disk size. However, the CO 3–2 velocity map does not show clear sign of the material falling into GG Tau Aa, and the velocity field near GG Tau Aa from the CO 6–5 velocity map is too complex to draw a conclusion. Because the resolutions of the CO maps obtained by Tang et al. [123] and Dutrey et al. [35] are relatively low (approximately $0.3''$ and $0.25''$ for the CO 3–2 and 6–5 maps, respectively), a higher-resolution observation may aid the further analysis of the velocity field in this disk.

2.4.3 Planet Formation

Based on the parameters given in Table 3 of Andrews et al. [3] and assuming a gas-to-dust ratio of 100:1, the Toomre Q parameter at disk radius 235 AU is ~ 5. Thus the ring is gravitationally stable, and a planet cannot form here through gravitational instability.

Previous CO (J=6–5, 3–2, and 2–1) images show a hotspot on the southwestern edge of the ring at a radius of approximately 250–260 AU that has a temperature of about 40 K, which is 20 K higher than those in other locations at the same distance from the GG Tau A binary [35, 123]. It has been suggested that this hotspot is a signature of a potential planet. However, we see no corresponding structure in the present *PI* image. The lack of such a structure could be due to a low degree of polarization. The mass of this CO hotspot reported by Tang et al. [123] was only approximately $2M_J$, thus it could be too faint to detect even in a NIR intensity image.

For the circumstellar disks around the binaries, if the mass of the outer disk ($0.15 M_{\odot}$; 36) and the total accretion rate of both stars ($5.1 \times 10^{-8}\, M_{\odot}/\mathrm{yr}$; 8) are taken in account, the circumbinary gas reservoir can sustain the inner disk for at least 3 Myr. Because some planets with similar ages have been discovered so far, such as LkCa 15 b with an age of 2 Myr [73, 113], a duration of 3 Myr could be sufficient for a planet to form.

Radio continuum observations (e.g., Dutrey et al. [35] and Tang et al. [123]) have revealed the presence of large dust structures in the circumstellar disk around GG Tau Aa. Minimum disk mass estimate of GG Tau Aa is approximately $1 M_{\mathrm{J}}$[35], which may not be enough for the formation of a Jupiter-like planet but may be feasible to form a Neptune-like or terrestrial mass planet [103].

The direct detection of the circumstellar disk around GG Tau Ab has not been reported yet. Some studies such as that by Skemer et al. [118], and the presence of streamer to GG Tau Ab, give indirect evidence of the presence of the circumstellar disk. Moreover, because GG Tau Ab itself is a binary, Di Folco et al. [29] has noted that a putative disk associated with Ab would have been tidally truncated. As a result, the disk size around either GG Tau Ab1 or Ab2 must be less than 1/3 of the binary separation of GG Tau Ab, which is approximately 4.2 AU, and its circumbinary disk radius can be no larger than 13 AU. Therefore, the environment around GG Tau Ab binary may be hostile to planet formation.

2.5 Conclusion

Using Subaru/HiCIAO with the AO188 system, a high-spatial-resolution ($0.07''$) image of the circumbinary disk around the GG Tau A binary was successfully obtained. In comparison with previous observations, the present polarimetry observations provide a much more detailed view of the disk structure inside the circumbinary ring. The present results indicate that the circumbinary disk around the binary is asymmetric and the binary is much closer to the northern edge of the ring than to the southern edge. By analyzing the sizes of the ring's inner edge and the circumstellar disk around GG Tau Aa, it was determined that the large semi major axis solution of 62 AU for the binary orbit is more likely than the small semi major axis solution of 32 AU. An arc structure north of GG Tau Ab called the north arc in this paper and a possible circumstellar disk structure around GG Tau Aa were observed inside the circumbinary ring. A comparison of the present observation results with previous observations and theoretical calculations suggests that the north arc may be part of a large streamer extending from the circumbinary ring to GG Tau Ab. Based on previous estimates of the accretion rate and the outer disk mass, the streamer to the circumstellar disk around each star may provide enough material for sub-Jovian planets to form in the disk around GG

Tau Aa. Considering the circumstellar disk around each star, it seems that GG Tau Aa has a better chance to form a Neptune-like or terrestrial planet than GG Tau Ab. This discovery may help reveal one aspect of the formation process of planets located in close binaries such as γ Cep Ab, and it may be helpful in improving our understanding of the planet formation process in binary star systems.

Chapter 3

A High-contrast Polarimetry Observation of T Tau Circumstellar Environment

3.1 Introduction

As a prototype of the large class of T Tauri pre-main sequence stars, T Tau has attracted considerable attention from astronomers studying star and planet formation processes. It is located about 146.7±0.6 pc from us [80] and has an age of about 1–2 Myr [65]. It is actually a triple system, consisting of the north single star T Tau N and the south binary T Tau Sa/Sb. T Tau N, which has a mass of about 1.95 $M_{\odot}$ [67], is believed to be a Class II young stellar object (YSO) [45, 81]. T Tau S, located about 0.7″ south from T Tau N, was first discovered by Dyck et al. [37] and could be a Class I YSO [45, 81]. Koresko [68] discovered that T Tau S is actually a binary Sa/Sb with a separation about 0.1″, with masses of 2.12±0.10 $M_{\odot}$ for Sa and 0.53±0.06 $M_{\odot}$ for Sb [67]. The orbit of T Tau Sa/Sb has a semi-major axis of $12.5^{+0.6}_{-0.3}$ AU and an eccentricity of $0.56^{+0.07}_{-0.09}$, while the orbit of T Tau N-S system is not well constrained; it is likely to have a semi-major axis of 430^{+790}_{-250} AU and an eccentricity of $0.7^{+0.2}_{-0.4}$ [67].

Although T Tau has been studied extensively for a long time, there are still some important issues needed to be resolved in this system. First issue is the circumstellar disk structures in this system. Akeson et al. [2] in their 3-mm continuum observations, estimated that T Tau N might have a nearly face-on disk with an outer radius of about 41 AU, but their beam-size (0.″59 × 0.″39) was not sufficient to reveal the details. Other researches, like Gustafsson et al. [49] gave an estimation of 85–100 AU, corresponding to about 0.″6–0.″7, based on a spectral

energy distribution (SED) simulation, and [100] derived 110-AU size based on their CN 5-4 line observations. T Tau S binary has extinction ($A_V = 15$, Duchêne et al. [32]) much higher than that of T Tau N ($A_V = 1.95$, Kenyon and Hartmann [65]). This difference is attributed to a compact edge-on circumbinary disk around T Tau S [32], or the blockage of the light due to the circumstellar disk around T Tau N [54, 9]. Besides the possible edge-on circumbinary disk, T Tau Sa may be surrounded by an edge-on disk of radius 2–3 AU [32], and oriented north–south, while the circumstellar disk around T Tau Sb may not be far from face-on, based on the middle infrared interferometry observations and SED simulations [106]. So far, the discussion of the disk structures in this system are mainly based on the indirect measurement, therefore, a direct view of the disks in this system with sufficiently high resolution is crucial in the understandings of the disk system.

Second is about the sources of its outflows. Several outflows have been reported in previous observations of this system. Bohm and Solf [13] observed T Tau with a spectrograph mounted on the 2.2-m telescope at the Calar Alto Observatory and reported the discovery of an east–west outflow (hereafter, the E-W outflow) and a southeast–northwest outflow (hereafter, the northwest outflow) from this system. But it is still under debate which stars trigger which outflow. Some research, e.g., Bohm and Solf [13] and Gustafsson et al. [48], attributed T Tau N to the E-W outflow and T Tau S to the northwest outflow, but Ratzka et al. [106] claimed that T Tau S should be responsible for the E-W outflow. In addition, Gustafsson et al. [48] suggested another southwest outflow coming from T Tau Sb based on near infrared hydrogen emission observations. Kasper et al. [61] also detected a coil-like structure extending to the southwest of the T Tau system in their multi-band near-infrared high-contrast imaging study. This structure can be attributed to a precessing outflow, but it is still unknown whether this originates from T Tau N or S. Identification of these outflow features will be beneficial for learning the evolution of the stars in the multiple system.

Near infrared high-contrast polarimetry imaging is sensitive to the disk and envelope structures around the young binaries, and can reach a spatial resolution smaller than $0.''1$. It has helped resolved some protoplanetary disks (e.g., Oh et al. [94]), and Murakawa [89] ever simulated the polarized image of young stellar objects with bipolar outflow cavities, showing that for edge-on disks with outflow cavities, the vectors near the disk plane tend to be aligned with the disk. Therefore, through polarimetry imaging it is possible to detect the outflow cavity structures from the directions of the vectors, and distinguish the disk and envelope.

In this paper, we will introduce the results of near infrared high contrast polarimetry observations of the T Tau system. Section 3.2 presents the observations and data reduction methods. In Section 3.3, the observation results are introduced. Section 3.4 contains

discussions of circumstellar disks and outflows based on the observation results. In Section 3.5, a conclusion is made.

3.2 Observations and Data reductions

Observations of T Tau, part of the Strategic Explorations of Exoplanets and Disks with Subaru (SEEDS) survey started in 2009, was conducted on January 8th 2015, Hawaii Standard Time, using the High Contrast Instrument for the Subaru Next Generation Adaptive Optics (HiCIAO, Tamura et al. [122]) and the Adaptive Optics (AO) system AO188 [51] mounted on the 8.2-m Subaru Telescope. This observation was in H-band, and the quad-polarized differential imaging (qPDI) mode was used in this observation. In this mode, a double-Wollaston prism is used to split the incident light into four 512×512-pixel channels, corresponding to two o-polarization and two e-polarization channels. The detector has a pixel scale of 9.50 mas pixel^{-1}, and the AO system helps to limit the full width at half maximum (FWHM) of the stellar point-spread function (PSF) to 0.07″. To calibrate the Stokes parameters, a half-wave plate was rotated among four angles: 0°, 45°, 22.5°, and 67.5°. Finally 36 frames, each with an exposure time of 5 seconds and four coadds, were collected, corresponding to a total integration time of 12 minutes.

The data were reduced using the Image Reduction and Analysis Facility (IRAF) pipeline. Generally the reduction steps include correction of stripes and the flat field, removal of bad pixels and distortions, and generation of a polarized intensity (PI) image. To obtain the PI image, the Stokes $+Q$, $+U$, $-Q$, and $-U$ images were first obtained by subtracting the e-images from the o-images, and then the formulas $Q = ((+Q) - (-Q)/2$ and $U = ((+U) - (-U))/2$ were used to construct the Stokes Q and Stokes U images. After correcting the instrumental polarization, the PI image could be obtained from the Stokes Q and U images using $PI = \sqrt{Q^2 + U^2}$. Through this reduction process the unpolarized light from the stars is removed, leaving only the polarized light from the circumstellar disk or envelopes. The Stokes I image, or intensity image, which contains both polarized and unpolarized light, was obtained by averaging the sum of the o- and e-images in all frames.

3.3 Results

The PI image of T Tau is in Figure 3.1, which shows an area of about $4.''9 \times 4.''9$ around this triple star system. This is one of the highest resolution polarization images of T Tau ever made and has revealed a number of new structures not previously reported before. All three stars in this system, T Tau N and T Tau Sa/Sb, as well as the nebula-like structures

surrounding them, can be seen in this PI image. We measured the distance between T Tau Sa and Sb to be about $0.10 \pm 0.''01$, and their position angle to be about $342^\circ \pm 1^\circ$ (measured from north to east). These results are consistent with those obtained on December 2014 and January 2015 by Köhler et al. [67], which indicated that the T Tau Sa/Sb system has a separation of $0.11''$ and a position angle of about 345° in the Brγ and Ks bands. T Tau N is saturated within about $0.1''$. Even though the accurate determination of the stellar position is not straightforward, the circular shape of the saturation allows us to have reasonable estimate of its central location with a $0.''01$. Using the center of the saturated circle as the position of T Tau N with a $0.01''$ uncertainty, the distance between T Tau N and Sa is estimated to be $0.68 \pm 0.01''$, consistent with the result of Köhler et al. [67] on December 2014 ($0.69''$) in the Brγ band.

Since the light scattered by the dust around the stars is polarized, while the light directly from the stars is non-polarized, polarimetry observations readily resolve the circumstellar disks and envelopes near the stars. There are several petal-like nebular structures that appear to extend from the T Tau stars, nearly filling the whole field of view. The polarization vector maps of this system are shown in Figure 3.2. The vectors show the polarization position angles θ_p, which are calculated using the formula $\theta_p = 0.5\tan^{-1}(U/Q)$. It can be seen that the vectors overplotted on these structures are centrosymmetric around either T Tau Sa/Sb or T Tau N, implying that they are real structures associated with these point sources. After comparing them with the results of previous observations, these surrounding structures are believed to be the inner part of the envelopes surrounding the triple system, as suggested by Mayama et al. [85], as well as the circumstellar disk around T Tau N and the circumbinary disk around T Tau S. A detailed discussion will be presented in Section 3.4.1.

There are some dark regions in the PI image, indicating these areas lack reflected polarized light, but it does not necessarily mean that there are no scattered light or scattering structures (e.g., Perrin et al. [98]). There is a clear large hole in the northwest with an opening angle of about 40° from T Tau N. In a J-band T Tau image obtained by the Canada France Hawaii Telescope (CFHT) [109][1], there is also a dark region located in the northwest of the nebular structure, but considering this data is too old, we hope future observations can bring more evidence about it. Also, in the eastern area there are two clear dark lines at position angles of 50° and 100°, which have never been reported in any previous observations. There are also dark regions in the southern and western areas, the south area is about $1.''8$ from T Tau N, while the western one is about $2.''2$ from T Tau N. A comparison with the H-band image by Mayama et al. [85], the southern and western boundaries of the nebular structures they

[1] A false color image is viewable at: http://www.cfht.hawaii.edu/Science/Astros/Imageofweek/ciw290500.html

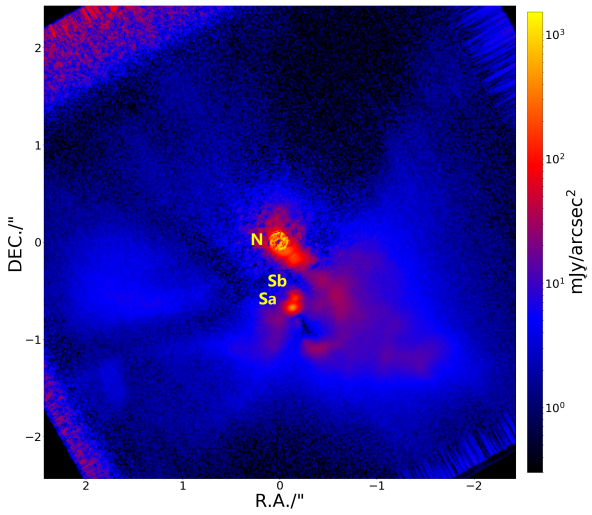

(a)

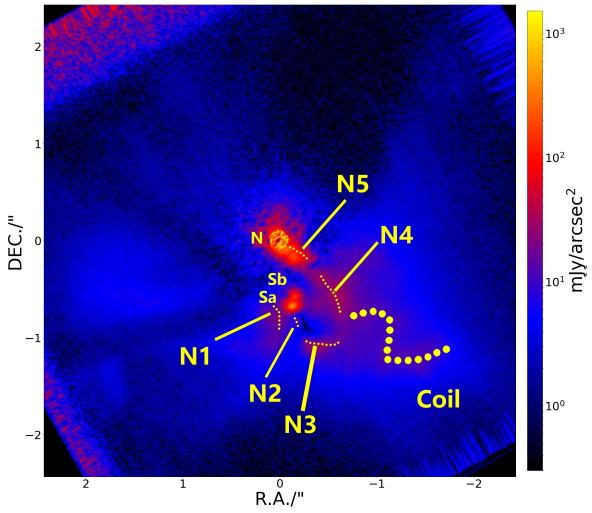

(b)

Fig. 3.1 a: PI image of T Tau, taken by Subaru/HiCIAO in H-band; b: same as (a) but with outflow-related structures labeled.

Table 3.1 Comparison of outflow structures

This paper	Herbst et al. [52]	Gustafsson et al. [48]	Kasper et al. [61]
N1	C4	1a/b, 2	R1
N2	–	–	R2
N3	C3	3	R3
N4	C1, C2	5, 6	R4

detected in H-band are about $2''$ from T Tau N, generally consistent with our results. This suggest that these dark regions could represent the boundaries of the envelope.

In the nebular structures, especially the southwestern area, there are some complicated structures shown in red. For clarification, they are labeled N1–N5 and “coil" in Figure 3.1 (b). To help understand what these structures are, we made detailed comparisons with previous observations, including the multi-band (J, H, K, and several hydrogen emission lines) observations in 2014 and 2015 using VLT/SPHERE-IRDIS, IRDIFS [61], the H_2 $v = 1-0$ $S(1)$ emission line observations performed in 2004 using VLT/SINFONI [48], and the H_2 $v = 1-0$ $S(1)$ emission line observations using VLT/NACO with a Fabry–Perot interferometer [52]. The comparisons are done by carefully overlapping their images on our image, matching the positions of stars (for T Tau S, we use the barycenter of them as reference) and scales, to see the differences of the structures. A brief summary of the comparison results is given in Table 3.1.

In our PI image, the N1 structure is associated with T Tau S, and extending to about $0.''5$ southeast from T Tau Sa. Its position is near the R1 structure reported by Kasper et al. [61], the 1 and 2 structure reported by Gustafsson et al. [48], and the C4 structure reported by Herbst et al. [52].

The position of the N2 structure appears to match the position of the R2 structure reported by Kasper et al. [61], but in our H-band image it looks much shorter (about $0.''1$) than the R2 in the J band image of Kasper et al. [61] (about $0.''25$). N3 structure is about $0.''4$ from T Tau Sa, and has a length of about $0.''4$. Its position also overlaps well with the position of the R3 structure in the J-band data of Kasper et al. [61]. It is just about $0.''2$ below structure 3 reported by Gustafsson et al. [48] and the C3 structure reported by Herbst et al. [52].

For the N4 structure, in our image it is more extended: its brightest part (shown in dashed line) has a length of about $0.''5$, and width of about $0.''2$. This feature covers the positions of the R4 structure reported by Kasper et al. [61], structures 5 and 6 reported by Gustafsson et al. [48], the C1 and C2 structures reported by Herbst et al. [52], and the “N1" knot-like structure (hereafter “knot") reported by Saucedo et al. [114] based on their HST/STIS Lyα observation. Also, it seems to be connected with N3, N5 and the coil in our image.

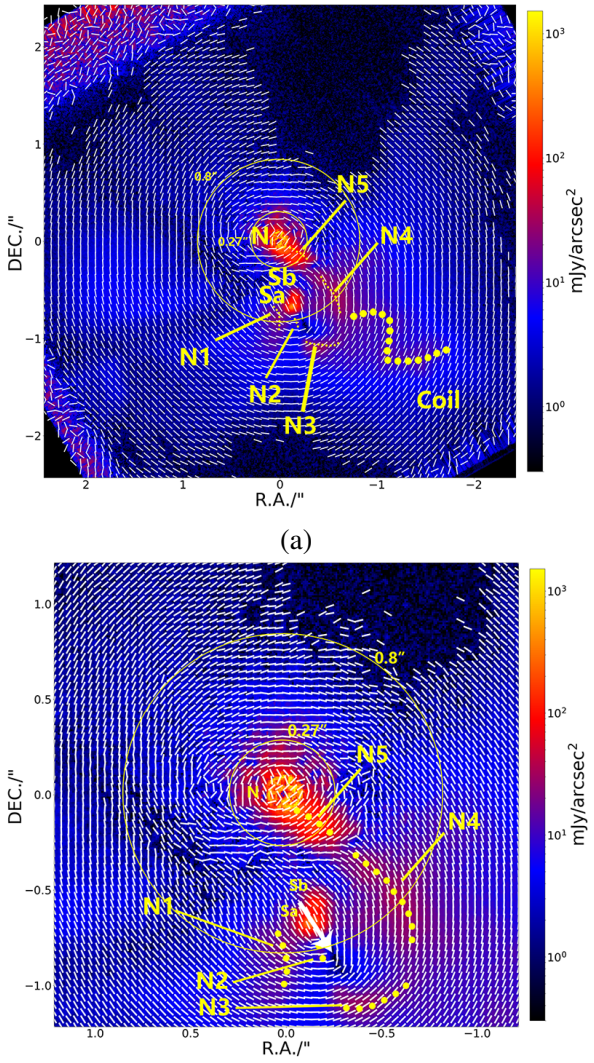

Fig. 3.2 a: PI image of T Tau with polarization vector map overplotted, the vectors are calculated using the formula $\theta_p = 0.5tan^{-1}(U/Q)$ in bins of 8 pixels; b: the central $2'' \times 2''$ region of (a), while the vectors are calculated in bins of 4 pixels. Only the areas with signal-noise ratio larger than 4 are overplotted with vectors.

N5 appears to start at T Tau N and extends to about 0.″4, or 59 AU and PA ∼220° from the star T Tau N. This structure does not have any counterparts reported in previous observations, hence it is a newly detected structure. Although it looks like to be connected with N4, the polarization vectors overplotted on N5 are centrosymmetric with respect to T Tau N, while the vectors for N4 are centrosymmetric with respect to T Tau S. This implies that N5 and N4 are illuminated by different sources, and could be different structures. Ray et al. [107] suggested a structure T Tau R near T Tau N, and Csépány et al. [22] reported a tentative object 144 milliarcseconds south of T Tau N. The position of N5 does not fit the object reported by Csépány et al. [22]. If T Tau R is an object orbiting T Tau N, its position angle should have changed from about 44° to about 240° over the past 22 years, considering its location to be 0″.3 or 44 AU from T Tau N. As a result, N5 is also unlikely to be related to T Tau R. In addition, the vectors overplotted on N5 surround only T Tau N, and thus another luminous object near it can be excluded. Therefore, we conclude that N5 could be part of the circumstellar disk around T Tau N.

The coil structure, first reported by Kasper et al. [61], is clearly seen in our PI image. Its appearance is similar to the J-band structure observed by Kasper et al. [61]. In our image, it looks like to connect with N4 structure, and extends to about 2.″1, or 294 AU, with position angle about 230° from T Tau N. The T Tau NW structure, which was reported by Herbst et al. [52] and could be related to the southeast-northwest outflow, is not found in our image. After comparing the results of Kasper et al. [61], it is likely that this structure is just at the northwestern edge of our field of view so that it cannot be seen in our image.

3.4 Discussions

3.4.1 Circumstellar Disks

In this section, we focus on the circumstellar disks in the T Tau system. Akeson et al. [2] reported that T Tau N might have a nearly face-on disk with an outer radius of about 41 AU, and previous SED fitting [49] and CN line observations (e.g., Podio et al. [100]) suggested that it has a circumstellar disk of about 100 AU. The disk of this scale should be able to be detected within the field view of our observation, although it is not easy to distinguish from the envelope. For the structures around T Tau N, the structures close to 0.11″ (16 AU) may correspond to the previously reported circumstellar disks.

Considering the inner boundary of the “hole" to the northwest of T Tau N is about 0.″8, or 117 AU, its circumstellar disk should not exceed it. However, for the south, from the vector map in Figure 3.2 it can be seen that only the vectors with distances smaller than

$\sim$0.″27 or 40 AU are centrosymmetric with respect to T Tau N. As described in Section 3.3, N4 and N5 could be independent structures, and structure N5 could be related to T Tau N, because the vectors on it is centrosymmetric with respect to T Tau N. Even if N5 is part of its disk, its outer size will be only about 59 AU. It could be a little strange that the disk is such asymmetric. One possible explanation is that the light from T Tau S and its surroundings is strong enough to penetrate the disk around T Tau N, and T Tau N contributes part of the extinctions of T Tau S.

In addition, considering the best orbital parameters derived by Köhler et al. [67], namely that the N-S orbit has a semi-major axis of about 430 AU and an eccentricity about 0.7, its periastron distance is about 130 AU. Regály et al. [108] simulated a binary system with a semi-major axis of 40 AU and an eccentricity of 0.5, and found that the circumprimary disk around one of the stars is about 10 AU, just half of its orbit periastron distance. In this case, a disk with about 117 AU seems too large for this periastron distance. The most possible explanation is that the orbital parameter Köhler et al. [67] derived is still not accurate, like the semi-major axis of T Tau N-S orbit is 430^{+790}_{-250} AU and eccentricity of $0.7^{+0.2}_{-0.4}$, 430 AU and 0.7 may not be the best solution, in this case the periastron distance will be at a range of 18 (for semi-major axis 180 AU and eccentricity 0.9) to 854 AU (for semi-major axis 1220 AU and eccentricity 0.3), corresponding to possible disk size about 9-427 AU. Future observations are still needed to constrain the orbit of T Tau N-S. While the projected distance of T Tau N and S is about 0.″64, or 91 AU, and we expect that a periastron distance suitable for the protoplanetary disk should be 2 times more larger than the disk size, thus the orbit plane of T Tau N-S should be very inclined ($> 60^\circ$) relative to the sky plane.

For T Tau S, some vectors in the southeast and northwest show centrosymmetric characteristics, whereas others such as those in the northeast appear to be aligned in one direction with position angles about 210° but still have some centrosymmetric characteristics, like the white arrow in Figure 3.2 (b) shows. This aligned centrosymmetry is consistent with the presence of a “polarization disk" (e.g., Tamura et al. [121], Murakawa [89]), and is considered to be a result of multiple scattering in dense regions of the disk. The light is scattered multiple times in the optically thick disk, but it is scattered less in the optically thin region, like the bipolar outflow cavities. According to the simulation results of Murakawa [89], the vectors near the disk plane seem to be aligned with the disk’s orientation, but the vectors in other areas, such as the outflow cavities, will still be centrosymmetric, as the light in those regions may only be scattered once. Considering that T Tau S itself is a Class I object, this gives a reasonable explanation. Also, an optically thick inclined disk will cause a large extinction, which is consistent with previous findings that T Tau S has a very large extinction. The rough range of the “polarization disk" is consistent with the real disk size as Murakawa

[89] suggested, so based on this we estimate that the disk should have a radius of about 0.3″, or 44 AU. The actual inclination of this circumbinary disk is a little hard to estimate from just the vector map, while from the simulation derived by Murakawa [89], the aligned vectors near the disk plane first appeared in their result of H=0.3, α_{max}=0.25μm, θ_{inc}=60°, in which they used a small maximum dust size α_{max}. Considering the actual maximum dust size in the disk around T Tau S could be larger, in this case its inclination should also be larger to make the vectors aligned with the disk. Therefore, it seems that its inclination should at least larger than 60°. We hope future ALMA observation of the gas velocity around it could give a more accurate result.

Considering that T Tau S is a binary with a semi-major axis of about 13 AU, as Köhler et al. [67] suggested, it should open a central gap in the circumbinary disk. From the simulation results of Artymowicz and Lubow [5] (Table 3 in their paper), a binary with mass ratio of 3:7 and an orbital eccentricity of 0.7 should open a gap with a size about 3.1 times of its semi-major axis. Therefore, for T Tau S whose mass ratio is about 1:4, the gap size is estimated to be about 30–40 AU, which would not allow much space for the circumbinary disk. While our observations shows that material surrounds the binary, there is no evidence of gap clearance. It could be the case that this Class I object has not had enough time to clear its surroundings or inflow has delayed its clearance. But it can be simply explained by the theory that the gap opened in an inclined disk is smaller than a coplanar one (e.g., Miranda and Lai [88]). We will make a discussion in Chapter 5. In addition, Köhler et al. [67] suggested that the inclination of T Tau Sa-Sb orbit is about 20°, so it is nearly face-on, but this binary system holds a nearly edge-on circumbinary disk, which means that the circumbinary disk is largely misaligned with the binary's orbit (at least 40°). This leaves the problem that how this kind of circumbinary disk forms. Some research (e.g., Martin and Lubow [83]) suggested that binary can truncate the disk, make the inner disk become misaligned with the outer disk. This made us think that maybe T Tau S also did the same thing to its surroundings. However, the simulation of Martin and Lubow [83] is focused on normal protoplanetary disks, i.e., Class II objects, it is still unknown that if this effect will happen on Class I object like T Tau S. Future theory and simulation work may help solve this problem.

3.4.2 Outflow

In this section, we briefly analysis the structures associated with the outflows. As mentioned in Section 3.4.1, N5 looks like to be part of the circumstellar disk around T Tau N. The other structures, N1–N4, as well as the coil, could be related to the outflows in this system. For the T Tau S system, as discussed in Section 3.4.1, it has a nearly edge-on disk

Table 3.2 Summary of the outflows

Star	Structure	Outflow
T Tau S	N1,N4	E-W
T Tau S	N2,N3	South
T Tau S	Coil	Southwest
T Tau N	e.g., Herbst et al. [52]	Northwest

oriented about 210°, and N1 and N4 just locate at its opposite sides. Therefore, N1 and N4 are likely to represent two opposite outflow cavities of T Tau S.

Based on the simulation results reported by Murakawa [89], the direction of the aligned vectors should be generally perpendicular to the direction of the bipolar outflow cavity. Therefore, from the vector map, we can estimate the position angles of the outflow cavities as about 120° and 300°. Eislöffel and Mundt [39] derived the tangential velocity position angle for HH 155, an object located $\sim 30''$ west of T Tau and believed to be caused by the E-W outflow, to be about 305°. Therefore, T Tau S is the most likely source responsible for the E-W outflow. In addition, Kasper et al. [61] reported a “T Tau SE" structure in their H_2 image pointing from T Tau S to southeast with position angle of 119° (Figure 8 in their paper), even though the signal-to-noise ratio was too low to confirm its presence. We notice that the position angle of T Tau SE is close to the position angle of the outflow cavities we derived, so this structure could be related to the outflow from the binary and it could be another evidence of our interpretation.

Gustafsson et al. [48] suggested that their structure 3 could represent a southwest outflow, which we here refer to as a “south" outflow, to distinguish the southwest outflow corresponding to the coil. Since our N2 and N3 structures are located near it, their connection to the outflow is readily implied. For the coil, as Kasper et al. [61] suggested, it is likely to be a precessing outflow, but its origin remains a mystery. There have been no reports about this structure before Kasper et al. [61]. One possible related report was a “bow" structure mentioned by Gustafsson et al. [48]. Since it is located in the envelope around T Tau S, we suggest that the coil is more likely to be related to the T Tau S system. There are then three outflows that could be related to T Tau S; however, up till now only two stars have been detected in this system. A simple hypothesis is that there is yet another companion star that has not been detected. Another possibility is that some structures, such as N2 and N3, are not caused by the outflow but by an inflow. Future observations, especially high-resolution spectroscopy observations, as well as the high resolution CO gas emission line observations like ALMA, will help address this problem. In addition, the T Tau NW structure is possibly located at the northwest edge of the field of view near the big hole, so we suggest that this

hole is much likely to be caused by the northwest outflow. Since the polarization vectors for the envelope structures near the hole are generally centrosymmetric with respect to T Tau N, the remaining northwest outflow is likely to be related to T Tau N.

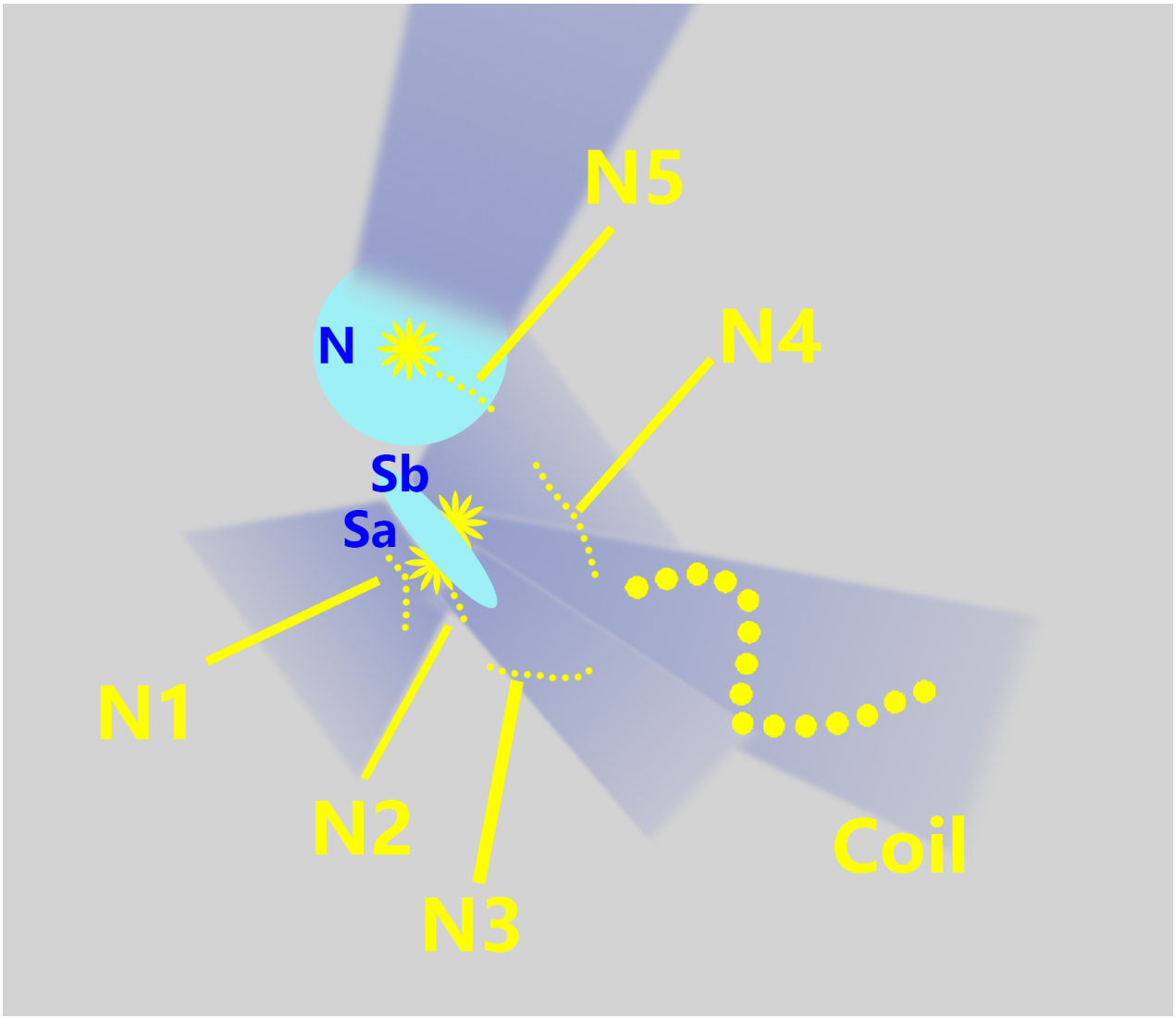

Fig. 3.3 Illustration of suggested T Tau surrounding structures. The three stars are believed to be surrounded by envelopes (gray), and there are some possible outflows from this system (blue). In addition, both the T Tau N and T Tau S systems may contain disks (light blue).

3.5 Conclusion

Using the HiCIAO instrument mounted on the Subaru Telescope, we successfully resolved nearby structures around the T Tau triple star system, and give new insights about the disks

and outflows in this system. From the PI image, we found out that this triple system is surrounded by petal-like envelopes, and some structures found in these envelopes could be associated to outflows from the stars. Based on the vector map, we suggest that the disk of T Tau N is no larger than $0.''8$, or 117 AU in the north and east, and at least has size of about $0.''27$ or 40 AU in the south, also a new structure N5 extends to about 59 AU from T Tau N is discovered, and could be part of the disk around T Tau N. As for T Tau S, the vector map implies that it holds a highly inclined disk with radius about 44 AU with position angle about 30°. Considering the semi-major axis and eccentricity of T Tau Sa-Sb orbit, there is not much room for the disk if the possible gap size of 30-40 AU is considered. It could be explained that the gap opened in the inclined disk is smaller than a coplanar one, and observing gap in an inclined disk like T Tau S could be hard.

We also try to find out the sources of previously discovered outflows. We believe that T Tau S should trigger the famous E-W outflow, because it has a nearly north-south circumbinary disk, and the outflow related structures N1 and N4 just locate at the opposite places of it. Since the coil is found in the envelope around T Tau S, we suggest that it is more likely to be triggered by T Tau S rather than T Tau N. The N2 and N3 structures look like to represent an outflow extending to the south, but in this case there should be one more star undetected in T Tau S system. Finally, since the existence of the large hole to the northwest of T Tau N, we suggest that the SE-NW outflow could be related to it.

Chapter 4

Subaru/HiCIAO Observations of FS Tau A and Coku Tau 4

4.1 Introduction

In Chapter 2 and Chapter 3, we have introduced two young binary systems with disk structures. In this Chapter, we will briefly introduce two more binary targets observed in SEEDS survey: FS Tau A and Coku Tau 4, both targets locates at about 140 pc from us in the Taurus star formation region[64, 80, 127, 128, 126].

FS Tau is a young multiple T-Tauri star system with age about 2.8 Myr [96]. It consists of FS Tau A and FS Tau B. FS Tau A is a binary system with total mass about $0.78\pm0.25M_{\odot}$, semi-major axis about $0.275''$, eccentricity 0.168 [120]. while FS Tau B, also called Haro 6-5B, is a single star and famous for its bipolar outflows which has been studied a lot(e.g., Liu et al. [79]). However, the research towards FS Tau A is still limited. Hioki et al. [53] suggested that it has a large circumbinary disk extending to about 630 AU, and is inclined by 30° to 40° based on Subaru Telescope/CIAO observations, and the southeast side is likely to be closer to us if the southeast side is brighter than the northwest side in the H-band due to the forward scattering of dust. They also discovered two cavities with position angle 220° to 250° and suggested that they could represent outflow cavities. This is inconsistent with their circumbinary disk model, which indicates that the position angle of the circumbinary disk is 105° to 135°, or 285° to 315°, so the outflow direction should be generally 195° to 225°. Therefore, they suggested that their circumstellar disks could be misaligned with the circumbinary disk. As for the structures near the binaries, like the possible circumstellar disks misaligned with the circumbinary disk, we still know little about it. With HiCIAO instrument mounted on Subaru Telescope, we are able to resolve structures close to $\sim0.''1$

from the star. So by executing observations with HiCIAO instrument, we may be able to resolve these misaligned circumstellar disks for the first time.

Coku Tau 4 is a young binary system with age about 4 Myr [96]. Ireland and Kraus [57] discovered that it is a binary system with projected separation about 8 AU. For its circumbinary disk, our knowledge is still limited, only D'Alessio et al. [27] and Nagel et al. [90] suggested that it should have an inner hole $\sim$10 AU based on spectrum and SED modeling. Therefore, it is also a good target for near-infrared band observations.

In this chapter, we will show that based on Subaru/HiCIAO near-infrared data as well as ALMA CO 2-1 data, we successfully revealed that FS Tau has a nearly face-on outer disk, and a inclined inner disk. As for Coku Tau 4, our observations catch a dark structure in the center of the disk, possibly representing a gap.

4.2 Observations and Data reduction

The H-band near infrared observations of FS Tau A was performed on Dec. 26th, 2011, using the the High Contrast Instrument for the Subaru Next Generation Adaptive Optics (HiCIAO, Tamura et al. [122]) and the adaptive optics (AO) instrument AO188 [51] mounted on the Subaru Telescope. This observation was part of the survey program Strategic Explorations of Exoplanets and Disks with Subaru (SEEDS), which began in 2009. This observation employed the standard-polarized differential imaging (sPDI) mode, which uses a Wollaston prism to split the light into two 2048×1024 channels on the detector, each corresponded to o- and e-polarizations, with pixel scale of 9.50 mas/pixel. The AO system helped limit the full width at half maximum of the stellar point spread function to $0.07''$, which is close to the diffraction limit of $0.04''$. A half-wave plate was used in the observation, and it was rotated among position angles of 0°, 22.5°, 45°, and 67.5° to measure the Stokes parameters. This cycle was repeated 13 times during observation. Finally 52 frames were collected, each with an exposure time of 50s, making the total integration time about 43 minutes.

As for the Coku Tau 4 data, it was taken on Dec. 30th, 2011, with Subaru Telscope and HiCIAO instrument. The observation consists of 20 cycles, 80 frames, each with an exposure time of 20s. The total integration time was about 27 minutes.

The data reduction of FS Tau A and Coku Tau 4 data is similar with the reduction of GG Tau A and T Tau S. Firstly we corrected flat field, then stripes, bad pixels, and distortions were removed. After these steps, the images were first cross-correlated in different channels then we derived the Stokes parameters $+Q$, $+U$, $-Q$, and $-U$ by subtracting the e-images from the o-images. In the next step, the Q and U images were constructed as $Q = ((+Q) - (-Q))/2$,

$U = ((+U) - (-U))/2$. The Stokes *I* image, or intensity image, was derived by averaging the sum of the o- and e- images in all frames. After the instrumental polarization was corrected, a polarized intensity (*PI*) image can be constructed as $PI = \sqrt{U^2 + Q^2}$.

The CO 2-1 ALMA observation data of FS Tau is downloaded from ALMA data archive. It was observed with ALMA Band 6 receiver (project "2013.1.00105.S"), on Sep. 19, 2015, with 36 antennas. The beam size of it is about $0.''22 \times 0.''16$, with position angle about 26.24°. Also the 1.3 mm continuum image was taken to show the position of the stars.

4.3 Results

From the stokes *I* image, Figure 4.1, we can see the star is a binary, although not resolved well. The primary star looks much brighter than the secondary star. The separations between them is estimated to be about $0.''28$, or 40 AU, with a position angle about 120°. The secondary star's position angle looks consistent with the orbit derived by Tamazian et al. [120].

For the Stokes *PI* image of FS Tau A in Figure 4.2a, the vectors on its vector map, Figure 4.2b, the vectors near the central star are generally centrosymmetric, indicating real structures. While some vectors near the central stars are aligned with one direction with position angle about 60°, generally consistent with the position angles of the symmetric dark regions. This could be a result of "polarization disk" suggested by Murakawa [89], which indicates a highly inclined optically thick disk. However, it could also be a result of uncorrected PSF halo like we have shown in Chapter 2. To clarify this we tried the PSF halo correction process on this PI image, by creating an artificial PSF halo for Stokes Q and U images based on Stokes *I* image, subtracting them from the original Stokes Q and Stokes U images, and generating PSF halo corrected *PI* image. The *PI* image and its vector map after correction is shown in Figure 4.3, from the vector map Figure 4.3b we can see that the vectors near the central star have become cenntrosymmetric. This indicates that the aligned vectors are should be a result of PSF halo. The following analysis will be based on the corrected *PI* image, e.g., Figure 4.3.

On the vector map, Figure 4.3b, the yellow vectors indicate the area where the signal noise ratio (SNR) is larger than 4, suggesting that their signal is strong enough to be regarded as a discovery in polarimetry observations. However, the 4-σ area around FS Tau A is too small, and there are still some structures can be seen in the right of the image, so we try to lower the acceptable SNR to 3σ, and these area are shown in red vectors. From the vector map, it can be seen that generally all the structures seen in the *PI* image are covered with

vectors, indicating that they generally have SNR larger than 3. While of course for the area whose SNR is larger 3 but smaller than 4, other observation is still necessary for confirmation.

From the corrected *PI* image of FS Tau A in Figure 4.3a, one structure in the east and southeast extends to about 1.″2, or 168 AU in 4σ level, if we consider the 3σ structures are real, then it extends to about 1.″6, or 224 AU from the stars. One arm extends from the star first to the north, to about 1.″6, or 226 AU, and then it seems to turn to the southwest of FS Tau A, its end is at a distance of about 0.″8 or 112 AU from the central star. However, its signal noise ratio is only about 3, so it remains doubt that if it is real. There is one dark region on the northeast of the stars, with position angles about 30-60°. On the opposite side there seems to be also one dark region between the southwest arm and the star.

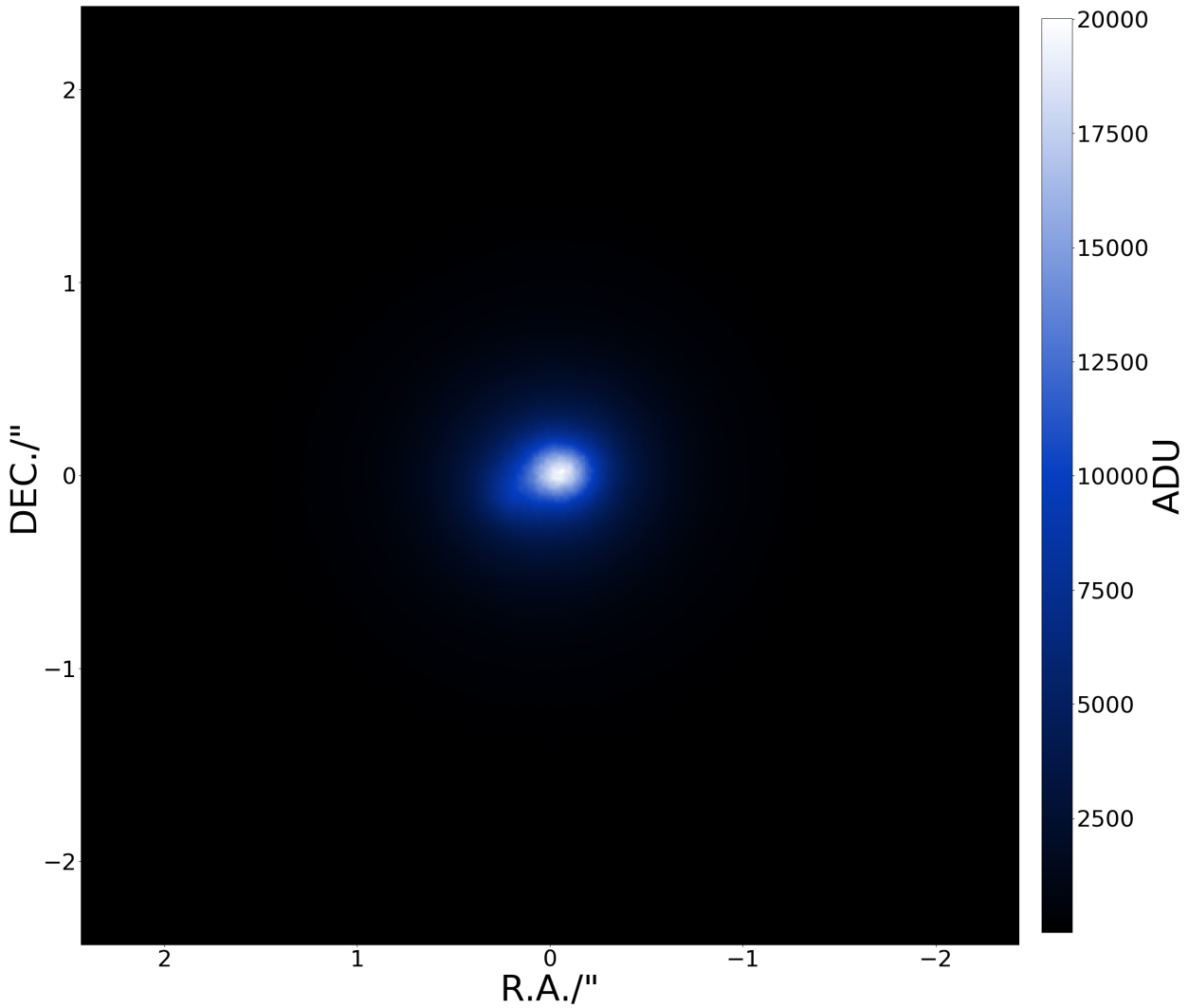

Fig. 4.1 Stokes *I* image of FS Tau A, taken by Subaru/HiCIAO in H-band.

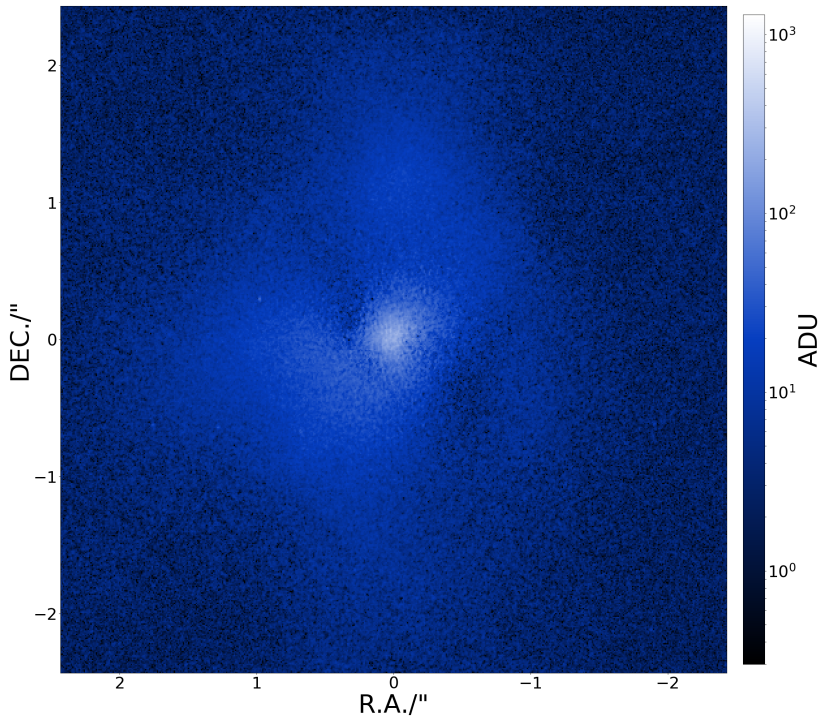

(a)

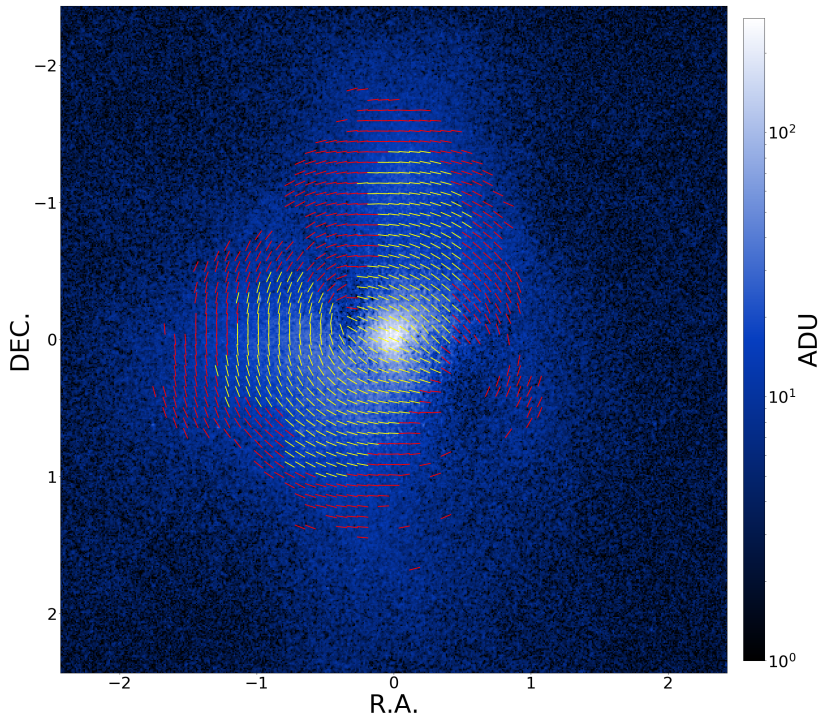

(b)

Fig. 4.2 (a): *PI* image of FS Tau A before PSF halo subtraction, taken by Subaru/HiCIAO in H-band; (b): vector map of FS Tau A before PSF halo subtraction. The yellow vectors indicate the area where signal noise ratio (SNR) σ is larger than 4, while the red vectors indicate the area where σ is larger than 3 but smaller than 4.

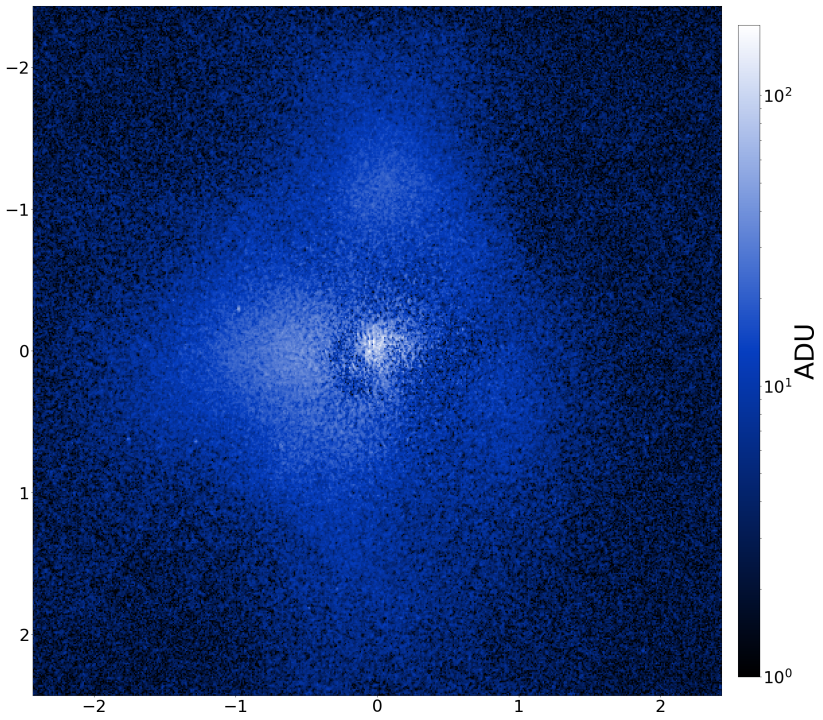

(a)

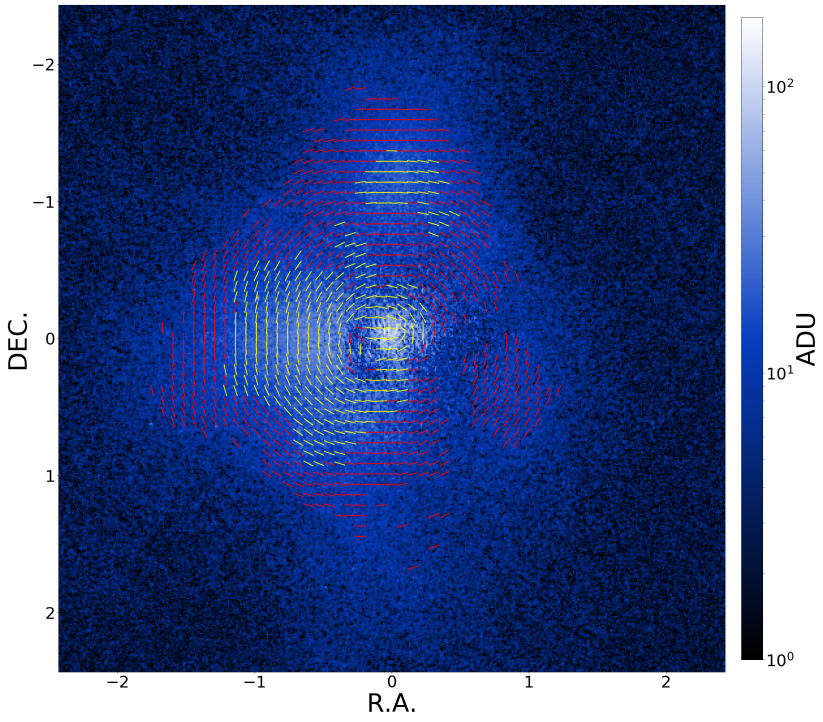

(b)

Fig. 4.3 (a): *PI* image of FS Tau A after PSF halo subtraction, taken by Subaru/HiCIAO in H-band; (b): vector map of FS Tau A after PSF halo subtraction. The yellow vectors indicate the area where signal noise ratio (SNR) σ is larger than 4, while the red vectors indicate the area where σ is larger than 3 but smaller than 4.

In the channel map of FS Tau A CO 2-1 image shown in Figure 4.4, we can see that no emission is detected in channel 6.27km/s, 6.90km/s and 7.54km/s, which may indicate that two independent components are detected in ALMA CO 2-1 image. In this case, we integrate these two independent components individually.

Component 1 is integrated from channel 1-8 (1.19-5.64 km/s), and its moment 0, 1 and 2 images are shown in Figure 4.5. In the moment 0 image, two obvious structures can be seen. One structure which we label as structure A extends from the star to about 0.″4 or 56 AU with position angle about 10°, in the central part of this structure there is a velocity dispersion of about 1.6 km/s. While another structure, a bar-like structure which we label as structure B, locates at about 0.″5 or 70 AU from the star, it has two peaks in the moment 0 image, with separation about 0.″7 or 98 AU and position angle about 40°. In the moment 1 map, this “bar” has a nearly-same velocity about 5 km/s, and it seems to have two velocity dispersion peaks in moment 2 map, just corresponding to the two peaks in moment 0 map.

As for component 2, it is integrated from channel 12-25 (8.17-16.43km/s) and its moment 0, 1, 2 images are shown in Figure 4.6. From the moment 0 intensity image and moment 1 velocity image, we can see that some structures extend to about 1″ (140 AU) to the south and southeast, and in the center there is clearly a bright “arm" extending from the star to ∼0.″25 (35 AU) with position angle ∼110°, and there is also a secondary arm extending to the north to about 1″ (140 AU), and turning to southwest to about 1.″1 (154 AU) from the turning point.

We also give the ALMA CO 2-1 images of FS Tau A with both component 1 and 2 included. These images are given in Figure 4.7. From the moment 1 image, we can see that the structure B, the “bar” of component 1 coincides with the southeast structure of component 2, while for the structure A, its south part does not coincide with component 2 well while the central part near the star seems to be consistent with some structures in component 2.

As for Coku Tau 4, our Subaru/HiCIAO observations show a inclined disk, with projected semi-major axis 0.″5 (70 AU), and semi-minor axis 0.″3 (42 AU), shown in Figure 4.8. If the disk is circular, its inclination is about 53°. These is a dark structure which can be seen in the center of the disk, with projected radius about 0.″1 (14 AU) from the central star and position angle -45°. If the circumbinary disk is generally circular, this dark structure has a radius of about 23 AU.

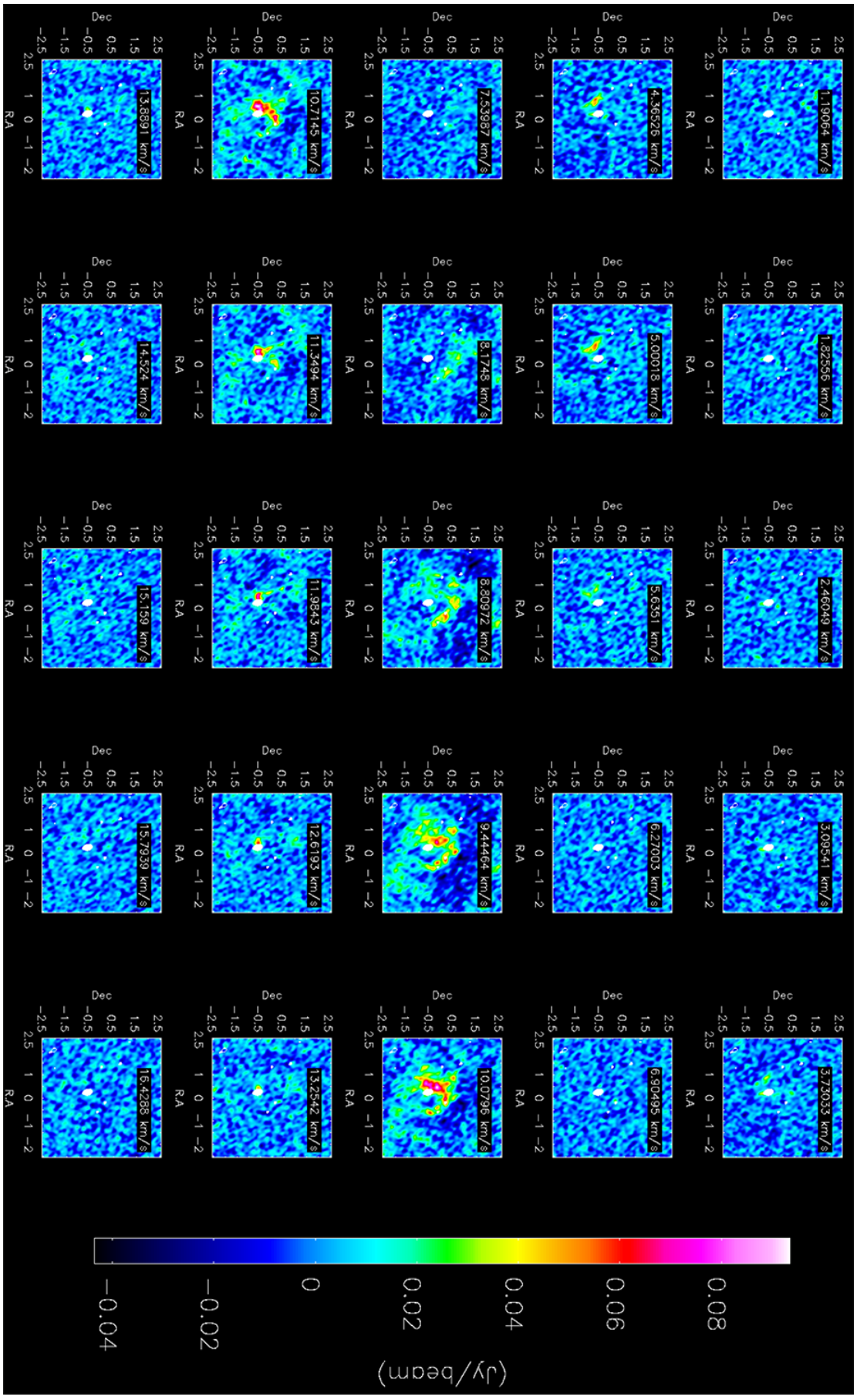

Fig. 4.4 ALMA CO 2-1 channel map of FS Tau A. Contours represent ALMA 1.3 mm continuum image, showing 0.2, 0.4, 0.6 and 0.8 of the peak intensity 2.08 mJy/beam.

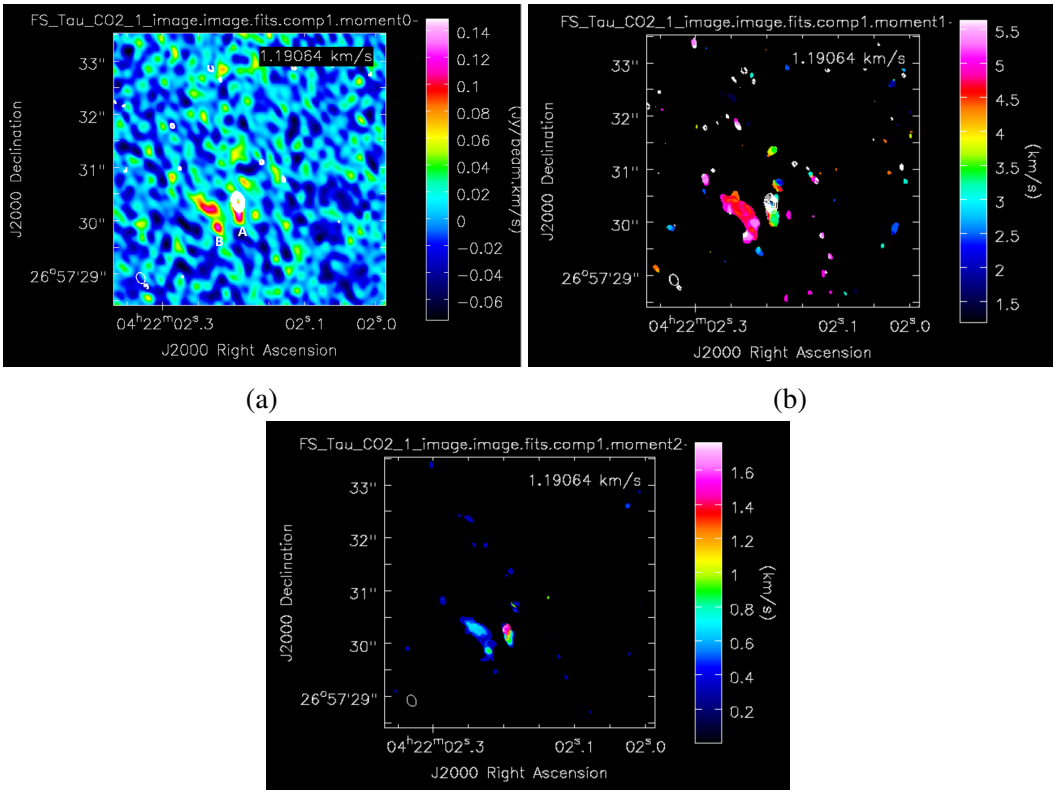

(a) (b)

(c)

Fig. 4.5 ALMA CO 2-1 component 1 images, corresponding to velocity 1.19-5.64 km/s. (a): ALMA CO 2-1 moment 0 image of FS Tau A component 1; (b): ALMA moment 1 image of FS Tau A component 1; (c) ALMA moment 2 image of FS Tau A component 1. The white contour in moment 0 and 1 images is the continuum emission image showing the position of the central stars, showing 0.2, 0.4, 0.6 and 0.8 of the peak intensity 2.08 mJy/beam.

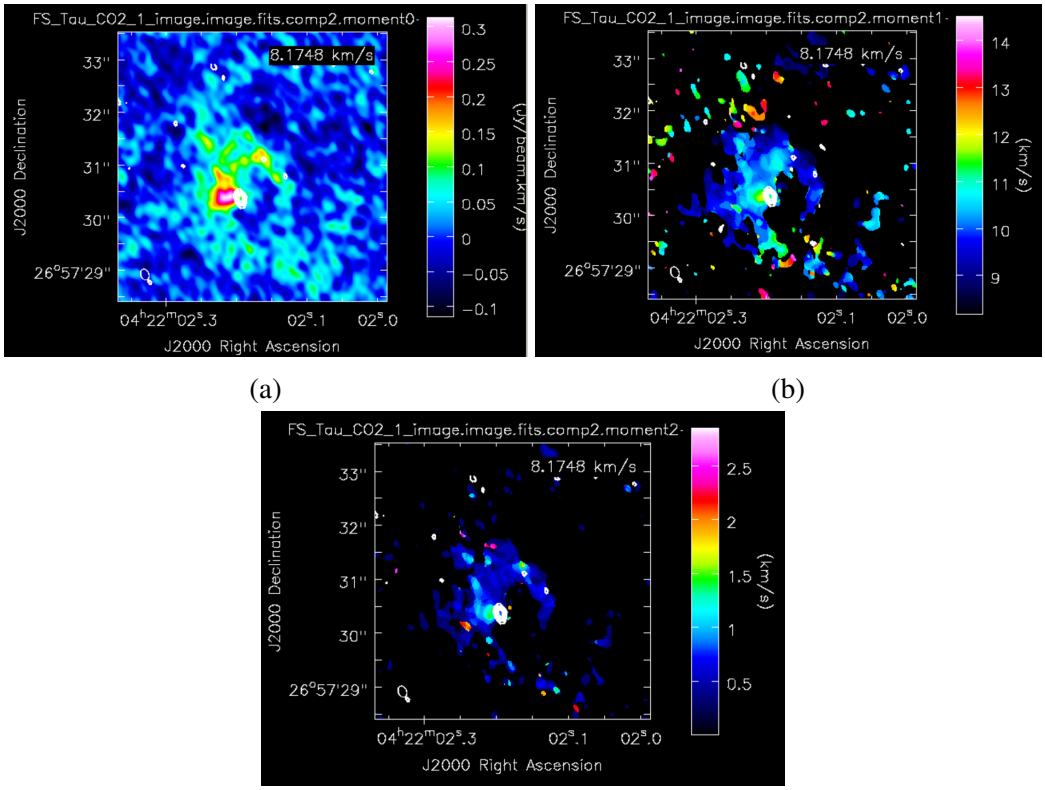

(a) (b)

(c)

Fig. 4.6 ALMA CO 2-1 component 2 images, corresponding to velocity 8.17-16.43km/s. (a): ALMA CO 2-1 moment 0 image of FS Tau A component 2; (b): ALMA moment 1 image of FS Tau A component 2; (c) ALMA moment 2 image of FS Tau A component 2. Contours represent ALMA 1.3 mm continuum image, showing 0.2, 0.4, 0.6 and 0.8 of the peak intensity 2.08 mJy/beam.

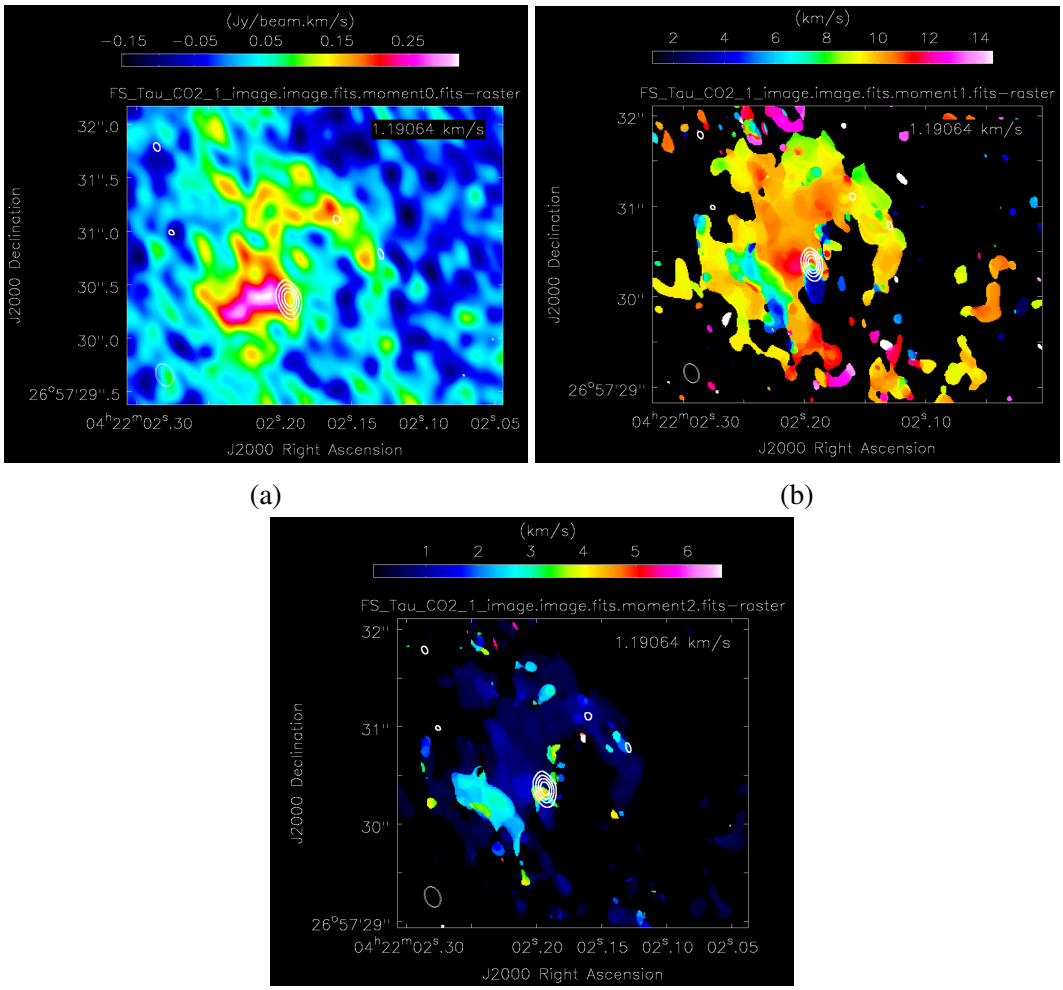

Fig. 4.7 ALMA CO 2-1 images of FS Tau A, including component 1 and component 2. (a): ALMA CO 2-1 moment 0 image of FS Tau A; (b): ALMA moment 1 image of FS Tau A; (c) ALMA moment 2 image of FS Tau A. Contours represent ALMA 1.3 mm continuum image, showing 0.2, 0.4, 0.6 and 0.8 of the peak intensity 2.08 mJy/beam.

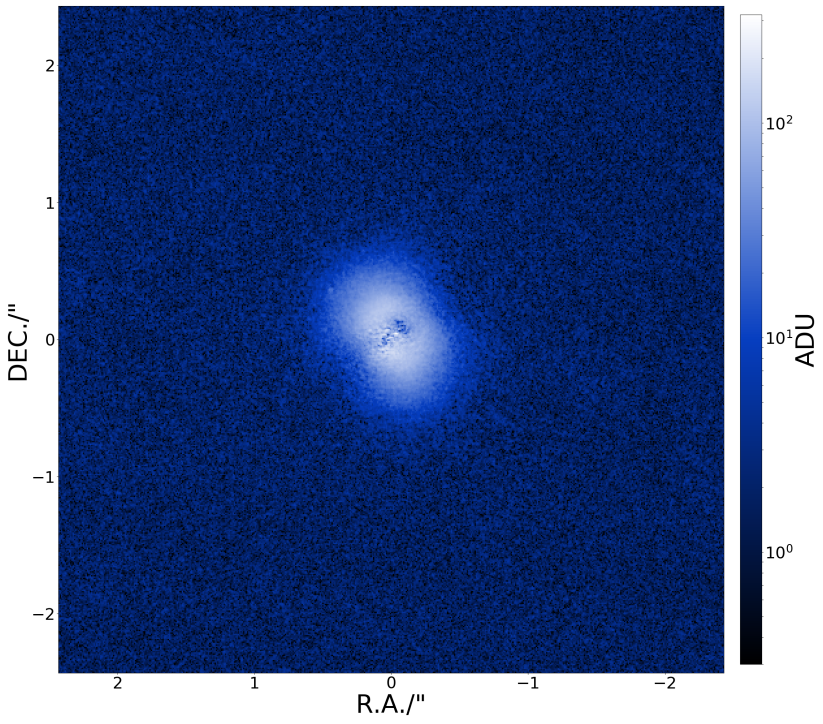

(a)

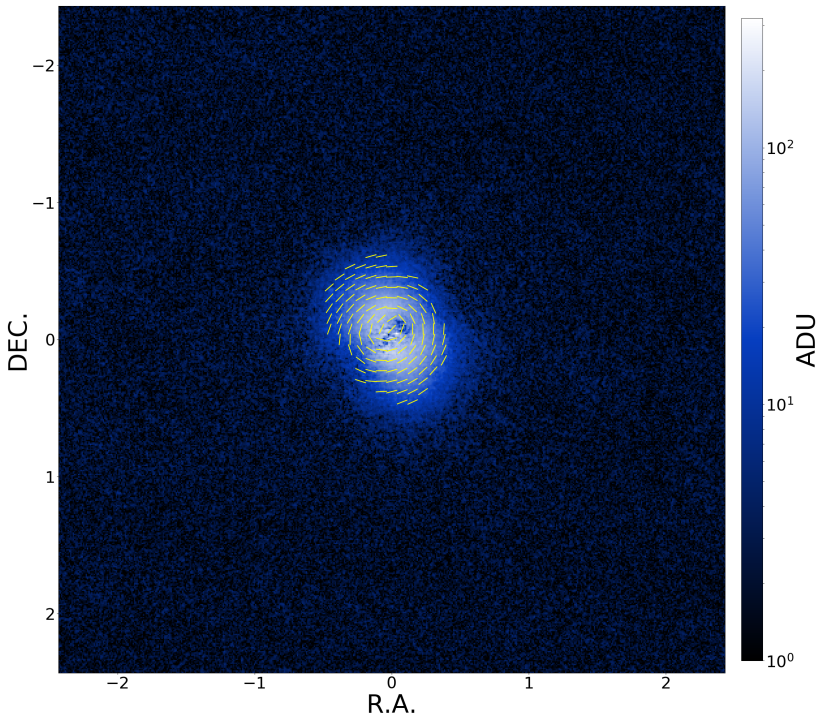

(b)

Fig. 4.8 (a): *PI* image of Coku Tau 4, taken by Subaru/HiCIAO in H-band; (b): vector map of Coku Tau 4.

4.4 Discussion

4.4.1 Component 1

To understand the structure A in Component 1, we draw a position-velocity (P-V) map of FS Tau A's central region for all the channels (Figure 4.9). The P-V map is drawn along with position angle 10°, radius 0.″6 and width 1 pixel from the central stars. From the P-V map, we can see that there exists two different velocity components: one is at the bottom left of the P-V map, with average velocity about 4 km/s while the other is at the top right of the map, with average velocity about 11 km/s. The 10 km/s component should belong to component 2, but the two components seem to be symmetric respect to 7.5 km/s, which is the general velocity of Taurus star formation region, so they could be related.

One possible reason causing these opposite velocities is the bipolar outflows from the central stars. However, previous observations did not report any outflows of this system. Woitas et al. [132] did not find any evidence of high-velocity jets from the stars in their optical emission line observations, like [SiII] and Hα, and the possible outflow suggested by Hioki et al. [53] is with position angle about 220-250°, which is inconsistent with our observations.

Another possible explanation is the disk in the binary. Since the outer boundary of structure A is about 0.″4 or 56 AU, while the semi-major axis of the binary is about 0.″258 or 36 AU, so if it is a disk, it should be a circumbinary one. Considering a Keplerian disk with velocity 3.5 km/s at 0.″4 or 56 AU, the central stellar mass should be about $0.77M_{\odot}$, just consistent with the previous mass estimation $0.78\pm0.25M_{\odot}$ by Tamazian et al. [120]. So this explanation seems to be more reasonable and this disk should be a nearly edge-on one, generally consistent with its appearance. However, we should point out that the possibility of outflow cannot be totally excluded, and hope following observations from other bands can bring better results to help make a judgement of this.

To distinguish the nearly edge-on circumbinary disk in ALMA CO 2-1 image from the large circumbinary disk suggested by Hioki et al. [53], I name this circumbinary ring as "inner circumbinary disk" of FS Tau A, while the circumbinary disk suggested by Hioki et al. [53] is named as "outer circumbinary disk". Tamazian et al. [120] suggested that the binary orbital plane of FS Tau A is about 19.7±5°, while this circumbinary disk around FS Tau A is nearly edge-on, this indicates that its orbital plane is highly misaligned ($\sim 70°$) with the inner circumbinary disk. The outer circumbinary disk has an inclination about 30° to 40°, thus the binary orbital plane is also misaligned with the outer circumbinary disk, and the inner circumbinary disk is misaligned with the outer circumbinary disk. A detailed discussion of this topic will be made in Chapter 5.

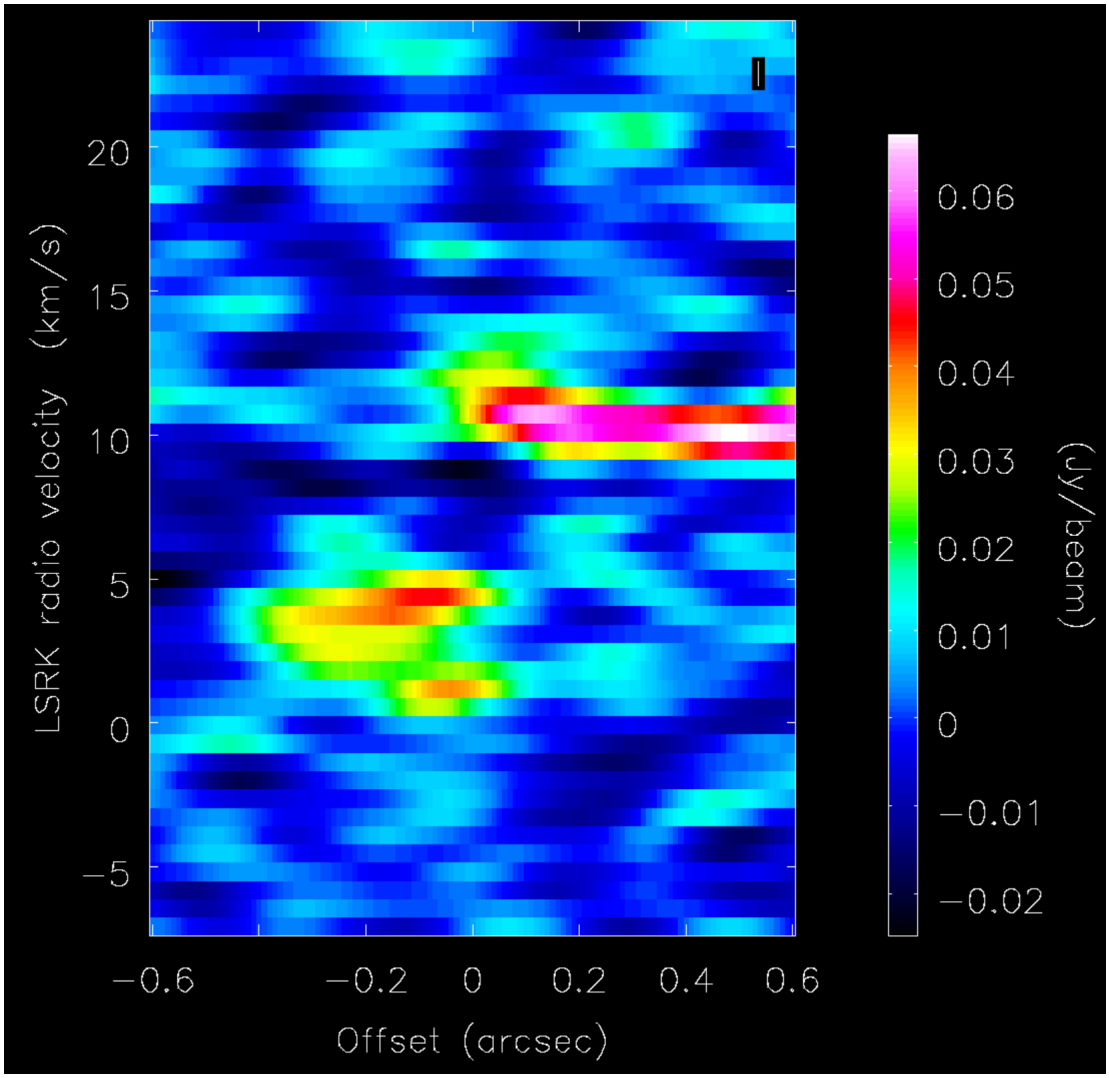

Fig. 4.9 PV map of FS Tau A ALMA CO 2-1 image central region. The image is drawn along a slit with position angle 10°, radius 0.″6 and width 1 pixel.

For structure B, the “bar" structure to the southeast of FS Tau A, from Figure 4.10a we can see that it is consistent with the southeast bright structure in H-band, but just from our observations it is hard to tell what it is. It could be a hot region heated by accretion, and the two peaks in this structure seen in moment 0 map may represent some embedded objects, to confirm this firstly we need to know its temperature. Future observations of some special emission lines, like observations from near infrared hydrogen emission line may be helpful.

4.4.2 Component 2

The velocity of component 2 is larger than $\sim$7.5 km/s, in this case the structures of component 2 are all “red-shifted". No “blue-shifted” structures with the same size as component 2 are detected around FS Tau A in ALMA CO 2-1 image, or our near-infrared H-band image. To understand what the structures of component 2 we detected in near-infrared H-band and CO 2-1 emission image are, we make a comparison of CO 2-1 image and H-band image, by overplotting the component 2 CO 2-1 image on H-band image. This image is shown in Figure 4.10b.

From Figure 4.10b, we can see that, the southeast structures of component 2 are generally consistent with the southeast structures in near-infrared band, and for the structures in the north and northwest, the near-infrared data and CO 2-1 emission data are quite consistent. This result indicates that the dust grains are generally couple with the gas.

Based on current observation data, it is still not easy to tell what component 2 is. But we give some hypotheses here, and hope future observational and theoretical work can help solve that. One hypothesis of these structures is that component 2 corresponds to a circumbinary ring. while the velocity of component 2 is all red-shifted, not consistent with the systemic velocity, this could be a little strange for a circumbinary ring. One possible explanation to this is that the blue-shifted part of the ring is almost lost due to some mechanisms like the interactions with the binary.

Another hypothesis is that, component 2, especially the arm in the northwest, is an arm triggered by an undetected object. Because this undetected object interacts with component 2, it may influence the velocities of the materials in this arm, which may lead their velocities different from the systematic velocity. However, we do not detect such a kind of object with the similar distance of this arm from the star, previous observations also did not report any objects at this distance. Some theoretical work needs to be done to give an estimation of the orbit and mass of this possible object.

In addition, in the Subaru/HiCIAO as well as ALMA observation results, we do not find out any structure that could be related to the outflow Hioki et al. [53] suggested, so the outflow cavities they suggested could just be areas where dust surface density is low.

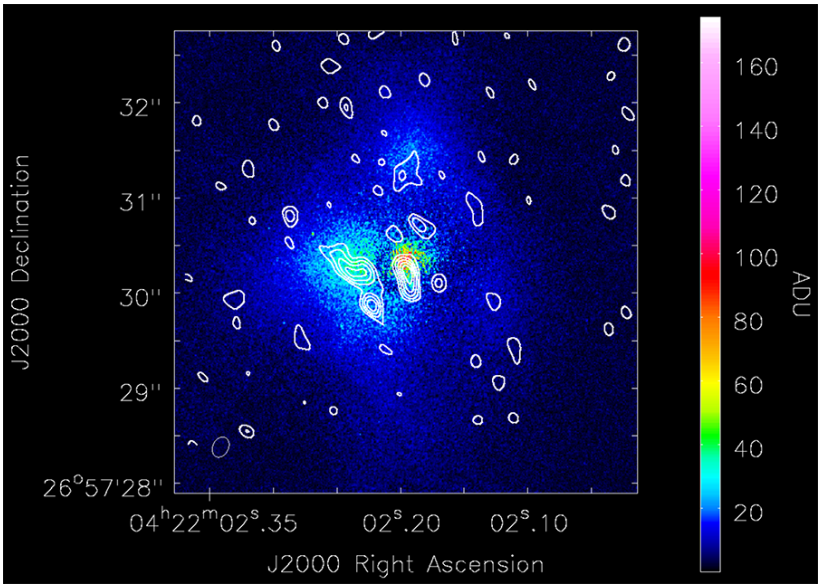

(a)

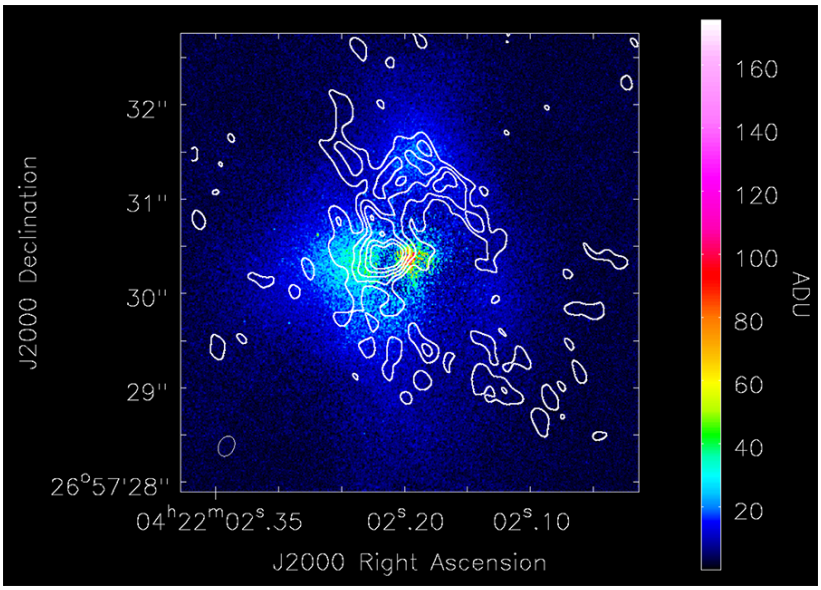

(b)

Fig. 4.10 (a): FS Tau A *PI* image (color scale) with ALMA CO 2-1 component 1 image (contour) overplotted. Contours are 0.5, 0.6, 0.7, 0.8, 0.9 of the peak intensity 0.149 Jy/beam; (b): FS Tau A *PI* image (color scale) with ALMA CO 2-1 component 2 image (contour) overplotted. Contours are 0.4, 0.5, 0.6, 0.7, 0.8 of the peak intensity 0.314 Jy/beam.

4.4.3 Coku Tau 4

As for Coku Tau 4, the Subaru/HiCIAO H-band shows a dark structure in the center of the circumbinary disk. If it is a gap structure, its real size could reach 23 AU, larger than the previous SED fitting results. However, considering the binary has a separation about 8 AU, if it is its semi-major axis, the gap size is not far from 3 times of its semi-major axis, which is the usual gap size as Artymowicz and Lubow [5] suggested. However, it is still necessary to point out that this gap could still be a result of backscattering light, like Perrin et al. [98] shows.

4.5 Conclusion

Our Subaru/HiCIAO observations successfully resolved the disk structures near the young binary FS Tau A and Coku Tau 4. For FS Tau A, we detect some structures extend to about 200 AU from the stars, and from the CO 2-1 emission image got by ALMA, we find out that these structures can be divided into blue-shifted component 1 and red-shifted component 2. For component 1, we detect two structures A and B, and suggest that the structure A could represent the blue-shifted part of a nearly edge-on inner circumbinary disk with size about $0.''4$ (56 AU) from the central binary. As for component 2, the structures in ALMA CO 2-1 image are generally consistent with the structures detected in near-infrared band, indicating that the gas and dusts are couple well. We suggest that component 2 could be a circumbinary ring, or an arm triggered by an undetected object, however future observational and theoretical works are needed to clarify this.

For Coku Tau 4, our near-infrared observation shows that it has a cirucmbinary disk with size about 70 AU, and inclination about 53° if it is circular. There is also one dark structure discovered in the center of the disk, with projected size 14 AU and position angle about -45°. If it is a gap caused by the binary, its real size should be about 23 AU, which is significant larger than the previous SED fitting results, but considering the separations of the binary, it is still consistent with the predicted gap size in circumbinary disks.

Chapter 5

Overall Discussion

In this chapter, we will discuss the disk evolutions in binary/multiple systems based on the appearance of the disks around binaries we have observed. We will mainly discuss the disk gap opening and disk misalignment in circumbinary disks, and a brief interpretation of the planet formation process in binary systems.

During the SEEDS survey, we have investigated 4 young binary/multiple stars with disks: GG Tau A, T Tau, FS Tau A, and Coku Tau 4. For GG Tau A, our near-infrared high-contrast observations show that its circumbinary ring has an inner edge of about 140 AU and is asymmetric, mostly like to be truncated by the binary; and one streamer is discovered connecting the circumbinary ring and the possible disk structure around GG Tau Ab, bringing materials from the ring to the disk. For T Tau S binary system, our observations show that it is surrounded by a nearly edge-on disk with radius about 44 AU, which is highly misaligned ($>40^\circ$) with its binary orbit. In our investigations of FS Tau A, we found that the component 1 in ALMA CO 2-1 image could represent a nearly edge-on circumbinary disk with size about $0.''4$, and highly misaligned ($\sim 70^\circ$) with the binary's orbit. For Coku Tau 4, it has a possible central gap structure with a size of about 23 AU. In summary, we find out gaps in the circumbinary disk around GG Tau A and Coku Tau 4, and misaligned circumbinary disks in T Tau S and FS Tau A. A summary of the observed binary parameters has been given in Table 5.1.

5.1 Disk Gap Opening

In this section, we mainly discuss the gaps opened in the circumbinary disk, based on HiCIAO observation results. According to the simulation like Artymowicz and Lubow [5], the binaries open gaps in the circumbinary disks, it can be seen in GG Tau A, as well as in Coku Tau 4. However, we do not see this kind of gaps in young binaries like T Tau S or FS

Table 5.1 A summary of the binary/multiple systems with disks observed by Subaru/HiCIAO

Star	M_s	t_a	a	e	r_e	r_g	r_d	Reference
T Tau S	2.12/0.53	1.2	12.5	0.56	∼39	–	**44**	[67, 96]
FS Tau A	0.78*	2.8	38.5	0.168	>80	–	∼**56**	[120, 96]
Coku Tau 4	0.6/0.5	4	∼8	unknown	>14	∼**23**	–	[57, 90, 96]
GG Tau A	0.73/0.64	2.7	62	<0.35	124-186	∼**140**	–	[10, 96]

M_s: stellar mass in solar mass; t_a: age of binary in Myr, given by Palla and Stahler [96]; a, semi-major axis of binary orbit in AU; e: eccentricity of binary orbit; r_e: expected gap size in AU, estimated from Artymowicz and Lubow [5]; r_g observed circumbinary disk gap size in AU, **derived by this work**; r_d: observed misaligned disk size in AU, **derived by this work**; M_s, a and e are given by Köhler et al. [67] (T Tau S), Tamazian et al. [120] (FS Tau A), Ireland and Kraus [57], Nagel et al. [90] (Coku Tau 4), and Beust and Dutrey [11] (GG Tau A)
*: total mass of this binary system;

Tau A. Instead, we see circumbinary disk highly misaligned with the binary's orbit in T Tau S, and FS Tau A system.

From these results, we wonder why we do not see gaps in T Tau S and FS Tau A systems. To help analysis, we estimated the gap sizes which the four binaries should open based on the simulation results of Artymowicz and Lubow [5].

For GG Tau A system, its mass ratio $\mu = M_b/(M_a + M_b)$ is about 0.47, here M_b is the mass of the secondary star, while M_a is the mass of the primary star. From the simulation results summarized in Table 3 of Artymowicz and Lubow [5], a binary system with $\mu = 0.3$ and $e = 0.3$ will open a gap with size about 2.72 times of their semi-major axis, and in their table it can be seen that a higher μ will lead to a larger gap size. Since the eccentricity of GG Tau A binary orbit is smaller than 0.35, it seems reasonable to suggest that the tidal radius of GG Tau A is about 3 times of their semi-major axis if its binary orbit has an eccentricity of about 0.3. For small orbital eccentricity case, Artymowicz and Lubow [5] suggested that for $\mu = 0.3$ and $e = 0$ the binary will open a gap about 1.8 times of the orbital semi-major axis. Since GG Tau A's mass parameter is larger, it should open a little larger gap. Therefore, we suggest that if GG Tau A has a low eccentric orbit, its tidal radius should be around 2 times of the semi-major axis. In summary, the tidal radius of GG Tau A should be about 2-3 times of the binary orbital semi-major axis. In Chapter 2 we have suggested that 62 AU is a more reasonable semi-major axis than 32 AU, so the expected gap size of GG Tau A is about 124-186 AU.

For T Tau S system, its mass ratio μ is about 0.2 and eccentricity is about 0.6, so in this case the expected gap size should also near 3 times of its semi-major axis, or 39 AU.

For FS Tau A system, we do not actually know the primary and secondary star masses, but from the Stokes I image of FS Tau A it seems that the secondary star is much fainter than

the primary star. So it is reasonable to suggest that the secondary star is much less massive than the primary star. Its orbital eccentricity is about 0.168. In the case of mass ratio $\mu = 0.1$ and orbital eccentricity $e = 0.1$ in the simulation of Artymowicz and Lubow [5], it should open a gap with size about 2.1 times of the orbital semi-major axis. So for FS Tau A, its expected gap size should be at least larger than about 2.1 times, i.e., about 80 AU.

Finally, for Coku Tau 4 system, its mass ratio μ is about 0.45, while orbital eccentricity remains unknown. However, considering that in the case of $\mu = 0.3$ and $e = 0$ the binary can open gaps about 1.8 times of the orbital semi-major axis, thus the gap size opened by Coku Tau 4 should at least larger than 1.8 times, i.e., about 14 AU.

Then, we compared the expected gap sizes with observation results. For GG Tau A, the observed gap size is about 140 AU, consistent with the expected gap size we estimate. So it shows that truncation from the binary could explain the formation of the gaps.

For Coku Tau 4, the observed dark structure has a projected size of about 14 AU from the stars, if the disk has an inclination of $\sim 53^\circ$, the real size of the dark structure is about 23 AU. If it is a gap opened by this binary, it is larger than the minimum expected gap size we estimate. It is foreseeable that if this binary has an eccentric orbit, they will open larger gaps to $\sim$3 times of its semi-major axis. This gap radius is just about 3 times of the semi-major axis, so this result is acceptable.

The problem is T Tau S and FS Tau A. Based on the expected gap sizes we estimate, they should open gaps with sizes about 39 AU and 80 AU, which are observable with the Subaru Telescope. However, we do not see any gap-like structures around them, while our observations suggest that they hold inclined, nearly edge-on disks. For T Tau S, its expected gap size is comparable with the observed disk size, while for FS Tau A, its expected gap size is significantly larger than the observed disk size. This raises the problem that why the circumbinary disk around T Tau S and FS Tau A could exist.

One possible explanation is that in misaligned circumbinary disks, the opened gap sizes are smaller than coplanar circumbinary disks. The simulation of Artymowicz and Lubow [5] is based on coplanar circumbinary disk. Miranda and Lai [88] discussed the opened gap sizes in circumbinary disks with different inclinations based on the calculations of Lindblad torques. In the work of Miranda and Lai [88], they has shown that for misaligned circumbinary disks, the gaps binaries open are significantly smaller than coplanar disks. In their calculation, Miranda and Lai [88] suggested that for a binary with mass ratio about 0.3 and misaligned inclination 45° and 90°, the cleared gap size is generally around 2-2.5 times of binary's semi-major axis. Considering T Tau S systems is a binary with mass ratio about 0.2, and misaligned inclination at least 40°, the opened gap size should be smaller than 2-2.5 times of its semi-major axis, i.e., 26-33.5 AU. This will bring much room for the

circumbinary disk. In addition, it could be hard to observe cleared gaps in inclined disks even in near-infrared band. For example, considering a 30-AU gap in a circumbinary disk with inclination 60° relative to the sky plane, its projected “semi-minor axis" is 15 AU, quite near the inner working angle (∼14 AU) of HiCIAO, and the disk itself could have thickness, which will make the gap harder to observe. This can explain why we do not see gaps in the circumbinary disk of T Tau S.

As for FS Tau A, a gap size with twice of its semi-major axis is still too large for its inner circumbinary disk to exist. However, Miranda and Lai [88] showed that for some special cases, like mass ratio 0.1 and a disk with misaligned angle 90°, the opened gap size could be as small as 1.3 times of binary's semi-major axis when orbital eccentricity is around 0.2. This result indicates that for highly-misaligned disk-binary systems, the opened gap size could be extremely small under some special binary parameters. Considering FS Tau A has an orbit with eccentricity about 0.168, and should be a low mass-ratio binary, the opened gap size could just be about 1.3 times of its orbital semi-major axis, i.e., 50 AU, smaller than the disk size I observed. And the inner circumbinary disk around FS Tau is generally edge-on, so observing gap in the disk could be really hard.

Gap opening can be finished in a few binary orbital periods. Like the simulation result shown in Figure 9 of Artymowicz and Lubow [5], a binary can open a gap with radius twice of its semi-major axis in 30 orbital periods. As for T Tau S and FS Tau A, 30 orbital periods are very short time (810 and 8100 year, respectively). In this case, it can be said that their cirumbinary disks are born with gaps, so circumbinary disks with sizes comparable with 2-3 times of their semi-major axes, like the disks around T Tau S and FS Tau A, may be still difficult to form. But considering the disk could have initial misalignment due to accretions, it may be explained by assuming that these systems hold proper misaligned angles (even a retrograde one, in this case it will be hard to open gaps in the disk [93]) at the very beginning, then they evolve to current misaligned angles in a few Myrs. In summary, the circumbinary disks of T Tau S and FS Tau A can exist, but to understand how they forms, theoretical and observational works are still needed to be done in the future.

Similar gap structures are also observed in other binaries. One example is L1551 NE. L1551 NE is a Class I object. This binary has a projected separation ∼70 AU. In ALMA 0.9 mm dust-continuum image, this binary holds a misaligned (∼ 12° and ∼ 21° relative to the circumstellar disks) circumbinary ring with radius about 300 AU [119]. The inner radius of the circumbinary ring, or the gap radius, is about 140 AU, and the radii of circumstellar disks around the binaries are about 20 AU. Considering the gap radii for misaligned angles 0° and 22.5° are nearly the same [88], the radii of the gap and the circumstellar disks in L1551 NE

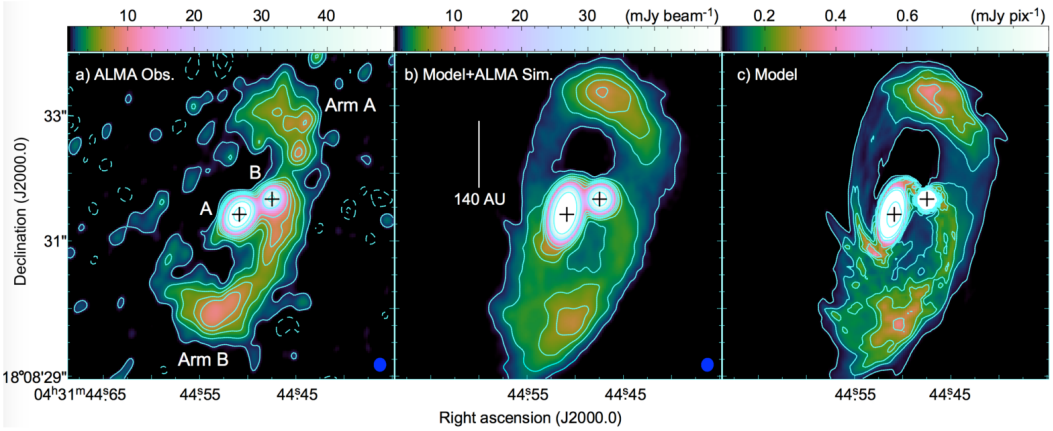

(a)

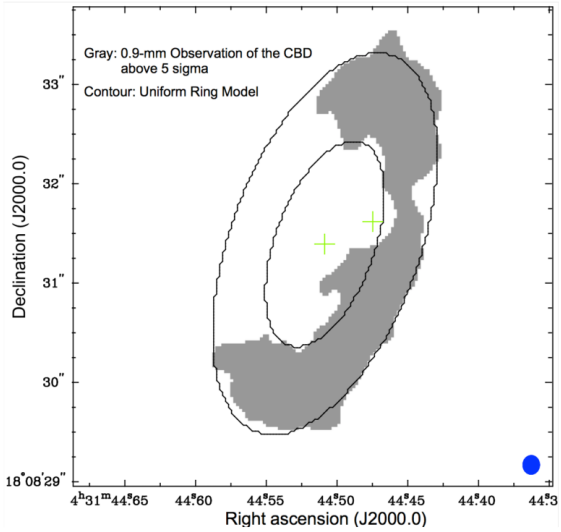

(b)

Fig. 5.1 (a): Figure 1 in Takakuwa et al. [119]. *left*: ALMA 0.9-mm continuum image of L1551NE; *middle*: simulated ALMA observation image of L1551NE; *right*: theoretical predicted image of L1551NE, based on the calculations of radiative transfer and 3D hydrodynamical model; (b): Figure 2 in Takakuwa et al. [119]. A simple fitting model of the circumbinary disk around L1551NE.

seem to be consistent with theoretical predictions, if the semi-major axis of this binary is $\sim$70 AU. In any case, L1551 NE looks like a younger version of GG Tau A.

There is another gap discovered in the circumbinary disk around HD 142527A. The binary HD 142527A has a semi-major axis $\sim$20 AU, and eccentricity about 0.5; its circumbinary disk has a gap about 90 AU, and $\sim 70^\circ$ misaligned [7, 77]. Considering its disk is highly misaligned with the binary orbital plane, and the secondary star is a low mass ($0.13M_\odot$) star, it is unexpected that its gap radius can reach about 4.5 times of the binary semi-major axis. Even considering the uncertainties of the semi-major axis (140^{+120}_{-70} milli-arcsecond, corresponding to about 20^{+17}_{-10} AU), the gap radius is still a little large. One possible explanation is that the initial separation between the binary is larger than the current separation, and other explanations include mechanisms like photo-evaporation, or one more (sub-) stellar object in the gap can also contribute to its gap opening scenario. Anyway, future research is still needed to understand the gap opening scenario like HD 142527A.

5.2 Disk Misalignment

In this section, we focus on the disk misalignment in young binary systems. Based on the targets observed during SEEDS survey, at least T Tau S and FS Tau A hold circumbinary disks misaligned with their binary orbital planes. For GG Tau A, Cazzoletti et al. [20] suggested that the disk around GG Tau A could also be misaligned with an angle of about 30°, although our observations suggest that the gap size can be explained by a coplanar binary orbit, and the simulation work of Nelson and Marzari [91] also suggest coplanar disk and binary orbit could be possible. Future astrometric calibration is needed to clarify this. For Coku Tau 4, till now no calibration about its binary orbital inclination has been made, we hope some future work can help reveal it.

For circumbinary disk misalignment with the binary orbit, it is usually believed that for very close (sub-AU) binaries, circumbinary disks tend to align the binary orbits, while for binaries a little wider (e.g., tens of AUs), their circumbinary disks can be misaligned. Some mechanisms have been suggested to explain the misalignment in binary systems. Accretion from different directions can lead the evolution of the angular momentum of the circumbinary disk and make the disk misaligned with the binary orbit, but the binary will usually drag the disk to its orbital plane, resulting in small inclinations ($< \sim 4^\circ$) within a few Myrs [43, 44]. The interactions between the disk and binary will cause the misalignment, and this kind of mechanisms has been studied a lot and can explain large misaligned angles (e.g., Martin and Lubow [83], Zanazzi and Lai [136]), while most of the simulations of these mechanisms started with a relatively large initial misalignment (tens of degrees). Zanazzi and Lai [136]

suggested that, to make a disk precess to a polar one rather than a coplanar one, the system requires to reach a critical misaligned angle I_{circ} between the disk and binary orbital plane:

$$I_{circ} = cos^{-1}\sqrt{\frac{5e^2}{1+4e^2}} \tag{5.1}$$

In addition, a companion out of the circumbinary disk can also make the disk become misaligned. Owen and Lai [95] suggested that the interactions between a circumstellar disk and an outer companion can cause "precession resonance" to make the circumstellar disk misaligned with the binary orbit. Their calculations show that this mechanism can start from a very small misaligned angles, and can lead to large misalignment between the circumstellar disk and the binary orbit. It is foreseeable that if there is one small object just outside of a circumbinary disk, the same mechanism will be triggered. Therefore, it looks like to be a promising mechanism.

As mentioned in the previous section, the sizes of the circumbinary disks around FS Tau A and T Tau S are comparable with their expected gap sizes, i.e., 2-3 times of the binary orbital semi-major axis. In the simulation work of Martin and Lubow [83], the radius of the misaligned circumbinary disk is 2-5 times of the binary orbital semi-major axis. Therefore, it is reasonable to doubt that interaction between the circumbinary disk and the binary is responsible for the misalignment. It is believed that disk-binary interaction will make the disk precess, then the disk will become misaligned with the binary orbital plane. In details, T Tau S has an eccentric orbit ($e \sim 0.56$), and its circumbinary disk is at least 40° misaligned with the binary orbit, this result is consistent with the expectation that eccentric close binary can have misaligned circumbinary disk. The disk-binary interaction suggested by Martin and Lubow [83] and Zanazzi and Lai [136] is likely to be responsible for its misalignment. Of course one initial misaligned angle (33°) is necessary to make the disk become misaligned, which could be caused by the accretion when the disk is formed.

For FS Tau A, its orbital eccentricity is relatively low (0.168). As Zanazzi and Lai [136] suggested, the critical inclination of an eccentricity 0.168 orbit can reach to about 69°. However, the observations of us and Hioki et al. [53] suggest that it has an outer circumbinary disk with misaligned angle $\sim 10^\circ$, and an inner circumbinary disk with misaligned angle $\sim 70^\circ$. It seems hard to explain the misalignment just from the disk-binary interactions. For the misalignment of the outer circumbinary disk, maybe the disk has an initial angle tens of degrees, and the binary still needs time to drag it to be coplanar, but for the inner circumbinary disk, neither initial misaligned angle nor the precession triggered by the binary can explain well about its misaligned angle. So it could have other mechanisms, like a

planetary mass object just outside of the inner circumbinary disk, to make the disk become misaligned.

Considering that four targets is still a small number, to have a better understanding of circumbinary disk evolution, more targets are necessary. In this case, we check other observations of binaries and their circumbinary disks. For my PhD study focuses on the disk evolution in close binary systems, i.e., binaries with separations smaller than $\sim$100 AU, so this time we just investigate young close binary systems.

The first kind of binaries we investigate is very close binaries. This kind of binaries have very short orbital periods, typically only a few days, which indicates that their orbital semi-major axes are quite small. Now protoplanetary disks have been found around some very close binaries like, DQ Tau, UZ Tau E, AK Sco and V4046 Sgr.

DQ Tau is a very close binary with orbital period only about 15.8 days. Czekala et al. [25] showed that it has a circumbinary disk about 100 AU, and the angle between its binary orbital plane and its disk is smaller than 3°.

UZ Tau E is also a very close binary with orbital period about 19 days. Prato et al. [101] found out that its orbit has an inclination of about 59.8°, consistent with its surrounding circumbinary disk.

AK Sco has a orbital period about 13.6 days. Czekala et al. [24] showed that its orbital plane is coplanar ($< 2°$) with its circumbinary disk observed by ALMA.

The orbital period of V4046 Sgr is only 2.4 days. Rosenfeld et al. [112] showed that its orbital plane is well consistent ($< 1°$) with its circumbinary disk observed by SMA.

From these results, we can see that, for very close binaries, like DQ Tau, UZ Tau E, AK Sco, V4046 Sgr, whose orbital periods are only a few days, their circumbinary disks seem to be general coplanar with their orbital planes. Although no observational reports about the gap structures they opened, it is foreseeable that the gaps they open, or the misaligned disk they truncated, if exist, are too small to be observed, because they all have very short semi-major axes. Their disk plane are generally coplanar with their orbital plane, and the small misaligned angle can be explained by the accretion mechanism suggested by Foucart and Lai [43, 44].

The binary system KH 15D has a stellar mass $1.3M_{\odot}$, orbital period about (48 days), corresponding to semi-major axis about 0.28 AU and orbital eccentricity 0.68-0.8 [60]. Its circumbinary disk has a mean radius about 3 AU and misaligned about 10-20° [21, 19]. Considering that it has a very eccentric orbit, its critical inclination could be very small, thus disk-binary interaction can still make its circumbinary disk misaligned. And it could be an evidence of why we did not see disk misalignment in very close binaries like DQ Tau; it is just because that they are too far for their truncated, misaligned inner disk to be observed.

There is one possible exception, TWA 3A. TWA 3 is a triple star system, consists of a very close binary TWA 3A, and a single star TWA 3B, locates at about 34 ± 4 pc from us [82]. The orbit of TWA 3A has an orbital period about 35 days with eccentricity about 0.63, its semi-major axis is estimated to be $\sim$0.19 AU [62]. while TWA 3B is located at a projected separation about $1.''55$ [125], or $\sim$50 AU from TWA 3A. Andrews et al. [4] suggested that its circumbinary disk has an inner radius at $\sim$1 AU, and outer radius of 15-25 AU. Kellogg et al. [62] suggested that its disk plane is misaligned with either TWA 3A orbital plane or TWA 3A-B orbital plane: these 3 planes, disk plane, TWA 3A orbital plane and TWA 3A-B, are likely misaligned with at least $\sim 30^\circ$. This misalignment may be related to the truncation from TWA 3B. However, HD 98800B, a similar binary system also located in the TW Hya association with a semi-major axis about $0.''023$ [12] (0.92 AU for a distance of $\sim$40 pc [82]) and eccentricity about 0.78, has a circumbinary disk generally coplanar with its orbital plane, despite the existence of HD 98800A $0.''8$ (32 AU) far away from it [4]. So it seems that future research is still needed to find out the reason of disk misalignment in the TWA 3 system.

Next we investigate some binaries with semi-major axis about tens of AU, just the same semi-major axis scale as our targets observed in SEEDS survey. The targets we investigate include L1551 NE, HD 142527A, 99 Her, and GW Ori.

For L1551 NE, as we have mentioned in Section 5.1, misaligned ($\sim 25^\circ$) circumbinary ring with radius about 300 AU [119]. If the semi-major axis of this binary is $\sim$70 AU, the disk size is comparable with the gap size the binary should open. The binary also has circumstellar disks around each star with size $\sim$20 AU and $\sim$10 AU, both are misaligned with the circumbinary ring . Therefore, the disk misalignment in L1551 NE system is likely to be a result of disk-binary interaction or precession resonance.

As for HD 142527A, its circumbinary disk has an inclination of $\sim 70^\circ$ relative to the inner circumstellar disk. As mentioned before, the precession resonance mechanism suggested by Owen and Lai [95] seems to be able to explain it.

99 Her is a binary system with total mass about $1.4 M_\odot$, and semi-major axis about 16 AU. Kennedy et al. [63] observed it using PACS and SPIRE instruments mounted on Herschel Telescope, suggesting that it holds a debris ring with a radius about 120 AU. It could be near-polar, or have 30° misalignment relative to the binary orbit. Although the ring size is a little large compared to the binary orbital semi-major axis, Kennedy et al. [63] still suggested one precession model that could explain the misalignment. This result seems to suggest that the precession triggered by the binary can affect as far as $\sim$8 times of the binary orbital semi-major axis.

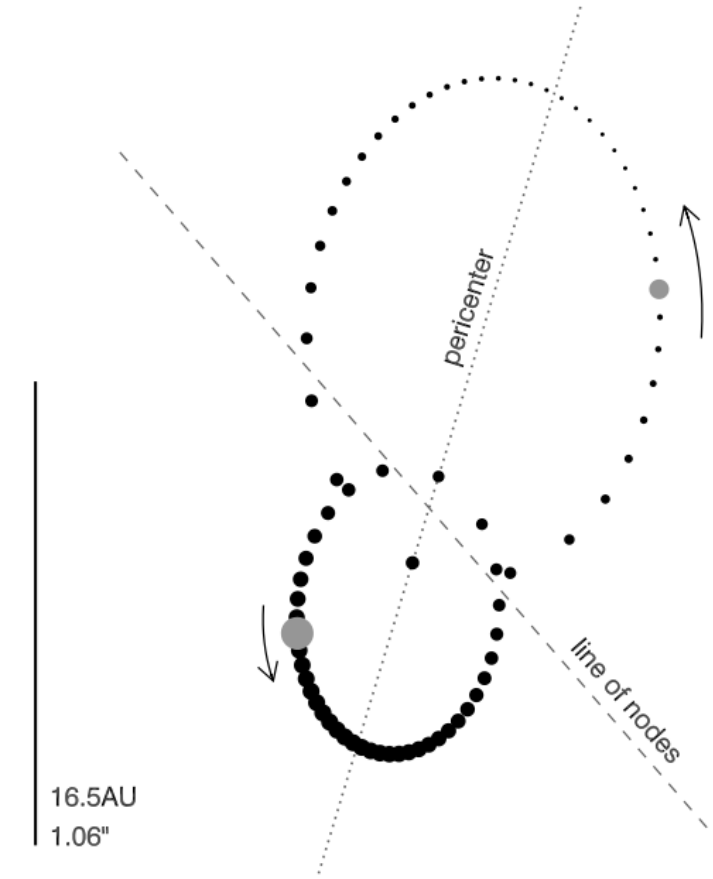

(a)

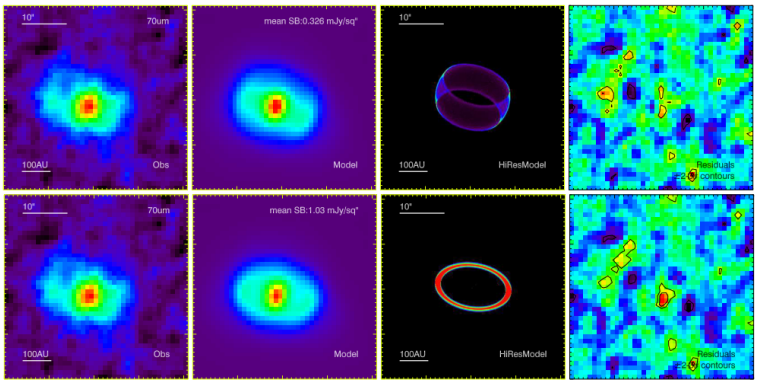

(b)

Fig. 5.2 (a): 99 Her orbit seen in the sky. Figure 1 in Kennedy et al. [63]; (b): 99 Her and its circumbinary disk. *top*: from left to right: 99 Her image in Hershcel/PACS 70μm band, simulated observation of a near-polar circumbinary ring, the appearance of the circumbinary ring, and the residuals between observation and simulations; *bottom*: generally the same but for the case of a circumbinary ring with 30° misalignment relative to the binary orbital plane. Figure 9 and 10 in Kennedy et al. [63].

GW Ori is a hierarchical triple system with total mass about $5.3M_{\odot}$, and GW Ori A/BC has a semi-major axis of about 10 AU [26]. It is located at about 388 pc from us [70]. Its circumtriple disk, has a radius of about 800 AU in 226 GHz continuum and CO lines emission observed by ALMA, and is misaligned about 45° with its orbital plane [26]. Considering that the disk size is about 80 times of the binary orbital semi-major axis, it looks hard for (only) disk-binary interaction to contribute to the disk misalignment. Some other mechanisms may contribute to it, like an undetected (sub-)stellar object near the disk truncates the disk from outside, or the binary orbit changes its orbital plane during its evolution. Future theoretical and observational work could help solve this problem.

In summary, for binaries with separations a little larger, like tens of AUs, it seems to be common that their circumbinary disks are not coplanar with their orbital planes. Based on the analyses of these binary systems, it can be seen that disk-binary interaction combined with procession resonance between the circumbinary disk, circumstellar disk and the binary suggested by Owen and Lai [95] can help explain much disk misalignment in binary systems. However, some of them cannot be explained by these mechanisms well, like TWA 3A, GW Ori, and the circumbinary disks of FS Tau A. Other mechanisms, like truncation from an outer object, or the binary changes the orbit plane itself during evolution, can be responsible for them. Future theoretical and observational work is still necessary to have a better understand of the mechanism triggered disk misalignment.

5.3 Planet formation in binary systems

It is inevitable to talk about planet formation process when we talk about disk evolution. Based on near infrared observation results, it is still not enough to describe the whole planet formation process in binary systems. However, some discussions can still be made, like what kind of binaries can have planets, or which area in the circumbinary disk where planet can form.

For wide (separation > $\sim$100 AU) binaries, researches like Duchêne [31] have shown that their disk evolutions do not have much difference from single stars, so planet formation in wide binaries could be just the same as in single star systems. And for very close (separation < $\sim$ 1 AU) binaries like DQ Tau with large circumbinary disks, it seems that their circumbinary disks are not affected much by the binaries, so planet formation in this kind of disks could be the same as it in disks around single stars.

The most complicated system is close binary, i.e., binary with separation about tens of AU. From our SEEDS observations, as well as observations from other telescopes, the disks in this kind of binaries are affected much by their host stars. The truncations from the binary

Table 5.2 A summary of the binary/multiple systems with disks we discussed from other observations

Star	M_s	t_a	a	e	r_g	Δi	Reference
L1551 NE	0.68/unknown	unknown	∼70	unknown	∼140	∼12/21*	[119]
HD 142527A	2.0/0.13	5.0/1.0**	∼20	0.5	∼90	70*	[7, 87, 77]
DQ Tau	1.3***	1-2	0.13	0.57	–	<2	[25]
UZ Tau E	1.3***	1-2	0.15	0.33	–	<5	[101]
AK Sco	2.5***	18	0.15	0.47	–	<2	[24]
V4046 Sgr	1.8***	10	0.04	∼0	–	<1	[112]
KH 15D	1.3***	∼3	0.28	0.68-0.8	–	10-20	[21, 60, 19]
TWA 3A	∼0.12/0.10	∼10	0.19	0.63	–	>∼30	[4, 62]
HD 98800B	∼0.70/0.58	∼10	∼0.92	∼0.78	–	<∼3	[12, 4]
99 Her	1.4***	6-10 Gyr	16	0.766	–	30or90	[55, 63]
GW Ori	2.7/1.7/0.9	∼1	∼10	unknown	–	∼45	[26]

M_s: stellar mass in solar mass; t_a: age of binary in Myr; a, semi-major axis of binary orbit in AU; e: eccentricity of binary orbit; r_g observed circumbinary disk gap size in AU; Δi: observed misaligned angles between the circumbinary disk and the binary orbital plane;
*: misaligned angle between the circumbinary disk and the circumstellar disks;
**: according to Lacour et al. [77], the ages of the two companions are different
***: the total mass of the binary

significantly changes the disk appearance. A typical disk system in close binary, like GG Tau A, includes a large circumbinary ring with inner edge about 2-3 times of binary orbital semi-major axis, and circumstellar disk around each star, usually one third to one half of binary orbital semi-major axis.

The area between the circumstellar disks and the circumbinary ring is a kind of gap with little materials, cleared by the binary. Although materials in the circumbinary ring can penetrate this kind of gap to go to the circumstellar disks around the stars, as we show in GG Tau A system, it seems hard for materials to have stable orbits in the gap area, and planet formation is also not likely to happen. And since materials can penetrate the gap to reach the circumstellar disks, the circumstellar disks will not dissipate soon, so planet will have the opportunity to form in them, as we have discussed in Chapter 2. As for the circumbinary ring, for GG Tau A system it seems that it is gravitational stable so that at least now it is not suitable for planet formation through gravitational instability, but for other binary systems, it could be gravitational instable for planet to form. And of course, planet formation process like core accretion, is still possible to happen in circumbinary disks. In summary, for a binary system with coplanar circumbinary and circumstellar disks, planet formation can happen in the circumbinary ring, usually farther than 2-3 times of the binary orbital semi-major axis from the binary, or the circumstellar disks, with sizes usually one third to one half of

the binary orbital semi-major axis. For the other areas, planet formation process could be difficult, or it could be hard to detect a planet whose orbital semi-major axis is smaller than twice and larger than half of the binary orbital semi-major axis.

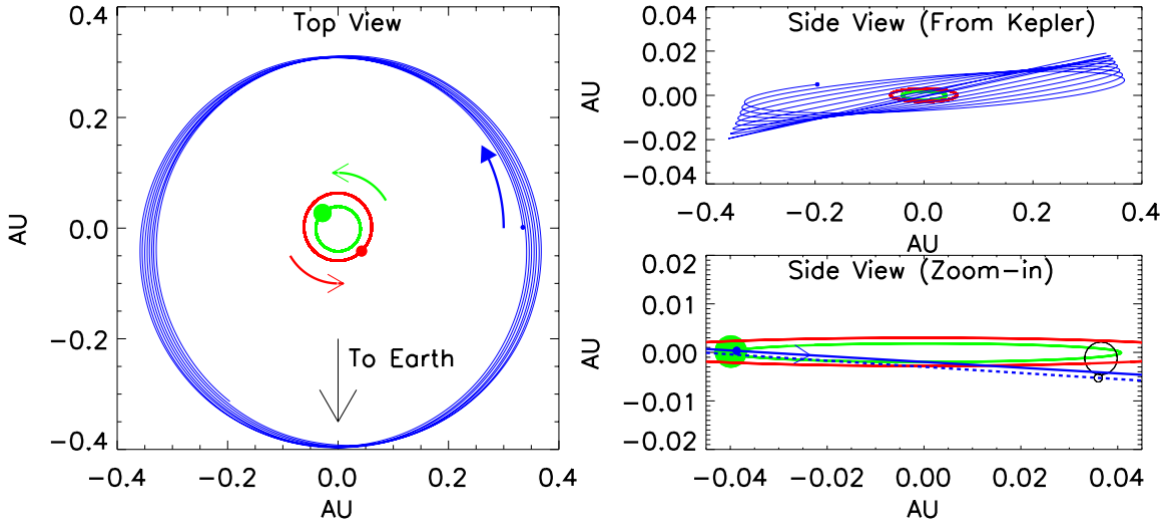

Fig. 5.3 Orbits of the circumbinary planet Kepler-413b and its host binary. *left*: the orbits from top view; *right*: the orbits from side view, it can be seen that there is a small angle between the binary orbital plane and the planet orbital plane. Figure 11 in Kostov et al. [69].

Our observations have shown that, binaries are not only to clear gaps in the disk, but also make the disk misaligned with the binary orbital plane. This rises the problem that if planet can form in these misaligned disks. Although the disk is precessing, dust grain growth can still happen, even if the actual grain growth process could be different from the disks in single star systems. But till now we have not discovered planet whose orbital plane is largely misaligned with the binary orbital plane yet. The only discovery is Kepler-413b, whose orbital plane has an inclination about 2.5° relative to the binary orbital plane, and it could be a result of misaligned circumbinary disk [69]. However, the misaligned angle of Kepler-413b orbital plane is too small, smaller than the possible misaligned angle ranges of the generally coplanar circumbinary disks, like DQ Tau. So in our criteria it can be regarded as generally "coplanar".

However, it does not mean that planet formation in misaligned disks is difficult. The non-detection of planets misaligned with their binary orbital plane is more likely to be a selection effect, because it is not easy to detect planet whose orbital plane is highly misaligned with binary orbital plane through transit. One promising method is eclipsing time variation, which keeps an eye on the variation of binary eclipsing time. Anyway, to detect planet with highly misaligned orbit, we still have many things to do.

Chapter 6

Future scope

In my PhD research, we have observed 4 young binary targets, analyzed the disks around them, showed that how disk evolution is disturbed by the binary. As the binary systems like GG Tau A shows, binary can open gaps in the circumbinary disk, and streamers triggered by the binary can penetrate the gap to sustain the circumstellar disks around each star in the binary system. And in the binary systems like T Tau S, the circumbinary disk becomes misaligned with its host binary orbital plane due to disk-binary interactions. These results can be explained well by current theories.

Of course, as mentioned in Section 5, some structures in some circumbinary disks cannot be explained well by current theory, like the gap size in the circumbinary disk around HD 142527A, and the disk misalignment in binary system like TWA 3A and GW Ori. To solve them, new circumbinary disk evolution theory should be developed.

For observations, we still need to observe more targets to help improve current disk evolution theory. This can be classified into two aspects. One is the observations of circumbinary disks, in this study, we mainly discuss the disk morphology in near-infrared H-band, it is still unknown that if the influence from the binary is wavelength-independent, or if the influence from the binary is the same towards all kinds of materials in the disk. To understand this, we need to observe more disks in different bands. With the help of Subaru Telescope and instrument SCExAO/CHARIS/VAMPIRES we can easily get the disk image in different near infrared bands (J, H, K), and from the ALMA observation data we can get the disk image in sub-millimeter bands, then based on these data we can make a discussion about this topic.

Another is the observations of the binary itself. As my PhD study has shown that, the binary parameters, like the binary mass, orbital semi-major axis and eccentricity, are very important in determining the disk morphology, and it is foreseeable that these parameters can also be related to the grain growth and temperature distributions in the disk. However, from our studies we found out that the parameters of many binaries, especially young binaries,

have not been determined well. In this case, we need observe more young binaries, especially the binary with known circumbinary disks in different methods like radial velocity and direct imaging to get a better constrain of their orbital parameters, then we can have a better discussion of the disk evolutions in these systems.

One more problem we hope to understand is the planet formation process in the disks around binary systems. As we have pointed out in Chapter 5, planet formation can happen in the circumbinary disks around the two stars, and since materials in the circumbinary disks can penetrate the gap between the circumbinary disks and the circumstellar disks around the stars, the circumstellar disks around each star will not dissipate so quickly, this gives the chance for planet formation. This can help explain some planets discovered in close binary systems, like γ Cep Ab. However, just from the disk structures observed in near-infrared band, it is not enough to learn the detailed planet formation process in binary systems. To learn the details, we need to know more parameters of the circumbinary disks, like the distributions of gas, large dusts and temperature.

As planet formation starts from grain growth, to learn it we need to know the grain growth in the disk, so it is necessary for us to investigate the distributions of large dust in the disk. Optical/Near infrared band observation by large ground-based telescope, like Keck telescopes, Subaru Telescope have given us a good view of the distribution of small dusts $\sim \mu m$ in circumbinary disks. For dusts with sizes $\sim$1 mm, now ALMA has given us a good spatial resolution, like Takakuwa et al. [119]. Besides large dusts distributions, ALMA can also give us the gas distributions in the disk with a good spatial resolution. I hope in the future we can learn more from ALMA observations. In addition, for gas giant formation via core accretion, the environmental temperature around the core should not be too high. This indicates that, disk temperature is also one of the important parameters for planet formation. In binary systems, the binary will affect the disk temperature by affecting the motion of the dusts and gas in the disk, so to understand planet formation in binary systems, it is important to know the temperature distributions in the disks. To investigate temperature, we can use some special molecule emission lines, like the molecule hydrogen emission line in near-infrared band (e.g., Beck et al. [8]), or the CO 6-5 emission line (e.g., Dutrey et al. [35]). In summary, to learn the details of planet formation process in binary systems, it is important to combine observational data in different wavelengths and different methods.

It could be better if we can catch a forming planet directly. Currently there is only one forming planet candidate discovered, LkCa 15 b [74, 113]. We still need more surveys to discover more forming planet, especially in binary systems. Also, the accretion in the circumplanetary disk will significantly raise the temperature, this makes it possible to find

out planets in the disk by investigating some high temperature area via some special molecule emission lines.

In addition, our observations show that as least T Tau S and FS Tau hold misaligned circumbinary disks relative to their host stars' orbital plane, but till now we have not detected any planets with highly-misaligned orbits. As I have pointed out in Chapter 5, this is more likely to be a selection effect, so there should exist planets whose orbital plane is misaligned with their host binaries. For transit method, as I have mentioned in Chapter 5, the binary eclipse time variation could be a promising method. With the help of transit observing satellite like Kepler Telescope, and TESS telescope which will be launched in 2018, we may be able to do it.

Direct imaging on large telescopes should also be one method in detecting planets in binary systems and constraining their orbital parameters. The next-generation telescopes like the future 30-m telescope Thirty Meter Telescope (TMT), will have a much better spatial resolution and sensitivity. With its help, we will be able to detect faint planets in binary systems, observe disks in more faint binaries, to resolve the detailed structures in the disks around the binaries, especially with the next generation coronagraph we will be able to observe disks closer than $\sim$1 AU in the binary systems, which will be crucial for us to learn the disk evolution as well as planet formation in binary systems. Middle infrared observations from space telescopes like James Webb Space Telescope (JWST), a 6.5m telescope which will be launched in 2019 and work at the second Lagrangian point, will bring us a good view of the distributions of colder, and larger dusts than those traced at near-infrared in the disk. Now some young binaries, like DQ Tau, are too faint to observe with current instruments, but with the next generation telescopes like TMT, we will be able to get their high-resolution images, which will be good supplement for ALMA observations.

Stars tend to form in binary or multiple systems, so planet formation usually occurs in binary or multiple systems. Therefore, to learn the planet formation process, it is quite important for us to investigate the protoplanetary disks in young binaries. The research of disks in young binaries has developed rapidly in the recent years, and in the upcoming future, with extensive observations with ALMA as well as the commission of the next generation telescopes like JWST and TMT, we will be able to combine excellent observation results in different wavelengths, to learn more about the disk evolution, as well as planet formation, in binary systems.

References

[1] Adelman-McCarthy, J. K. and et al. (2009). VizieR Online Data Catalog: The SDSS Photometric Catalog, Release 7 (Adelman-McCarthy+, 2009). *VizieR Online Data Catalog*, 2294.

[2] Akeson, R. L., Koerner, D. W., and Jensen, E. L. N. (1998). A Circumstellar Dust Disk around T Tauri N: Subarcsecond Imaging at $\lambda = 3$ Millimeters. *The Astrophysical Journal*, 505(1):358–362.

[3] Andrews, S. M., Chandler, C. J., Isella, A., Birnstiel, T., Rosenfeld, K. a., Wilner, D. J., Pérez, L. M., Ricci, L., Carpenter, J. M., Calvet, N., Corder, S. a., Deller, a. T., Dullemond, C. P., Greaves, J. S., Harris, R. J., Henning, T., Kwon, W., Lazio, J., Linz, H., Mundy, L. G., Sargent, a. I., Storm, S., and Testi, L. (2014). RESOLVED MULTIFREQUENCY RADIO OBSERVATIONS OF GG Tau. *The Astrophysical Journal*, 787:148.

[4] Andrews, S. M., Czekala, I., Wilner, D. J., Espaillat, C., Dullemond, C. P., and Hughes, A. M. (2010). Truncated disks in TW Hya association multiple star systems. *Astrophysical Journal*, 710(1):462–469.

[5] Artymowicz, P. and Lubow, S. H. (1994). Dynamics of binary-disk interaction. 1: Resonances and disk gap sizes. *The Astrophysical Journal*, 421:651.

[6] Arzoumanian, Z., Joshi, K., Rasio, F. A., and Thorsett, S. E. (1996). Orbital Parameters of the PSR B1620-26 Triple System. In Johnston, S., Walker, M. A., and Bailes, M., editors, *IAU Colloq. 160: Pulsars: Problems and Progress*, volume 105 of *Astronomical Society of the Pacific Conference Series*, pages 525–530.

[7] Avenhaus, H., Quanz, S. P., Schmid, H. M., Meyer, M. R., Garufi, A., Wolf, S., and Dominik, C. (2014). Structures in the Protoplanetary Disk of Hd142527 Seen in Polarized Scattered Light. *The Astrophysical Journal*, 781(2):87.

[8] Beck, T. L., Bary, J. S., Dutrey, A., Piétu, V., Guilloteau, S., Lubow, S. H., and Simon, M. (2012). CIRCUMBINARY GAS ACCRETION ONTO A CENTRAL BINARY: INFRARED MOLECULAR HYDROGEN EMISSION FROM GG Tau A. *The Astrophysical Journal*, 754:72.

[9] Beck, T. L., Prato, L., and Simon, M. (2001). Evidence for Extinction and Accretion Variability in T Tauri South. *The Astrophysical Journal*, 551(2):1031–1036.

[10] Beust, H. and Dutrey, A. (2005). Dynamics of the young multiple system GG Tauri. I. Orbital fits and inner edge of the circumbinary disk of GG Tau A. *Astronomy & Astrophysics*, 439(2):585–594.

[11] Beust, H. and Dutrey, A. (2006). Dynamics of the young multiple system GGTauri II. Relation between the stellar system and the circumbinary disk. *Astronomy and Astrophysics*, 446(1):137–154.

[12] Boden, A. F., Sargent, A. I., Akeson, R. L., Carpenter, J. M., Torres, G., Latham, D. W., Soderblom, D. R., Nelan, E., Franz, O. G., and Wasserman, L. H. (2005). Dynamical Masses for Low-Mass Pre–Main-Sequence Stars: A Preliminary Physical Orbit for HD 98800 B. *The Astrophysical Journal*, 635(1):442–451.

[13] Bohm, K.-H. and Solf, J. (1994). A sub-arcecond-scale spectroscopic study of the complex mass outflows in the vicinity of T Tauri. *The Astrophysical Journal*, 430:277.

[14] Bourgés, L., Lafrasse, S., Mella, G., Chesneau, O., Bouquin, J. L., Duvert, G., Chelli, A., and Delfosse, X. (2014). The JMMC Stellar Diameters Catalog v2 (JSDC): A New Release Based on SearchCal Improvements. In Manset, N. and Forshay, P., editors, *Astronomical Data Analysis Software and Systems XXIII*, volume 485 of *Astronomical Society of the Pacific Conference Series*, page 223.

[15] Brogi, M., Snellen, I. A. G., de Kok, R. J., Albrecht, S., Birkby, J., and de Mooij, E. J. W. (2012). The signature of orbital motion from the dayside of the planet τ Boötis b. *Nature*, 486(7404):502–504.

[16] Butler, R. P., Marcy, G. W., Williams, E., Hauser, H., and Shirts, P. (1997). Three New "51 Pegasi-Type" Planets. *The Astrophysical Journal*, 474(2):L115–L118.

[17] Butler, R. P., Wright, J. T., Marcy, G. W., Fischer, D. A., Vogt, S. S., Tinney, C. G., Jones, H. R. A., Carter, B. D., Johnson, J. A., McCarthy, C., and Penny, A. J. (2006). Catalog of Nearby Exoplanets. *The Astrophysical Journal*, 646(1):505–522.

[18] Campbell, B., Walker, G. A. H., and Yang, S. (1988). A search for substellar companions to solar-type stars. *The Astrophysical Journal*, 331(1978):902.

[19] Capelo, H. L., Herbst, W., Leggett, S. K., Hamilton, C. M., and Johnson, J. A. (2012). Locating the trailing edge of the circumbinary ring in the KH 15D system. *Astrophysical Journal Letters*, 757(1):1–5.

[20] Cazzoletti, P., Ricci, L., Birnstiel, T., and Lodato, G. (2017). Testing dust trapping in the circumbinary disk around GG Tauri A. *Astronomy & Astrophysics*, 599(1994):A102.

[21] Chiang, E. I. and Murray-Clay, R. A. (2004). The Circumbinary Ring of KH 15D. *The Astrophysical Journal*, 607(2):913–920.

[22] Csépány, G., van den Ancker, M., Ábrahám, P., Brandner, W., and Hormuth, F. (2015). Examining the T Tauri system with SPHERE. *Astronomy & Astrophysics*, 578:L9.

[23] Currie, T., Daemgen, S., Debes, J., Lafreniere, D., Itoh, Y., Jayawardhana, R., Ratzka, T., and Correia, S. (2014). DIRECT IMAGING AND SPECTROSCOPY OF A CANDIDATE COMPANION BELOW/NEAR THE DEUTERIUM-BURNING LIMIT IN THE YOUNG BINARY STAR SYSTEM, ROXs 42B. *The Astrophysical Journal*, 780(2):L30.

[24] Czekala, I., Andrews, S. M., Jensen, E. L. N., Stassun, K. G., Torres, G., and Wilner, D. J. (2015). A DISK-BASED DYNAMICAL MASS ESTIMATE FOR THE YOUNG BINARY AK SCO. *The Astrophysical Journal*, 806(2):154.

[25] Czekala, I., Andrews, S. M., Torres, G., Jensen, E. L. N., Stassun, K. G., Wilner, D. J., and Latham, D. W. (2016). A DISK-BASED DYNAMICAL CONSTRAINT ON THE MASS OF THE YOUNG BINARY DQ TAU. *The Astrophysical Journal*, 818(2):156.

[26] Czekala, I., Andrews, S. M., Torres, G., Rodriguez, J. E., Jensen, E. L. N., Stassun, K. G., Latham, D. W., Wilner, D. J., Gully-Santiago, M. A., Grankin, K. N., Lund, M. B., Kuhn, R. B., Stevens, D. J., Siverd, R. J., James, D., Gaudi, B. S., Shappee, B. J., and Holoien, T. W.-S. (2017). The Architecture of the GW Ori Young Triple-star System and Its Disk: Dynamical Masses, Mutual Inclinations, and Recurrent Eclipses. *The Astrophysical Journal*, 851(2):132.

[27] D'Alessio, P., Hartmann, L., Calvet, N., Franco-Hernández, R., Forrest, W. W. J., Sargent, B., Furlan, E., Uchida, K., Green, J. D. J., Watson, D. D. M., Chen, C. H. C., Kemper, F., Sloan, G. C., Najita, J., Franco-Hernandez, R., Forrest, W. W. J., Sargent, B., Furlan, E., Uchida, K., Green, J. D. J., Watson, D. D. M., Chen, C. H. C., Kemper, F., Sloan, G. C., and Najita, J. (2005). The Truncated Disk of CoKu Tau/4. *The Astrophysical Journal*, 621(1):461–472.

[28] Degl'innocenti, E. L. and Landolfi, M. (2004). *Polarization in Spectral Lines*. Springer Netherlands, Dordrecht.

[29] Di Folco, E., Dutrey, A., Le Bouquin, J.-B., Lacour, S., Berger, J.-P., Köhler, R., Guilloteau, S., Piétu, V., Bary, J., Beck, T., Beust, H., and Pantin, E. (2014). GG Tauri: the fifth element. *Astronomy & Astrophysics*, 565:L2.

[30] Doyle, L. R., Carter, J. a., Fabrycky, D. C., Slawson, R. W., Howell, S. B., Winn, J. N., Orosz, J. a., Prša, A., Welsh, W. F., Quinn, S. N., Latham, D., Torres, G., Buchhave, L. a., Marcy, G. W., Fortney, J. J., Shporer, A., Ford, E. B., Lissauer, J. J., Ragozzine, D., Rucker, M., Batalha, N., Jenkins, J. M., Borucki, W. J., Koch, D., Middour, C. K., Hall, J. R., McCauliff, S., Fanelli, M. N., Quintana, E. V., Holman, M. J., Caldwell, D. a., Still, M., Stefanik, R. P., Brown, W. R., Esquerdo, G. a., Tang, S., Furesz, G., Geary, J. C., Berlind, P., Calkins, M. L., Short, D. R., Steffen, J. H., Sasselov, D., Dunham, E. W., Cochran, W. D., Boss, A., Haas, M. R., Buzasi, D., and Fischer, D. (2011). Kepler-16: a transiting circumbinary planet. *Science*, 333(6049):1602–1606.

[31] Duchêne, G. (2010). Planet Formation in Binary Systems: a Separation-Dependent Mechanism? *The Astrophysical Journal*, 709(2):L114–L118.

[32] Duchêne, G., Ghez, A. M., McCabe, C., and Ceccarelli, C. (2005). The Circumstellar Environment of T Tauri S at High Spatial and Spectral Resolution. *The Astrophysical Journal*, 628(2):832–846.

[33] Duchêne, G. and Kraus, A. (2013). Stellar Multiplicity. *Annual Review of Astronomy and Astrophysics*, 51(1):269–310.

[34] Duquennoy, A. and Mayor, M. (1991). Multiplicity among solar-type stars in the solar neighbourhood. II - Distribution of the orbital elements in an unbiased sample. *Astronomy & Astrophysics*, 248:485–524.

[35] Dutrey, A., Di Folco, E., Guilloteau, S., Boehler, Y., Bary, J., Beck, T., Beust, H., Chapillon, E., Gueth, F., Huré, J.-M., Pierens, A., Piétu, V., Simon, M., and Tang, Y.-W. (2014). Possible planet formation in the young, low-mass, multiple stellar system GG Tau A. *Nature*, 514:600–602.

[36] Dutrey, A., Guilloteau, S., and Simon, M. (1994). Images of the GG Tauri rotating ring. *Astronomy & Astrophysics*, 286:149–159.

[37] Dyck, H. M., Simon, T., and Zuckerman, B. (1982). Discovery of an infrared companion to T Tauri. *The Astrophysical Journal*, 255:L103–L106.

[38] Eggl, S., Pilat-Lohinger, E., Funk, B., Georgakarakos, N., and Haghighipour, N. (2013). Circumstellar habitable zones of binary-star systems in the solar neighbourhood. *Monthly Notices of the Royal Astronomical Society*, 428(4):3104–3113.

[39] Eislöffel, J. and Mundt, R. (1998). Imaging and Kinematic Studies of Young Stellar Object Jets in Taurus. *The Astronomical Journal*, 115(4):1554–1575.

[40] Fabricius, C., Høg, E., Makarov, V. V., Mason, B. D., Wycoff, G. L., and Urban, S. E. (2002). The Tycho double star catalogue. *Astronomy & Astrophysics*, 384:180–189.

[41] Farris, B. D., Duffell, P., MacFadyen, A. I., and Haiman, Z. (2014). Binary Black Hole Accretion From a Circumbinary Disk: Gas Dynamics Inside the Central Cavity. *The Astrophysical Journal*, 783(2):134.

[42] Fischer, D. A., Marcy, G. W., Butler, R. P., Vogt, S. S., Laughlin, G., Henry, G. W., Abouav, D., Peek, K. M. G., Wright, J. T., Johnson, J. A., McCarthy, C., and Isaacson, H. (2008). Five Planets Orbiting 55 Cancri. *The Astrophysical Journal*, 675(1):790–801.

[43] Foucart, F. and Lai, D. (2013). ASSEMBLY OF PROTOPLANETARY DISKS AND INCLINATIONS OF CIRCUMBINARY PLANETS. *The Astrophysical Journal*, 764(1):106.

[44] Foucart, F. and Lai, D. (2014). Evolution of linear warps in accretion discs and applications to protoplanetary discs in binaries. *Monthly Notices of the Royal Astronomical Society*, 445(2):1731–1744.

[45] Furlan, E., Hartmann, L., Calvet, N., D'Alessio, P., Franco-Hernandez, R., Forrest, W. J., Watson, D. M., Uchida, K. I., Sargent, B., Green, J. D., Keller, L. D., and Herter, T. L. (2006). A Survey and Analysis of Spitzer Infrared Spectrograph Spectra of T Tauri Stars in Taurus. *The Astrophysical Journal Supplement Series*, 165(2):568–605.

[46] G. Martin, R., Armitage, P. J., and Alexander, R. D. (2013). Formation of Circumbinary Planets in a Dead Zone. *The Astrophysical Journal*, 773(1):74.

[47] Guilloteau, S., Dutrey, A., and Simon, M. (1999). GG Tauri: the ring world. *Astronomy & Astrophysics*, 348:570–578.

[48] Gustafsson, M., Kristensen, L. E., Kasper, M., and Herbst, T. M. (2010). The origin, excitation, and evolution of subarcsecond outflows near T Tauri. *Astronomy and Astrophysics*, 517:A19.

[49] Gustafsson, M., Labadie, L., Herbst, T. M., and Kasper, M. (2008). Spatially resolved H 2 emission from the disk around T Tau N. *Astronomy and Astrophysics*, 488(1):235–244.

[50] Hatzes, A. P., Cochran, W. D., Endl, M., McArthur, B., Paulson, D. B., Walker, G. A. H., Campbell, B., and Yang, S. (2003). A Planetary Companion to γ Cephei A. *The Astrophysical Journal*, 599(2):1383–1394.

[51] Hayano, Y., Takami, H., Oya, S., Hattori, M., Saito, Y., Watanabe, M., Guyon, O., Minowa, Y., Egner, S. E., Ito, M., Garrel, V., Colley, S., Golota, T., and Iye, M. (2010). Commissioning status of Subaru laser guide star adaptive optics system. In Ellerbroek, B. L., Hart, M., Hubin, N., and Wizinowich, P. L., editors, *Proceedings of the SPIE*, pages 77360N–77360N–8.

[52] Herbst, T. M., Hartung, M., Kasper, M. E., Leinert, C., and Ratzka, T. (2007). Molecular Hydrogen Outflows in the Central Arcseconds of the T Tauri System. *The Astronomical Journal*, 134(1):359–366.

[53] Hioki, T., Itoh, Y., Oasa, Y., Fukagawa, M., and Hayashi, M. (2011). High-Resolution Optical and Near-Infrared Images of the FS Tauri Circumbinary Disk. *Publications of the Astronomical Society of Japan*, 63(3):543–554.

[54] Hogerheijde, M. R., van Langevelde, H. J., Mundy, L. G., Blake, G. A., and van Dishoeck, E. F. (1997). Subarcsecond Imaging at 267 GH[CLC]z[/CLC] of a Young Binary System: Detection of a Dust Disk of Radius Less than 70 AU around T Tauri N. *The Astrophysical Journal*, 490(1):L99–L102.

[55] Holmberg, J., Nordström, B., and Andersen, J. (2009). The Geneva-Copenhagen survey of the solar neighbourhood. *Astronomy & Astrophysics*, 501(3):941–947.

[56] Horch, E. P., Howell, S. B., Everett, M. E., and Ciardi, D. R. (2014). Most Sub-Arcsecond Companions of Kepler Exoplanet Candidate Host Stars Are Gravitationally Bound. *The Astrophysical Journal*, 795(1):60.

[57] Ireland, M. J. and Kraus, A. L. (2008). The Disk Around CoKu Tauri/4: Circumbinary, Not Transitional. *The Astrophysical Journal*, 678:L59.

[58] Itoh, Y., Oasa, Y., Kudo, T., Kusakabe, N., Hashimoto, J., Abe, L., Brandner, W., Brandt, T. D., Carson, J. C., Egner, S., Feldt, M., Grady, C. A., Guyon, O., Hayano, Y., Hayashi, M., Hayashi, S. S., Henning, T., Hodapp, K. W., Ishii, M., Iye, M., Janson, M., Kandori, R., Knapp, G. R., Kuzuhara, M., Kwon, J., Matsuo, T., McElwain, M. W., Miyama, S., Morino, J.-I., Moro-Martin, A., Nishimura, T., Pyo, T.-S., Serabyn, E., Suenaga, T., Suto, H., Suzuki, R., Takahashi, Y. H., Takato, N., Terada, H., Thalmann, C., Tomono, D., Turner, E. L., Watanabe, M., Wisniewski, J., Yamada, T., Mayama, S., Currie, T., Takami, H., Usuda, T., and Tamura, M. (2014). Near-infrared polarimetry of the GG Tauri A binary system. *Research in Astronomy and Astrophysics*, 14:1438–1446.

[59] Jensen, E. L. N. and Akeson, R. (2014). Misaligned protoplanetary disks in a young binary star system. *Nature*, 511(7511):567–569.

[60] Johnson, J. a., Marcy, G. W., Hamilton, C. M., Herbst, W., and Johns-Krull, C. M. (2004). KH 15D: A Spectroscopic Binary. *The Astronomical Journal*, 128(3):8.

[61] Kasper, M., Santhakumari, K. K. R., Herbst, T. M., and Köhler, R. (2016). New circumstellar structure in the T Tauri system. *Astronomy & Astrophysics*, 593(2002):A50.

[62] Kellogg, K., Prato, L., Torres, G., Schaefer, G. H., Avilez, I., Ruíz-Rodríguez, D., Wasserman, L. H., Bonanos, A. Z., Guenther, E. W., Neuhäuser, R., Levine, S. E., Bosh, A. S., Morzinski, K. M., Close, L., Bailey, V., Hinz, P., and Males, J. R. (2017). The TWA 3 Young Triple System: Orbits, Disks, Evolution. *The Astrophysical Journal*, 844(2):1–47.

[63] Kennedy, G. M., Wyatt, M. C., Sibthorpe, B., Duchêne, G., Kalas, P., Matthews, B. C., Greaves, J. S., Su, K. Y. L., and Fitzgerald, M. P. (2012). 99 Herculis: host to a circumbinary polar-ring debris disc. *Monthly Notices of the Royal Astronomical Society*, 421(3):2264–2276.

[64] Kenyon, S. J., Dobrzycka, D., and Hartmann, L. (1994). A new optical extinction law and distance estimate for the Taurus-Auriga molecular cloud. *The Astronomical Journal*, 108(9):1872.

[65] Kenyon, S. J. and Hartmann, L. (1995). Pre-Main-Sequence Evolution in the Taurus-Auriga Molecular Cloud. *The Astrophysical Journal Supplement Series*, 101:117.

[66] Köhler, R. (2011). The orbit of GG Tauri A. *Astronomy & Astrophysics*, 530:A126.

[67] Köhler, R., Kasper, M., Herbst, T. M., Ratzka, T., and Bertrang, G. H.-M. (2016). Orbits in the T Tauri triple system observed with SPHERE. *Astronomy & Astrophysics*, 587:A35.

[68] Koresko, C. D. (2000). A Third Star in the T Tauri System. *The Astrophysical Journal*, 531:L147–L149.

[69] Kostov, V. B., McCullough, P. R., Carter, J. A., Deleuil, M., Díaz, R. F., Fabrycky, D. C., Hébrard, G., Hinse, T. C., Mazeh, T., Orosz, J. A., Tsvetanov, Z. I., and Welsh, W. F. (2014). Kepler-413B: A slightly misaligned, neptune-size transiting circumbinary planet. *Astrophysical Journal*, 784(1).

[70] Kounkel, M., Hartmann, L., Loinard, L., Ortiz-León, G. N., Mioduszewski, A. J., Rodríguez, L. F., Dzib, S. A., Torres, R. M., Pech, G., Galli, P. A. B., Rivera, J. L., Boden, A. F., Evans II, N. J., Briceño, C., and Tobin, J. J. (2017). THE GOULD'S BELT DISTANCES SURVEY (GOBELINS). II. DISTANCES AND STRUCTURE TOWARD THE ORION MOLECULAR CLOUDS. *The Astrophysical Journal*, 834(2):142.

[71] Kozai, Y. (1962). Secular perturbations of asteroids with high inclination and eccentricity. *The Astronomical Journal*, 67(1):591.

[72] Kraus, A. L. and Hillenbrand, L. a. (2009). The Coevality of Young Binary Systems. *The Astrophysical Journal*, 704:531–547.

[73] Kraus, A. L. and Ireland, M. J. (2012). LkCa 15: A YOUNG EXOPLANET CAUGHT AT FORMATION? *The Astrophysical Journal*, 745(1):5.

[74] Kraus, A. L., Ireland, M. J., Hillenbrand, L. a., and Martinache, F. (2012). THE ROLE OF MULTIPLICITY IN DISK EVOLUTION AND PLANET FORMATION. *The Astrophysical Journal*, 745(1):19.

[75] Krist, J. E., Stapelfeldt, K. R., Golimowski, D. A., Ardila, D. R., Clampin, M., Martel, A. R., Ford, H. C., Illingworth, G. D., and Hartig, G. F. (2005). HST/ACS Images of the GG Tauri Circumbinary Disk. *The Astronomical Journal*, 130(6):2778–2787.

[76] Krist, J. E., Stapelfeldt, K. R., and Watson, A. M. (2002). Hubble Space Telescope/WFPC2 Images of the GG Tauri Circumbinary Disk. *The Astrophysical Journal*, 570:785–792.

[77] Lacour, S., Biller, B., Cheetham, A., Greenbaum, A., Pearce, T., Marino, S., Tuthill, P., Pueyo, L., Mamajek, E. E., Girard, J. H., Sivaramakrishnan, A., Bonnefoy, M., Baraffe, I., Chauvin, G., Olofsson, J., Juhasz, A., Benisty, M., Pott, J.-U., Sicilia-Aguilar, A., Henning, T., Cardwell, A., Goodsell, S., Graham, J. R., Hibon, P., Ingraham, P., Konopacky, Q., Macintosh, B., Oppenheimer, R., Perrin, M., Rantakyrö, F., Sadakuni, N., and Thomas, S. (2016). An M-dwarf star in the transition disk of Herbig HD 142527. *Astronomy & Astrophysics*, 590:A90.

[78] Lidov, M. L. (1962). The evolution of orbits of artificial satellites of planets under the action of gravitational perturbations of external bodies. *Planetary and Space Science*, 9:719–759.

[79] Liu, C.-F., Shang, H., Pyo, T.-S., Takami, M., Walter, F. M., Yan, C.-H., Wang, S.-Y., Ohashi, N., and Hayashi, M. (2012). IS FS Tau B DRIVING AN ASYMMETRIC JET? *The Astrophysical Journal*, 749:62.

[80] Loinard, L., Torres, R. M., Mioduszewski, A. J., Rodriguez, L. F., Gonzalez Lopezlira, R. A., Lachaume, R., Vazquez, V., and Gonzalez, E. (2007). VLBA Determination of the Distance to Nearby Star-forming Regions. I. The Distance to T Tauri with 0.4% Accuracy. *The Astrophysical Journal*, 671(1):546–554.

[81] Luhman, K. L., Allen, P. R., Espaillat, C., Hartmann, L., and Calvet, N. (2010). the Disk Population of the Taurus Star-Forming Region. *The Astrophysical Journal Supplement Series*, 186(1):111–174.

[82] Mamajek, E. E. (2005). A Moving Cluster Distance to the Exoplanet 2M1207b in the TW Hydrae Association. *The Astrophysical Journal*, 634:1385.

[83] Martin, R. G. and Lubow, S. H. (2017). Polar Alignment of a Protoplanetary Disk around an Eccentric Binary. *The Astrophysical Journal*, 835(2):L28.

[84] Mayama, S., Tamura, M., Hanawa, T., Matsumoto, T., Ishii, M., Pyo, T.-S., Suto, H., Naoi, T., Kudo, T., Hashimoto, J., Nishiyama, S., Kuzuhara, M., and Hayashi, M. (2010). Direct imaging of bridged twin protoplanetary disks in a young multiple star. *Science*, 327(5963):306–8.

[85] Mayama, S., Tamura, M., Hayashi, M., Itoh, Y., Fukagawa, M., Suto, H., Ishii, M., Murakawa, K., Oasa, Y., Hayashi, S. S., Yamashita, T., Morino, J., Oya, S., Naoi, T., Pyo, T.-S., Nishikawa, T., Kudo, T., Usuda, T., Ando, H., Miyama, S. M., and Kaifu, N. (2006). Subaru Near Infrared Coronagraphic Images of T Tauri. *Publications of the Astronomical Society of Japan*, 58(2):375–382.

[86] Mayor, M. and Queloz, D. (1995). A Jupiter-mass companion to a solar-type star. *Nature*, 378(6555):355–359.

[87] Mendigutía, I., Fairlamb, J., Montesinos, B., Oudmaijer, R. D., Najita, J. R., Brittain, S. D., and Van Den Ancker, M. E. (2014). Stellar parameters and accretion rate of the transition disk star HD 142527 from X-shooter. *The Astrophysical Journal*, 790(1):4–11.

[88] Miranda, R. and Lai, D. (2015). Tidal truncation of inclined circumstellar and circumbinary discs in young stellar binaries. *Monthly Notices of the Royal Astronomical Society*, 452(3):2396–2409.

[89] Murakawa, K. (2010). Polarization disks in near-infrared high-resolution imaging. *Astronomy & Astrophysics*, 518:1–8.

[90] Nagel, E., D'Alessio, P., Calvet, N., Espaillat, C., Sargent, B., Hernández, J., and Forrest, W. J. (2010). WALL EMISSION IN CIRCUMBINARY DISKS: THE CASE OF CoKu TAU/4. *The Astrophysical Journal*, 708(1):38–50.

[91] Nelson, A. F. and Marzari, F. (2016). DYNAMICS OF CIRCUMSTELLAR DISKS. III. THE CASE OF GG Tau A. *The Astrophysical Journal*, 827(2):93.

[92] Neuhaeuser, R., Mugrauer, M., Fukagawa, M., Torres, G., and Schmidt, T. (2007). Direct detection of exoplanet host star companion gamma Cep B and revised masses for both stars and the sub-stellar object. *Astronomy & Astrophysics*, 462(6581):777–780.

[93] Nixon, C. and Lubow, S. H. (2015). Resonances in retrograde circumbinary discs. *Monthly Notices of the Royal Astronomical Society*, 448(4):3472–3483.

[94] Oh, D., Hashimoto, J., Carson, J. C., Janson, M., Kwon, J., Nakagawa, T., Mayama, S., Uyama, T., Yang, Y., Kudo, T., Kusakabe, N., Abe, L., Akiyama, E., Brandner, W., Brandt, T. D., Currie, T., Feldt, M., Goto, M., Grady, C. A., Guyon, O., Hayano, Y., Hayashi, M., Hayashi, S. S., Henning, T., Hodapp, K. W., Ishii, M., Iye, M., Kandori, R., Knapp, G. R., Kuzuhara, M., Matsuo, T., Mcelwain, M. W., Miyama, S., Morino, J.-I., Moro-Martin, A., Nishimura, T., Pyo, T.-S., Serabyn, E., Suenaga, T., Suto, H., Suzuki, R., Takahashi, Y. H., Takato, N., Terada, H., Thalmann, C., Turner, E. L., Watanabe, M., Yamada, T., Takami, H., Usuda, T., and Tamura, M. (2016). A RESOLVED NEAR-INFRARED IMAGE OF THE INNER CAVITY IN THE GM Aur TRANSITIONAL DISK. *The Astrophysical Journal*, 831(1):L7.

[95] Owen, J. E. and Lai, D. (2017). Generating large misalignments in gapped and binary discs. *Monthly Notices of the Royal Astronomical Society*, 469(3):2834–2844.

[96] Palla, F. and Stahler, S. W. (2002). Star Formation in Space and Time: Taurus-Auriga. *The Astrophysical Journal*, 581:1194–1203.

[97] Pelupessy, F. I. and Zwart, S. P. (2013). The formation of planets in circumbinary discs. *Monthly Notices of the Royal Astronomical Society*, 429(1):895–902.

[98] Perrin, M. D., Schneider, G., Duchene, G., Pinte, C., Grady, C. A., Wisniewski, J. P., and Hines, D. C. (2009). THE CASE OF AB AURIGAE'S DISK IN POLARIZED LIGHT: IS THERE TRULY A GAP? *The Astrophysical Journal*, 707(2):L132–L136.

[99] Piétu, V., Gueth, F., Hily-Blant, P., Schuster, K.-F., and Pety, J. (2011). High resolution imaging of the GG Tauri system at 267 GHz. *Astronomy & Astrophysics*, 528:A81.

[100] Podio, L., Kamp, I., Codella, C., Nisini, B., Aresu, G., Brittain, S., Cabrit, S., Dougados, C., Grady, C., Meijerink, R., Sandell, G., Spaans, M., Thi, W.-F., White, G. J., and Woitke, P. (2014). PROBING THE GASEOUS DISK OF T Tau N WITH CN 5-4 LINES. *The Astrophysical Journal*, 783(2):L26.

[101] Prato, L., Simon, M., Mazeh, T., Zucker, S., and McLean, I. S. (2002). Component Masses of the Young Spectroscopic Binary UZ Tau E. *The Astrophysical Journal Letters*, 579(2):L99–L102.

[102] Rafikov, R. R. (2013). PLANET FORMATION IN SMALL SEPARATION BINARIES: NOT SO SECULARLY EXCITED BY THE COMPANION. *The Astrophysical Journal*, 765(1):L8.

[103] Rafikov, R. R. and Silsbee, K. (2015). PLANET FORMATION IN STELLAR BINARIES. II. OVERCOMING THE FRAGMENTATION BARRIER IN α CENTAURI AND γ CEPHEI-LIKE SYSTEMS. *The Astrophysical Journal*, 798(2):70.

[104] Raghavan, D., Henry, T. J., Mason, B. D., Subasavage, J. P., Jao, W.-c., Beaulieu, T. D., and Hambly, N. C. (2006). Two Suns in The Sky: Stellar Multiplicity in Exoplanet Systems. *The Astrophysical Journal*, 646:523–542.

[105] Raghavan, D., McAlister, H. A., Henry, T. J., Latham, D. W., Marcy, G. W., Mason, B. D., Gies, D. R., White, R. J., and Ten Brummelaar, T. A. (2010). A survey of stellar families: Multiplicity of solar-type stars. *The Astrophysical Journal Supplement*, 190(1):1–42.

[106] Ratzka, T., Schegerer, a. a., Leinert, C., Ábrahám, P., Henning, T., Herbst, T. M., Köhler, R., Wolf, S., and Zinnecker, H. (2009). Spatially resolved mid-infrared observations of the triple system T Tauri. *Astronomy and Astrophysics*, 502(2):623–646.

[107] Ray, T. P., Muxlow, T. W. B., Axon, D. J., Brown, A., Corcoran, D., Dyson, J., and Mundt, R. (1997). Large-scale magnetic fields in the outflow from the young stellar object T Tauri S. *Nature*, 385(6615):415–417.

[108] Regály, Z., Sándor, Z., Dullemond, C. P., and Kiss, L. L. (2011). Spectral signatures of disk eccentricity in young binary systems I. Circumprimary case. *Astronomy & Astrophysics*, 528:A93.

[109] Roddier, C., Roddier, F., Graves, J., Northcott, M., Close, L., Surace, J., and Veran, J. (1999). Four-Year Observations of T Tauri With Adaptive Optics. In Bonaccini, D., editor, *ESO Conference and Workshop Proceedings*, volume 56 of *European Southern Observatory Conference and Workshop Proceedings*, page 389.

[110] Roddier, C., Roddier, F., Northcott, M. J., Graves, J. E., and Jim, K. (1996). Adaptive Optics Imaging of GG Tauri: Optical Detection of the Circumbinary Ring. *The Astrophysical Journal*, 463:326.

[111] Roell, T., Neuhäuser, R., Seifahrt, a., and Mugrauer, M. (2012). Extrasolar planets in stellar multiple systems. *Astronomy & Astrophysics*, 542:A92.

[112] Rosenfeld, K. a., Andrews, S. M., Wilner, D. J., and Stempels, H. C. (2012). A DISK-BASED DYNAMICAL MASS ESTIMATE FOR THE YOUNG BINARY V4046 Sgr. *The Astrophysical Journal*, 759(2):119.

[113] Sallum, S., Follette, K. B., Eisner, J. A., Close, L. M., Hinz, P., Kratter, K., Males, J., Skemer, A., Macintosh, B., Tuthill, P., Bailey, V., Defrère, D., Morzinski, K., Rodigas, T., Spalding, E., Vaz, A., and Weinberger, A. J. (2015). Accreting protoplanets in the LkCa 15 transition disk. *Nature*, 527(7578):342–344.

[114] Saucedo, J., Calvet, N., Hartmann, L., and Raymond, J. (2003). The Spatial Distribution of Fluorescent H 2 Emission near T Tauri. *The Astrophysical Journal*, 591(1):275–282.

[115] Schwarz, R., Funk, B., Zechner, R., and Bazsó (2016). New prospects for observing and cataloguing exoplanets in well-detached binaries. *Monthly Notices of the Royal Astronomical Society*, 460(4):3598–3609.

[116] Sigurdsson, S., Richer, H. B., Hansen, B. M., Stairs, I. H., and Thorsett, S. E. (2003). A Young White Dwarf Companion to Pulsar 1620-26: Evidence for Early Planet Formation. *Science*, 301(5630):193–196.

[117] Silber, J., Gledhill, T., Duchene, G., and Menard, F. (2000). Near-infrared imaging polarimetry of the GG Tau circumbinary ring. *The Astrophysical Journal*, 536(2):L89–L92.

[118] Skemer, A. J. I., Close, L. M., Greene, T. P., Hinz, P. M., Hoffmann, W. F., and Males, J. R. (2011). Dust Grain Evolution in Spatially Resolved T Tauri Binaries. *The Astrophysical Journal*, 740:43.

[119] Takakuwa, S., Saigo, K., Matsumoto, T., Saito, M., Lim, J., Hanawa, T., Yen, H.-W., and Ho, P. T. P. (2017). Spiral Arms, Infall, and Misalignment of the Circumbinary Disk from the Circumstellar Disks in the Protostellar Binary System L1551 NE. *The Astrophysical Journal*, 837(1):86.

[120] Tamazian, V. S., Docobo, J. A., White, R. J., and Woitas, J. (2002). Preliminary Orbits and System Masses for Five Binary T Tauri Stars. *The Astrophysical Journal*, 578(2):925–934.

[121] Tamura, M., Gatley, I., Joyce, R. R., Ueno, M., Suto, H., and Sekiguchi, M. (1991). Infrared polarization images of star-forming regions. I - The ubiquity of bipolar structure. *The Astrophysical Journal*, 378:611.

[122] Tamura, M., Hodapp, K., Takami, H., Abe, L., Suto, H., Guyon, O., Jacobson, S., Kandori, R., Morino, J.-I., Murakami, N., Stahlberger, V., Suzuki, R., Tavrov, A., Yamada, H., Nishikawa, J., Ukita, N., Hashimoto, J., Izumiura, H., Hayashi, M., Nakajima, T., and Nishimura, T. (2006). Concept and science of HiCIAO: high contrast instrument for the Subaru next generation adaptive optics. In McLean, I. S. and Iye, M., editors, *Proceedings of the SPIE*, volume 6269, pages 62690V–62690V–9.

[123] Tang, Y.-W., Dutrey, A., Guilloteau, S., Chapillon, E., Pietu, V., Di Folco, E., Bary, J., Beck, T., Beust, H., Boehler, Y., Gueth, F., Huré, J.-M., Pierens, A., and Simon, M. (2016). MAPPING CO GAS IN THE GG TAURI A TRIPLE SYSTEM WITH 50 au SPATIAL RESOLUTION. *The Astrophysical Journal*, 820(1):19.

[124] Thorsett, S. E., Arzoumanian, Z., and Taylor, J. H. (1993). PSR B1620-26 - A binary radio pulsar with a planetary companion? *The Astrophysical Journal*, 412:L33.

[125] Tokovinin, A. (2015). SPECTROSCOPIC SUBSYSTEMS in NEARBY WIDE BINARIES. *The Astronomical Journal*, 150(6):177.

[126] Torres, R. M., Loinard, L., Mioduszewski, A. J., Boden, A. F., Franco-Hernández, R., Vlemmings, W. H. T., and Rodríguez, L. F. (2012). VLBA DETERMINATION OF THE DISTANCE TO NEARBY STAR-FORMING REGIONS. V. DYNAMICAL MASS, DISTANCE, AND RADIO STRUCTURE OF V773 Tau A. *The Astrophysical Journal*, 747(1):18.

[127] Torres, R. M., Loinard, L., Mioduszewski, A. J., and Rodriguez, L. F. (2007). VLBA Determination of the Distance to Nearby Star-forming Regions. II. Hubble 4 and HDE 283572 in Taurus. *The Astrophysical Journal*, 671(2):1813–1819.

[128] Torres, R. M., Loinard, L., Mioduszewski, A. J., and Rodríguez, L. F. (2009). VLBA DETERMINATION OF THE DISTANCE TO NEARBY STAR-FORMING REGIONS. III. HP TAU/G2 AND THE THREE-DIMENSIONAL STRUCTURE OF TAURUS. *The Astrophysical Journal*, 698(1):242–249.

[129] von Braun, K., Tabetha, S. B., ten Brummelaar, T. A., Kane, S. R., van Belle, G. T., Ciardi, D. R., Raymond, S. N., López-Morales, M., McAlister, H. A., Schaefer, G., Ridgway, S. T., Sturmann, L., Sturmann, J., White, R., Turner, N. H., Farrington, C., and Goldfinger, P. J. (2011). 55 Cancri: Stellar Astrophysical Parameters, a Planet in the Habitable Zone, and Implications for the Radius of a Transiting Super-Earth. *The Astrophysical Journal*, 740(1):49.

[130] Wang, J., Fischer, D. A., Xie, J.-W., and Ciardi, D. R. (2015). INFLUENCE OF STELLAR MULTIPLICITY ON PLANET FORMATION. IV. ADAPTIVE OPTICS IMAGING OF KEPLER STARS WITH MULTIPLE TRANSITING PLANET CANDIDATES. *The Astrophysical Journal*, 813(2):130.

[131] Williams, J. P. and Cieza, L. A. (2011). Protoplanetary Disks and Their Evolution. *Annual Review of Astronomy and Astrophysics*, 49(1):67–117.

[132] Woitas, J., Eisloffel, J., Mundt, R., and Ray, T. P. (2002). The Environment of FS Tauri Observed with Hubble Space Telescope Wide Field Planetary Camera 2 in Narrowband Emission Line Filters. *The Astrophysical Journal*, 564(2):834–838.

[133] Wolszczan, A. and Frail, D. A. (1992). A planetary system around the millisecond pulsar PSR1257 + 12. *Nature*, 355(6356):145–147.

[134] Wu, Y. and Murray, N. (2003). Planet Migration and Binary Companions: The Case of HD 80606b. *The Astrophysical Journal*, 589(1):605–614.

[135] Yan, Z., Shen, Z.-Q., Yuan, J.-P., Wang, N., Rottmann, H., and Alef, W. (2013). Very long baseline interferometry astrometry of PSR B1257+12, a pulsar with a planetary system. *Monthly Notices of the Royal Astronomical Society*, 433(1):162–169.

[136] Zanazzi, J. J. and Lai, D. (2018). Inclination evolution of protoplanetary discs around eccentric binaries. *Monthly Notices of the Royal Astronomical Society*, 473(1):603–615.